

## AN ABSTRACT OF THE THESIS OF

Jason Polzin for the degree of Doctor of Philosophy in Chemical Engineering  
presented on April 28, 2005.

Title: Factors Influencing Halogenated Monoterpene Production in Microplantlets  
Derived from the Red Macroalga *Ochtodes secundiramea*

Abstract approved: \_\_\_\_\_ **Redacted for Privacy** \_\_\_\_\_

Gregory L. Rorrer

Halogenated monoterpene production by the red macroalga *Ochtodes secundiramea* was studied under different levels of nutrient, bromide, vanadium and light delivery. The key products formed were identified as myrcene, beta-elemene, the Z and E isomers of 10-bromomyrcene, 3-chloro-10E-bromomyrcene, Apakaocthodene A, and isomers of chloromyrcene and dibromomyrcene. The proposed pathway begins with an initial halogenation of myrcene to 3-chloromyrcene or 10-bromomyrcene. 10-bromomyrcene reacts with either chloride or bromide ions producing either 3-chloro-10E-bromomyrcene or 1,10-dibromomyrcene. The production of Apakaocthodene A starts from myrcene with 4 consecutive halogenation reactions, the first one forming the cyclic ring.

All fermentations were carried out in similar 2L photobioreactors. Temperature was controlled at 26°C, with a photoperiod of 14 hours on:10 hours off. Incident light intensity was 143  $\mu\text{E m}^{-2} \text{s}^{-1}$  for nutrient, bromide and vanadium delivery cultivations and the mean light intensity was set to 52.5, 125, and 240  $\mu\text{E m}^{-2} \text{s}^{-1}$  for light delivery cultivations. The pH was buffered to 8.0 with sodium bicarbonate, but not controlled. Air was supplied at 630  $\text{mL min}^{-1}$ , vvm of 0.3, and  $\text{CO}_2$  was supplied at 2  $\text{mL min}^{-1}$  for nutrient and light delivery cultivations and 0

mL min<sup>-1</sup> for bromide and vanadium delivery cultivations. For nutrient delivery cultivations, nitrate was delivered at 0.006, 0.076 and 0.74 mmol Nitrate L<sup>-1</sup> day<sup>-1</sup> and phosphate was delivered at 0.33, 3.99 and 38.4 µmol Phosphate L<sup>-1</sup> day<sup>-1</sup>. For semi-continuous delivery cultivations, bromide was delivered at 0.0, 0.0074, 0.013 and 0.13 mmol Bromide L<sup>-1</sup> day<sup>-1</sup> at a constant vanadium delivery of 6.38 to 7.35 nmol Vanadium L<sup>-1</sup> day<sup>-1</sup>, and vanadium delivery was set to 0.0 and 6.38 nmol Vanadium L<sup>-1</sup> day<sup>-1</sup> at a constant bromide delivery of 0.13 mmol Bromide L<sup>-1</sup> day<sup>-1</sup>. For fed-batch bromide and vanadium delivery cultivations the one time pulse of bromide raised the medium bromide concentration to 0.0, 0.038, 0.128 and 1.4 mmol Bromide L<sup>-1</sup>, with the vanadium concentration going to 416 to 520 nmol Vanadium L<sup>-1</sup>, and the pulse of vanadium raised the medium vanadium concentration to 0.0 and 515 nmol Vanadium L<sup>-1</sup>, with the bromide concentration going to 1.1 to 1.4 mmol Bromide L<sup>-1</sup>.

Factors Influencing Halogenated Monoterpene Production in Microplantlets  
Derived from the Red Macroalga *Ochtodes secundiramea*

by

Jason Polzin

A THESIS

submitted to

Oregon State University

in partial fulfillment of  
the requirements for the  
degree of

Doctor of Philosophy

Presented April 28, 2005

Commencement June 2005


Doctor of Philosophy thesis of Jason Polzin presented on April 28, 2005.

APPROVED:

Redacted for Privacy

\_\_\_\_\_  
Major Professor, representing Chemical Engineering

Redacted for Privacy

  
\_\_\_\_\_  
Head of the Department of Chemical Engineering

Redacted for Privacy

\_\_\_\_\_  
Dean

I understand that my thesis will become part of the permanent collection of Oregon State University libraries. My signature below authorizes release of my thesis to any reader upon request.

\_\_\_\_\_  
Redacted for Privacy

## ACKNOWLEDGEMENT

My road to the completion of this degree has followed a very non-traditional path. I am thankful that the efforts invested up to this point will be rewarded with my desired goal, and I am thankful to the people that have helped me along the way. Everyone feels obliged to thank their professor, but in my case Greg Rorrer has gone above and beyond to help me finish this degree. I, without a doubt, would never have been able to finish it without his patience and understanding as well as his excellent teaching and mentoring skills. I am currently employed in a position that has afforded me the opportunity to use my education with opportunities to develop my career, and that is a testament to his good work. Thanks a bunch Greg.

This research was fully supported by the National Science Foundation, Division of Bioengineering and Environmental Systems (Award number BES-9810797)

## TABLE OF CONTENTS

	<u>Page</u>
1. INTRODUCTION .....	1
1.1. LITERATURE REVIEW .....	2
1.1.1. Bioprocess Development for Marine Biotechnology.....	3
1.1.2. Tissue Culture of Marine Macroalgae.....	3
1.1.3. Halogenated Monoterpenes.....	4
1.1.4. Marine Haloperoxidase .....	5
1.1.5. Halogenated Monoterpene Biogenic Pathway .....	5
1.1.6. Growth Differentiation Balance Hypothesis.....	6
1.1.7. Light Effects on Marine Macroalgae .....	8
1.2. RESEARCH OBJECTIVES .....	9
1.3. REFERENCES .....	10
2. COMPOUND IDENTIFICATION.....	15
2.1. MATERIALS AND METHODS.....	15
2.1.1. Biomass Extraction .....	15
2.1.2. GC-MS Analysis .....	16
2.2. RESULTS AND DISCUSSION .....	17
2.2.1. GC-MS .....	17
2.2.2. NMR Analysis .....	19
2.2.3. Halogenated Monoterpene Structure Determination .....	19
2.3. REFERENCES .....	23
3. NUTRIENT DELIVERY .....	25
3.1. MATERIALS AND METHODS.....	25
3.1.1. Culture Maintenance .....	25
3.1.2. Photobioreactor Design and Operation .....	27
3.1.3. Cell Biomass, Nitrate and Phosphate .....	32
3.1.4. GC-FID Analysis .....	33
3.1.5. Specific Oxygen Evolution Rate.....	35

## TABLE OF CONTENTS (Continued)

	<u>Page</u>
3.1.6. Volumetric Oxygen Mass Transfer and CO <sub>2</sub> -TR.....	36
3.2. RESULTS AND DISCUSSION .....	37
3.2.1. Growth Data .....	37
3.2.2. Halogenated Monoterpene Kinetic Data.....	46
3.2.3. Dynamic Growth Model .....	52
3.3. REFERENCES .....	60
4. BROMIDE & VANADIUM DELIVERY .....	62
4.1. MATERIALS AND METHODS.....	63
4.1.1. Culture Maintenance .....	63
4.1.2. Photobioreactor Design and Operation .....	64
4.1.2.1. Semi-Continuous Cultivations .....	64
4.1.2.2. Fed-Batch Cultivations .....	74
4.1.3. Bromide.....	74
4.1.4. Estimation of Specific Growth Rate .....	75
4.1.5. Compound Production Rate Estimation.....	76
4.2. RESULTS AND DISCUSSION .....	78
4.2.1. Semi-continuous cultivations .....	78
4.2.1.1. Growth Data .....	78
4.2.1.2. Bromide Kinetic Data .....	85
4.2.1.3. Halogenated Monoterpene Kinetic Data.....	89
4.2.2. Fed-Batch Cultivations .....	101
4.2.2.1. Growth Data .....	101
4.2.2.2. Bromide Kinetic Data .....	107
4.2.2.3. Halogenated Monoterpene Kinetic Data.....	111
4.3. METABOLIC NETWORK ANALYSIS .....	123
4.3.1. Theory and Background .....	123
4.3.2. Biosynthetic Pathway .....	125
4.3.3. Metabolic Flux Model Development .....	127
4.3.4. Flux Rigidity .....	130

## TABLE OF CONTENTS (Continued)

	<u>Page</u>
4.4. REFERENCES .....	134
5. LIGHT DELIVERY .....	136
5.1. MATERIALS AND METHODS.....	136
5.1.1. Culture Maintenance .....	136
5.1.2. Photobioreactor Design and Operation .....	137
5.1.3. Mean Light Intensity .....	139
5.1.4. Specific Biomass Growth Rate .....	143
5.1.5. GC-MS Analysis .....	144
5.2. RESULTS AND DISCUSSION .....	145
5.2.1. Growth Data .....	145
5.2.2. GC-MS Analysis .....	153
5.2.3. Terpene Kinetic Data .....	154
5.3. REFERENCES .....	157
6. SUMMARY AND CONCLUSIONS .....	159
BIBLIOGRAPHY .....	165



## LIST OF FIGURES

Figure	Page
2-1. GC-TIC (a) and GC-FID (b) plots of DCM extracts of <i>Ochtodes Secundiramea</i> microplantlets.....	18
2-2. GC-TIC plots of DCM extracts of <i>Ochtodes secundiramea</i> microplantlets showing trace compounds E-J .....	19
2-3. Myrcene and octodane carbon backbone templates.....	20
2-4. Probable structures for dominate halogenated monoterpenes extracted from <i>Ochtodes secundiramea</i> microplantlets.....	21
3-1. Schematic diagram of 2-L photobioreactor.....	29
3-2. Experimental and estimated biomass density profiles for nutrient delivery cultivations.....	39
3-3. Photobioreactor medium nitrate concentration profiles for nutrient delivery cultivations.....	40
3-4. Photobioreactor medium phosphate concentration profiles for nutrient delivery cultivations.....	41
3-5. Net photosynthetic oxygen evolution rate vs. light intensity curves for nutrient delivery cultivation at $0.74 \text{ mmol N L}^{-1} \text{ day}^{-1}$ .....	43
3-6. Myrcene profiles for nutrient delivery cultivations.....	47
3-7. Compound A-2 (10(E)-bromomyrcene) profiles for nutrient delivery cultivations.....	48
3-8. Compound E (chloromyrcene) profiles for nutrient delivery cultivations .....	49
3-9. Compound B (bromochloromyrcene) profiles for nutrient delivery cultivations.....	50

## LIST OF FIGURES (Continued)

Figure	Page
3-10. Compound C (dibromomyrcene) profiles for nutrient delivery cultivations .....	51
3-11. Compound D-2 (apakaodotene B) profiles for nutrient delivery cultivations .....	52
3-12. Dynamic model prediction and experimental data of biomass density for nutrient delivery cultivation at $0.74 \text{ mmol N L}^{-1} \text{ day}^{-1}$ .....	57
3-13. Dynamic model prediction and experimental data of nitrate concentration for nutrient delivery cultivation at $0.74 \text{ mmol N L}^{-1} \text{ day}^{-1}$ .....	58
3-14. Dynamic model prediction and experimental data of phosphate concentration for nutrient delivery cultivation at $0.74 \text{ mmol N L}^{-1} \text{ day}^{-1}$ .....	59
4-1. Photobioreactor medium nitrate concentration profiles for semi-continuous bromide delivery cultivations .....	80
4-2. Photobioreactor medium nitrate concentration profiles for semi-continuous vanadium delivery cultivations .....	81
4-3. Photobioreactor medium phosphate concentration profiles for semi-continuous bromide delivery cultivations .....	82
4-4. Photobioreactor medium phosphate concentration profiles for semi-continuous vanadium delivery cultivations .....	83
4-5. Photosynthetic oxygen evolution rate vs incident light intensity (PI) curve for <i>Ochodes secundiramea</i> microplantlets .....	85
4-6. Photobioreactor medium bromide concentration profiles for semi-continuous bromide delivery cultivations .....	86

## LIST OF FIGURES (Continued)

Figure	<u>Page</u>
4-7. Photobioreactor medium bromide concentration profiles for semi-continuous bromide delivery cultivations .....	87
4-8. Photobioreactor medium bromide concentration profiles for semi-continuous vanadium delivery cultivations.....	88
4-9. Myrcene profiles for semi-continuous bromide delivery Cultivations .....	89
4-10. Compound A-2 (10(E)-bromomyrcene) profiles for semi-continuous bromide delivery cultivations .....	90
4-11. Compound E (chloromyrcene) profiles for semi-continuous bromide delivery cultivations.....	91
4-12. Compound B (bromochloromyrcene) profiles for semi-continuous bromide delivery cultivations .....	92
4-13. Compound C (dibromomyrcene) profiles for semi-continuous bromide delivery cultivations .....	93
4-14. Compound D-2 (apakaochtodene B) profiles for semi-continuous bromide delivery cultivations .....	94
4-15. Myrcene profiles for semi-continuous vanadium delivery cultivations .....	95
4-16. Compound A-2 (10(E)-bromomyrcene) profiles for semi-continuous vanadium delivery cultivations.....	96
4-17. Compound E (chloromyrcene) profiles for semi-continuous vanadium delivery cultivations .....	97
4-18. Compound B (bromochloromyrcene) profiles for semi-continuous vanadium delivery cultivations.....	98

## LIST OF FIGURES (Continued)

Figure	Page
4-19. Compound C (dibromomyrcene) profiles for semi-continuous vanadium delivery cultivations.....	99
4-20. Compound D-2 (apakaochtodene B) profiles for semi-continuous vanadium delivery cultivations.....	100
4-21. Photobioreactor medium nitrate concentration profiles for fed-batch bromide delivery cultivations.....	103
4-22. Photobioreactor medium nitrate concentration profiles for fed-batch vanadium delivery cultivations .....	104
4-23. Photobioreactor medium phosphate concentration profiles for fed-batch bromide delivery cultivations.....	105
4-24. Photobioreactor medium phosphate concentration profiles for fed-batch vanadium delivery cultivations .....	106
4-25. Photobioreactor medium bromide concentration profiles for fed-batch bromide delivery cultivations.....	108
4-26. Photobioreactor medium bromide concentration profiles for fed-batch bromide delivery cultivations.....	109
4-27. Photobioreactor medium bromide concentration profiles for fed-batch vanadium delivery cultivations .....	110
4-28. Myrcene profiles for fed-batch bromide delivery cultivations .....	111
4-29. Compound A-2 (10(E)-bromomyrcene) profiles for fed-batch bromide delivery cultivations.....	112
4-30. Compound E (chloromyrcene) profiles for fed-batch bromide delivery cultivations.....	113

## LIST OF FIGURES (Continued)

Figure	Page
4-31. Compound B (bromochloromyrcene) profiles for fed-batch bromide delivery cultivations.....	114
4-32. Compound C (dibromomyrcene) profiles for fed-batch bromide delivery cultivations.....	115
4-33. Compound D-2 (apakaodotodene B) profiles for fed-batch bromide delivery cultivations.....	116
4-34. Myrcene profiles for fed-batch vanadium delivery Cultivations .....	117
4-35. Compound A-2 (10(E)-bromomyrcene) profiles for fed-batch vanadium delivery cultivations .....	118
4-36. Compound E (chloromyrcene) profiles for fed-batch vanadium delivery cultivations .....	119
4-37. Compound B (bromochloromyrcene) profiles for fed-batch vanadium delivery cultivations .....	120
4-38. Compound C (dibromomyrcene) profiles for fed-batch vanadium delivery cultivations .....	121
4-39. Compound D-2 (apakaodotodene B) profiles for fed-batch vanadium delivery cultivations .....	122
4-40. Proposed biosynthetic pathway for production of halogenated monoterpenes in <i>Ochtodes secundiramea</i> microplantlets.....	126
4-41. Putative metabolic pathway from myrcene to identified halogenated monoterpenes.....	127
5-1. Photosynthetic oxygen evolution rate vs mean light intensity (PI) curve for <i>Ochtodes secundiramea</i> microplantlets.....	140

## LIST OF FIGURES (Continued)

Figure	<u>Page</u>
5-2. Dependence of light attenuation constant on biomass density .....	141
5-3. Calculated specific growth rate for light delivery cultivations based on measurements of biomass during cultivation, and from photosynthetic oxygen evolution calculation .....	149
5-4. Photobioreactor medium nitrate concentration profiles for light delivery cultivations .....	150
5-5. Photobioreactor medium phosphate concentration profiles for light delivery cultivations .....	151
5-6. GC-TIC plots of DCM extracts of <i>Ochtodes secundiramea</i> microplantlets showing terpenes and no halogenated compounds .....	152
5-7. Myrcene profiles for light delivery cultivations .....	156
5-8. beta-elemene profiles for light delivery cultivations .....	157

## LIST OF TABLES

Table	<u>Page</u>
2-1. Dominant Halogenated Monoterpenes in Dichloromethane Extracts of Photobioreactor Cultivated <i>O. secundiramea</i> Microplantlets .....	22
2-2. Trace Halogenated Monoterpenes in Dichloromethane Extracts of Photobioreactor Cultivated <i>O. secundiramea</i> Microplantlets .....	23
3-1. Experimental Process Conditions for Nutrient Delivery Cultivations .....	31
3-2. Medium Composition for Nutrient Delivery Cultivations .....	32
3-3. GC-FID Response Factors for Model C <sub>10</sub> Brominated Compounds .....	35
3-4. Photosynthetic Growth Parameters for Nutrient Delivery Cultivations .....	44
3-5. Dynamic Model Estimation Parameters.....	56
4-1. Experimental Process Conditions for Semi-continuous Bromide Delivery Cultivations .....	66
4-2. Experimental Process Conditions for Semi-continuous Vanadium Delivery Cultivations .....	67
4-3. Medium Composition for Semi-continuous Bromide Delivery Cultivations .....	68
4-4. Medium Composition for Semi-continuous Vanadium Delivery Cultivations .....	69
4-5. Experimental Process Conditions for Fed-batch Bromide Delivery Cultivations .....	70

## LIST OF TABLES (Continued)

Table	<u>Page</u>
4-6. Experimental Process Conditions for Fed-batch Vanadium Delivery Cultivations .....	71
4-7. Medium Composition for Fed-batch Bromide Delivery Cultivations .....	72
4-8. Medium Composition for Fed-batch Vanadium Delivery Cultivations .....	73
4-9. Estimated Specific Growth Rates for Semi-continuous Bromide and Vanadium Delivery Cultivations.....	79
4-10. Estimated Specific Growth Rates for Fed-batch Bromide and Vanadium Delivery Cultivations.....	102
4-11. Compound Production Rates for Key Halogenated Monoterpenes fro Semi-continuous Bromide and Vanadium Delivery Cultivations .....	130
4-12. Compound Flux for Semi-continuous Bromide and Vanadium Delivery Cultivations .....	131
5-1. Experimental Process Conditions for Light Delivery Cultivations .....	138
5-2. Medium Composition for Light Delivery Cultivations.....	139
5-3. Estimation of Mean Light Intensity .....	143
5-4. Measured Specific Growth Rates for Light Delivery Cultivations .....	147
5-5. Specific Growth Rate Calculated from Estimation of Photosynthetic Oxygen Evolution.....	148
5-6. Dominant Terpenes in DCM Extracts of Photobioreactor Cultivated <i>O. secundiramea</i> Microplantlets .....	154



# **Factors Influencing Halogenated Monoterpene Production in Microplantlets Derived from the Red Macroalga *Ochtodes secundiramea***

## **1. INTRODUCTION**

The discovery of naturally produced compounds, having novel structures and biological activities, is important to future pharmaceutical research. Compounds obtained from marine organisms are of particular interest because they produce a large number of bioactive compounds with structural features different than compounds obtained from terrestrial organisms (Ireland et al., 1988). Physiologically complex marine macroalgae, commonly known as seaweeds, are a particularly productive source of unique compounds with biological activities (Radmer, 1996). The three major phyla of marine macroalgae are the Chlorophyta (green macroalgae), Phaeophyta (brown macroalgae) and Rhodophyta (red macroalgae). Of the three phyla, the red macroalgae have shown the unique ability to produce halogenated monoterpenes and sesquiterpenes (Fennical, 1975), and many of these have potential as anti-cancer compounds in particular the pentahalogenated, acyclic monoterpene, halomon (Fuller et al., 1992, 1994).

Discovery is just the first step in a long process yielding valuable biological products. Three bioprocess development steps are required to transition from a novel compound to a useful drug. First, when an organism and target molecule are identified, an *in vivo* culture must be developed. Second, conditions, which affect the growth of marine macroalgae, such as light intensity, CO<sub>2</sub> delivery, nutrient concentrations, nutrient delivery and photobioreactor configuration can then be determined. Third, after the growth of the organism is understood, metabolic flux analysis is used to illuminate the metabolic control of the target compound under

different process conditions. Each new application of this procedure develops a tool kit to be used with the next organism and compound of interest. The ability to systematically alter conditions and analyze a response within a theoretical framework, is an application of the chemical engineering approach to marine natural products development.

### 1.1. LITERATURE REVIEW

My approach to understanding the factors affecting growth and metabolite production of marine macroalgae is made feasible by application of chemical engineering principles to the organism as a mini-factory. The following literature review will focus on the biological background that inspires the experimental approach.

The literature review will outline one class of biologically active compounds produced by Rhodophyta—halogenated monoterpenes. The discussion of halogenated monoterpenes will include the bioactivity of some halogenated monoterpenes and their proposed ecological function. The introduction will also address possible biogenic pathways of halogenated monoterpenes, take a more detailed look at the possible halogenation reactions, present the growth differentiation balance hypothesis as a rationale for influencing halogenated monoterpene production, discuss light quality effects on secondary metabolite production, and illustrate the bioprocess development for marine biotechnology.

#### 1.1.1. Bioprocess Development for Marine Biotechnology

The collection of marine macroalgae and the subsequent extraction, purification and identification of unique compounds has yielded a large library of bioactive compounds (Carte, 1996). However, only with the application of bioprocess development can these bioactive compounds find their way into commercial use.

Field collecting enough macroalga biomass to supply a candidate compound for drug testing and development could do significant damage to the local marine ecosystem (Rorrer et al., 1999). In addition to limited biomass supply, field collected macroalgae from different geographical and temporal locations can have variations in product composition (Puglisi and Paul, 1997). A solution to field collecting macroalgae is cultivation in mariculture or aquaculture, but these methods do not provide complete control over cultivation conditions. The problem facing direct synthesis of complex, bioactive compounds is preserving regio- and stereochemistry, which are vital for bioactivity (Rorrer et al., 1999).

#### 1.1.2. Tissue Culture of Marine Macroalgae

The above problems can be overcome by the controlled growth of marine macroalgae in photobioreactors (Rorrer et al., 1999). Once the compound of interest has been identified, the second step in the bioprocess development for marine biotechnology is the development of a suspension culture. Suspension cultures have been previously developed in our lab for the macroalgae *Laminar saccharina* (Qi and Rorrer, 1995), *Acrosiphonia coalita* (Rorrer et al., 1996), and the red macroalgae *Agardhiella subulata* (Huang et al., 1998, Huang and Rorrer,

2002a, Huang and Rorrer, 2002b, Huang and Rorrer, 2003) and *Ochtodes secundiramea* (Maliakal et al., 2001).

The technique for initiation of microplantlet suspension cultures from marine macroalgae was first developed in our lab for *Agardhiella subulata* (Huang et al., 1998) and then for *Ochtodes secundiramea* (Maliakal et al., 2001). In the *Agardhiella subulata* system, a sub-lethal shear stress was applied to filament clumps to initiate microplantlet formation (Huang et al., 1998). In the *Ochtodes secundiramea* system, microplantlet regeneration was achieved following nutrient deprivation of compact callus cells (Maliakal et al., 2001).

#### 1.1.3. Halogenated Monoterpenes

Halogenated monoterpenes (HMTs) are produced by many marine organisms including marine macroalgae (Gribble, 1992). The abundance of halogens within the marine environment, 19,000 mg/L Cl<sup>-</sup> and 65 mg/L Br<sup>-</sup>, readily allows marine organisms to incorporate halogens within organic compounds (Fenical, 1982). Within marine macroalgae, HMTs are abundant in Rhodophyta (Fennical, 1975, Gribble, 1992), particularly within the genera *Plocamium* (Crews, 1977, König et al., 1990), *Porteria* (Ichikawa et al., 1974, Burreson et al., 1975, Fuller et al., 1994) and *Ochtodes* (McConnell and Fenical, 1978, Paul et al., 1980, Gerwick, 1984).

Halogenated monoterpenes obtained from Rhodophyta have principally shown bioactivity in anti-cancer and anti-microbial assays. Halomon, an acyclic, pentahalogenated monoterpene, obtained from *Porteria hornemannii*, produced one of the most extreme examples of differential cytotoxicity to 60 different human cell lines representing eight major cancer subtypes in a National Cancer Institute screen

(Carte, 1996, Fuller et al., 1994). A group of cyclic compounds based on the ochtodane ring system has also shown biotoxicity in anti-insect and anti-cell division assays (Crews et al., 1984).

In nature, HMTs reduce grazing by herbivorous fish on algae lacking any morphological defense (Paul et al., 1980, 1987). In the coral reef environment, where many Rhodophyta are found, benthic marine algae must combat consumption by marine fish; either by growing quickly to outpace consumption or by making themselves unpalatable. The ability of Rhodophyta to produce HMTs gives them a potential evolutionary advantage.

#### 1.1.4. Marine Haloperoxidase

The halogenation of monoterpenes with bromine and chlorine ions in seawater is most likely promoted by a vanadium-dependent bromoperoxidase (Butler and Walker, 1993; Butler, 1999), which is present in *Ochtodes* (Tucker and Rorrer, 2001). Vanadium bromoperoxidase (V-BrPO) catalyzes the oxidation of bromide and to a lesser extent, chloride by hydrogen peroxide with subsequent reaction of the halonium ion with an array of organic substrates (Butler and Walker, 1993, Itoh et al., 1988, de Boer and Wever, 1988). Recently more understanding has been gained as to the mechanism of reaction, selectivity, and structure of binding site of vanadium haloperoxidases (Butler, 1999).

#### 1.1.5. Halogenated Monoterpene Biogenic Pathway

The biosynthesis of halogenated monoterpenes in macrophytic red algae is not very well understood (Wise and Croteau, 1999). Biogenic schemes proposed

by Naylor et al. (1983) suggest that ocimene is the common monoterpene precursor to all the halogenated monoterpenes found in *Plocamium*, whereas myrcene is common precursor to all the halogenated monoterpenes found in *Portieria*.

The production of HMTs involves the preparation of a monoterpene precursor, with subsequent halogenation by a haloperoxidase. It is widely held that all terpenes are formed by head to tail joining of isoprene units. Isoprene is prepared, as isopentenyl pyrophosphate, via several enzymatic steps from Acetyl-CoA (Bramley, 1997). Isopentenyl pyrophosphate then undergoes isomerization to form dimethylallyl pyrophosphate with subsequent reaction of isopentenyl pyrophosphate and dimethylallyl pyrophosphate to produce geranyl pyrophosphate (Bramley, 1997). Geranyl pyrophosphate is believed to be the precursor for cyclic and acyclic monoterpene production (Wise and Croteau, 1999). Both cyclic and acyclic monoterpenes are available to undergo halogenation to make HMTs; however, it has been proposed that cyclic HMTs are formed by a halonium ion induced cyclization from an acyclic monoterpene, with subsequent continued halogenation by haloperoxidases (Fenical, 1982, Wise and Croteau, 1999).

#### 1.1.6. Growth Differentiation Balance Hypothesis

The growth differentiation balance hypothesis (GDBH) was first proposed by Loomis in 1932 and further developed by Lorio in 1986 (Lerdau et al., 1994). The GDBH states there is a distinction between growth processes (primary metabolism) and differentiation processes (the production of specialized storage tissues and compounds not dedicated to resource capture, secondary metabolism), with each requiring photosynthate (Lerdau et al., 1994). Growth processes will dominate under conditions of high nutrient supply, but will no longer dominate when nutrients become limited. Under conditions of high carbon input, ie normal

to high light intensities, and low nutrient input, the production of carbon based secondary defenses will increase.

In aquatic environments, the GDBH more accurately predicts the response for polyphenolic producing plants than for monoterpene producing plants (Cronin and Hay, 1996). Polyphenolics varied inversely with nitrogen content for the brown alga *Fucus vesiculosus* (Ilvessalo and Tuomi, 1989). Phenolic content decreased with increasing media nitrate concentration for the brown alga *Lobophora variegata* (Arnold et al., 1995). However, the brown alga *Sargassum filipendula* showed no change in phenolic concentration with nutrient enrichment (Cronin and Hay, 1996).

Terpene concentrations within marine algae appear to contradict the GDBH. Terpene concentrations increased with nutrient enrichment for the brown alga *Dictyota ciliolata* (Cronin and Hay, 1996). The red alga *Portieria hornemannii* showed no change in ooctodene concentration with nutrient enrichment (Puglisi and Paul, 1997). The results for *Dictyota ciliolata*, however, are misleading because a material balance on the nutrient shows that the nutrient enriched cultures were not nutrient enriched—the nutrient pulse was completely washed out of the flow through tanks within 20 minutes following the pulse. The results for *Portieria hornemannii* may also be misleading because no quantification for the nutrient enrichment is presented. These organisms may or may not differ with the GDBH.

#### 1.1.7. Light Effects on Marine Macroalgae

According to the GDBH, increased light intensity will increase the carbon pool in the organism and thereby increase the production of carbon based secondary metabolites under nutrient deficiency. Decreasing the light intensity will shut down primary and secondary metabolism. An organism growing under conditions of sufficient nutrients may still not show increased primary metabolism, given the light intensity is insufficient.

The effect of light on *Dictyota ciliolata* and *Portieria hornemannii* production of terpenes contradict one another. *D. ciliolata* decreased terpene metabolites with increased light intensity (Cronnin and Hay, 1996), but *P. hornemannii* decreased octadecene concentrations following shading (Puglisi and Paul, 1997).

Terpene production in terrestrial plants follows more closely to the GDBH. The production of specialized monoterpene storage structures was shown to be light dependent in *Thymus vulgaris* (Yamamura et al., 1989), and low light intensities caused a decrease in terpene production in *Hedeoma drummondii* (Firmage, 1981).

Much work has been done to isolate and identify chemical structures of halogenated monoterpenes extracted from marine macroalgae (Gribble, 1992, Fennical, 1982, Fenical 1975) and to determine bioactivity of unique halogenated monoterpenes (Carte, 1996, Fuller et al., 1994, Crews et al., 1984), but no work has been completed to extract halogenated monoterpenes from tissue suspension cultures of marine macroalgae cultivated in photobioreactors.



Cultivation of tissue from the macroalgae *Laminaria saccharina*, *Acrosiphonia coalita* and *Agardhiella subulata* have been demonstrated in our lab in batch and fed-batch stirred tank photobioreactors (Qi and Rorrer, 1995, Rorrer et al., 1996), bubble column photobioreactors (Rorrer et al., 1995, Zhi and Rorrer, 1996, Huang et al., 1998, Huang and Rorrer, 2002a, Huang and Rorrer, 2002b, Huang and Rorrer, 2003), and tubular recycle photobioreactors (Rorrer et al., 1999). The proposed research builds on the state of the art in biotechnology for marine macroalgae established in our lab and enters into a new class of bioactive compounds.

## 1.2. RESEARCH OBJECTIVES

The overall goal of this research is to demonstrate the production of secondary metabolites by bioreactor cultivation of cell and tissue cultures derived from marine macroalgae. Efforts will focus on one model organism, the red alga *Ochtodes secundiramea*. The unique halogenation ability of this model alga has a wide range of applications ranging from pharmaceutical intermediates to the “green chemistry” production of brominated organic intermediates for petrol or specialty chemicals. To these ends, I will use photobioreactor cultivated microplantlets derived from the red macroalgae *Ochtodes secundiramea* to understand the factors affecting the metabolic pathways to halogenated monoterpenes. Determining the factors affecting halogenated monoterpene production will also require an understanding of what factors are important to growth. Possible limiting growth factors will be assessed. The factors affecting halogenated monoterpene production will then be studied at constant growth conditions. Specifically, the objectives of this thesis research are to

1. Assess the limiting environmental factors on growth, including CO<sub>2</sub> delivery, and light delivery, for the cultivation of *Ochtodes secundiramea* microplantlets in bubble column photobioreactors and airlift photobioreactors.
2. Identify key monoterpenes produced by *Ochtodes secundiramea* microplantlets, and determine the yield for key monoterpenes in biomass extracts of *Ochtodes secundiramea* microplantlets.
3. Determine the effect of medium components on production of halogenated monoterpenes within *Ochtodes secundiramea* microplantlets.
4. Determine the effect of medium components on growth of *Ochtodes secundiramea* microplantlets.
5. Determine the effect of mean light intensity on growth and halogenated monoterpene production within *Ochtodes secundiramea* microplantlets.
6. Develop a metabolic flux analysis for production of halogenated monoterpenes within *Ochtodes secundiramea* microplantlets, including production pathway, and quantification of key pathway steps. Propose limiting steps within the pathway based on metabolic flux analysis.

### 1.3. REFERENCES

Arnold, T.M., Tanner, C.E., and Hatch, W.I. 1995. Phenotypic variation in polyphenolic content of the tropical brown alga *Lobophora variegata* as a function of nitrogen availability. *Marine Ecology Progress Series* **123**: 177-183.

- Bramley, P.M. 1997. Isoprenoid metabolism. In: *Plant Biochemistry*, P.M. Dey and J.B. Harborne, Ed., Academic Press: San Diego, CA, pp 417-439.
- Burreson, B.J., Woolard, F.X., and Moore, R.E. 1975. Evidence for the biogenesis of halogenated myrcenes from the red alga *Chondrococcus hornemanni*. *Chemistry Letters*: 1111-1114.
- Butler, A., and Walker, J.V. 1993. Marine haloperoxidases. *Chemistry Reviews* **93**: 1937-1944.
- Butler, A. 1999. Mechanistic considerations of the vanadium haloperoxidases. *Coordination Chemistry Reviews* **187**: 17-35.
- Carte, B.K. 1996. Biomedical potential of marine natural products. *BioScience* **46**: 271-285.
- Crews, P. 1977. Monoterpene halogenation by the red alga *Plocamium oregonum*. *Journal of Organic Chemistry* **42**: 2634-2636.
- Crews, P., Myers, B.L., Naylor, S., Clason, E.L., Jacobs, R.S., and Staal, G.B. 1984. Bio-active monoterpenes from red seaweeds. *Phytochemistry* **23**: 1449-1451.
- Cronin, G., and Hay, M.E. 1996. Effects of light and nutrient availability on the growth, secondary chemistry, and resistance to herbivory of two brown seaweeds. *Oikos* **77**: 93-106.
- de Boer, E., and Wever, R. 1988. The reaction mechanism of the novel vanadium-bromoperoxidase. *Journal of Biological Chemistry* **263**: 12326-12332.
- Fenical, W. 1975. Halogenation in the rhodophyta—a review. *Journal of Phycology* **11**: 245-259.
- Fenical, W. 1982. Natural products chemistry in the marine environment. *Science* **215**: 923-928.
- Firmage, D. 1981. Environmental influences on the monoterpene variation in *Hedeoma drummondii*. *Biochemical Systematics and Ecology* **9**: 53-58.
- Fuller, R.W., Cardellina II, J.J., Kato, Y., Brinen, L.S., Clardy, J., Snader, K.M., and Boyd, M.R. 1992. A pentahalogenated monoterpene from the red alga *Portieria hornemannii* produces a novel cytotoxicity profile against a diverse panel of human tumor cell lines. *Journal of Medical Chemistry* **35**: 3007-3011.

Fuller, R.W., Cardellina II, J.J., Jurek, J., Scheuer, P.J., Alvarado-Lindner, B., McGuire, M., Gray, G.N., Steiner, J.R., Clardy, J., Menez, E., Shoemaker, R.H., Newman, D.J., Snader, K.M., and Boyd, M.R. 1994. Isolation and structure/activity features of halomon-related antitumor monoterpenes from the red alga *Portieria hornemannii*. *Journal of Medical Chemistry* **37**: 4407-4411.

Gerwick, W.H. 1984. 2-Chloro-1,6(S\*),8-tribromo-3-(8)(Z)-octodene: a metabolite of the tropical red seaweed *Ochtodes secundiramea*. *Phytochemistry* **23**: 1323-1324.

Gribble, G.W. 1992. Naturally occurring organohalogen compounds—a survey. *Journal of Natural Products* **55**: 1353-1395.

Huang, Y.M., Maliakal, S., Cheney, D.P., and Rorrer, G.L. 1998. Comparison of development and photosynthetic growth for filament clump and regenerated microplantlet cultures of *Agardhiella subulata* (Rhodophyta, Gigartinales). *Journal of Phycology* **34**: 893-901.

Huang, Y.M., and Rorrer, G.L. 2002a. Dynamics of oxygen evolution and biomass production during cultivation of *Agardhiella subulata* microplantlets in a bubble-column photobioreactor under medium perfusion. *Biotechnology Progress* **18**: 62-71.

Huang, Y.M.; Rorrer, G.L. 2002b. Optimal temperature and photoperiod for the cultivation of *Agardhiella subulata* microplantlets in a bubble-column photobioreactor. *Biotechnology and Bioengineering* **79**: 135-144.

Huang, Y.M., and Rorrer, G.L. 2003. Cultivation of microplantlets derived from the marine red alga *Agardhiella subulata* in a stirred tank photobioreactor. *Biotechnology Progress* **19**: 418-427.

Ichikawa, N., Naya, Y., and Enomoto, S. 1974. New halogenated monoterpenes from *Desmia (Chondrococcus) hornemanni*. *Chemistry Letters*: 1333-1336.

Ireland, C.M., Roll, D.M., Molinski, T.F., McKee, T.C., Zabriske, T.M., and Swersey, J.C. 1988. Uniqueness of the marine environment: categories of marine natural products from invertebrates. In: *Biomedical Importance of Marine Organisms*, D.G. Fautin, Ed., California Academy of Sciences: San Francisco, CA, pp. 41-57.

Itoh, N., Quamrul, H., Izumi, Y., and Yamada, H. 1988. Substrate specificity, regioselectivity and stereoselectivity of halogenation reactions catalyzed by non-

- heme-type bromoperoxidase of *Corallina pilulifera*. *European Journal of Biochemistry* **172**: 477-484.
- Ilvessalo, H., and Tuomi, J. 1989. Nutrient availability and accumulation of phenolic compounds in the brown alga *Fucus vesiculosus*. *Marine Biology* **101**: 115-119.
- Konig, G.M., Wright, A.D., and Sticher, O. 1990. A new polyhalogenated monoterpene from the red alga *Plocamium cartilagineum*. *Journal of Natural Products* **53**:1615-1618.
- Lerdau, M., Litvak, M., and Monson, R. 1994. Plant chemical defense: monoterpenes and the growth-differentiation balance hypothesis. *TREE* **9**: 58-61.
- Maliakal, S., Cheney, D.P., and Rorrer, G.L. 2001. Halogenated monoterpene production in regenerated plantlet cultures of *Ochtodes secundiramea*. *Journal of Phycology* **37**: 1010-1019.
- McConnell, O.J., and Fenical, W. 1978. Ochtodene and ochtodiol: novel polyhalogenated cyclic monoterpenes from the red seaweed *Ochtodes secundiramea*. *Journal of Organic Chemistry* **43**: 4238-4241.
- Naylor, S., Hanke, F.K., Manes, L.V., and Crews, P. 1983. XXX. *Prog. Chem. Nat. Prod.* **44**: 189.
- Paul, V.J., McConnell, O.J., and Fenical, W. 1980. Cyclic monoterpenoid feeding deterrents from the red marine alga *Ochtodes crockeri*. *Journal of Organic Chemistry* **45**: 3401-3407.
- Paul, V.J. Hay, M.E., Duffy, J.E., Fenical, W., and Gustafson, K. 1987. Chemical defense in the seaweed *Ochtodes secundiramea* (Montagne) Howe (Rhodophyta): effects of its monoterpenoid components upon diverse coral-reef herbivores. *Journal of Experimental Marine Biology and Ecology* **114**: 249-260.
- Puglisi, M.P., and Paul, V.J. 1997. Intraspecific variation in the red alga *Portieria hornemannii*: monoterpene concentrations are not influenced by nitrogen or phosphorus enrichment. *Marine Biology* **128**: 161-170.
- Qi, H., and Rorrer, G.L. 1995. Photolithotrophic cultivation of *Laminaria saccharina* gametophyte cells in a stirred-tank bioreactor. *Biotechnology and Bioengineering* **45**: 251-260.

Radmer, R.J. 1996. Algal diversity and commercial algal products. *BioScience* **46**: 263-270.

Rorrer, G.L., Mullikin, R., Huang, Y.M., Gerwick, W.H., Maliakal, S., and Cheney, D.P. Production of bioactive metabolites by cell and tissue cultures of marine macroalgae in bioreactor systems. 1999. In: *Plant Cell and Tissue Culture for the Production of Food Ingredients*, Fu et al., Ed., Kluwer Academic/Plenum: New York, pp 165-184.

Rorrer, G.L., Polne-Fuller, M., and Zhi, C. 1996. Development and bioreactor cultivation of a novel semi-differentiated tissue suspension derived from the marine plant *Acrosiphonia coalita*. *Biotechnology and Bioengineering* **49**: 559-567.

Rorrer, G.L., J. Modrell, C. Zhi, H.-D. Yoo, D.N. Nagle and W.H. Gerwick. 1995. Bioreactor seaweed cell culture for production of bioactive oxylipins. *Journal of Applied Phycology* **7**: 187-198.

Tucker and Rorrer, 2001. Bromoperoxidase activity in microplantlet suspension cultures of the macrophytic red alga *Ochtodes secundiramea*. *Biotechnology and Bioengineering* **74**: 389-395.

Wise, M.L., and Croteau, R. Monoterpene biosynthesis. 1999. In: *Comprehensive Natural Products*, S. Barton, K. Nakanishi, O.M. Cohn, and D.E. Cane, Ed., Elsevier: Amsterdam, pp 97-153.

Yamaura, T., Tanaka, S., and Tabata, M. 1989. Light-dependent formation of glandular trichomes and monoterpenes in thyme seedlings. *Phytochemistry* **28**: 741-744.

Zhi C., and Rorrer, G.L. 1996. Photolithotrophic cultivation of *Laminaria saccharina* gametophyte cells in a bubble-column bioreactor. *Enzyme and Microbial Technology* **18**: 291-299.

## 2. COMPOUND IDENTIFICATION

Identification of the compounds present in photobioreactor cultivated *O. secundiramea* microplantlets was critical for determining the factors affecting halogenated monoterpene production; GC-MS were performed to determine the molecular composition of halogenated monoterpenes. GC-MS analyses, supplemented with later NMR analyses described by Barahona and Rorrer (2003) were used to deduce the structure of halogenated monoterpenes that could be isolated by chromatographic methods.

### 2.1. MATERIALS AND METHODS

#### 2.1.1. Biomass Extraction

A 0.6 g fresh weight aliquot of plantlet tissue was added to a 100 mL mortar and pestle containing liquid nitrogen, and then ground until all the liquid nitrogen was evaporated. The ground plantlet tissue was weighed to a precision of  $\pm 0.1$  mg, then added to 2.0 mL dichloromethane (DCM, Mallinckrodt 4879, chromatography grade) containing  $50 \mu\text{g mL}^{-1}$  naphthalene (internal standard) within a 4.0 mL glass vial. The vial was sealed, vortexed for 3-5 seconds, and then allowed to stand at room temperature for 24 hours to ensure complete extraction. The vial contents were syringe filtered through a  $0.22 \mu\text{m}$  Teflon filter (Osmonics, Cameo 13F) and the dichloromethane extract was stored in a septum-capped vial at  $-20^\circ\text{C}$ . The dichloromethane extract sample was blown down to ca. 0.3 mL under nitrogen gas flow at room temperature to concentrate the sample for later gas chromatography analysis. The loss of naphthalene and myrcene during sample concentration was negligible.

### 2.1.2. GC-MS Analysis

Prior to gas chromatography - mass spectrometry (GC-MS) analysis, 0.3 mL aliquots of the dichloromethane extract were passed through a Pasteur pipette packed with SilicAR (Mallinckrodt) granular silica gel. Nonpolar monoterpenes and halogenated monoterpenes were adsorbed on the Silicar, whereas more polar compounds, including photosynthetic pigments and alcohols, passed through. Adsorbed monoterpenes, halogenated monoterpenes, the naphthalene internal standard, and other nonpolar compounds were eluted with 1.0 mL ether (Sigma-Aldrich ACS Grade, 0.0001% BHT stabilizer). Samples for gas chromatography analysis with flame-ionization detection (GC-FID) were not SilicAR-cleaned prior to analysis.

The SilicAR-cleaned dichloromethane extracts were analyzed by GC-MS using a Hewlett Packard 6890 gas chromatograph and quadrupole mass selective detector. Compounds were profiled on a 30 m by 0.25 mm Zebron ZB-5 capillary column (Phenomenex, 5% phenyl- 95% dimethylpolysiloxane film, 0.25  $\mu\text{m}$  thickness) under the following temperature program: injector temperature 250 °C, column temperature 50 °C initial, 20 °C  $\text{min}^{-1}$  ramp to 300 °C, 1.0 min hold at 300 °C, 40 °C  $\text{min}^{-1}$  ramp to 320 °C, 2.0 min hold at 320 °C. The carrier gas flowrate through the column was 0.7 mL  $\text{min}^{-1}$  at 3.3 psi column head pressure. The ionization voltage of the MS detector was 70 eV. Sample injection volume was 1.0  $\mu\text{L}$ . All reported mass spectra were obtained from the scan taken at the apex of the chromatographic peak corresponding to a given compound. The reported relative signal intensity for a given mass fragment was not averaged from several scans nor subtracted from the baseline abundance signal.



## 2.2. RESULTS AND DISCUSSION

### 2.2.1. GC-MS

The dichloromethane (DCM) extract from the photobioreactor cultured *O. secundiramea* plantlets was rich in halogenated monoterpenes. Gas chromatography (GC) profiles of a representative DCM extract using both TIC and FID modes of detection are presented in Figure 2-1. Mass spectral data from selected peaks profiled by GC-TIC are presented in Tables 2-1 and 2-2. The peak at 4.63 min retention time on GC-TIC was myrcene, C<sub>10</sub>H<sub>16</sub>, an acyclic monoterpene with characteristic mass signals at  $m/z$  136 (parent molecular ion M<sup>+</sup>), 93 (M<sup>+</sup> less  $m/z$  43 C<sub>3</sub>H<sub>7</sub> fragment), and  $m/z$  69 (C<sub>5</sub>H<sub>9</sub> fragment). No other monoterpenes were detected, even in trace amounts. Compounds labeled A-J contained chlorine and/or bromine and possessed MS fragmentation patterns characteristic of halogenated monoterpenes. Compounds A-D (Table 2-1) were present in sufficient amounts for quantification, whereas compounds E-J (Table 2-2) were present in only trace amounts, as shown in Figure 2-2. The M-X fragments (X = halogen) provided the key mass signals for compound identification. Furthermore, the mass fragmentation pattern of each halogenated monoterpene reflected the natural isotopic abundance of bromine (50.54 % <sup>79</sup>Br, 49.46% <sup>81</sup>Br), and chlorine (75.53% <sup>35</sup>Cl, 24.47% <sup>37</sup>Cl). For example, compound C, which possesses one Br and one Cl atom, has three permutations for its molecular formula: 248 (<sup>79</sup>Br and <sup>35</sup>Cl), 250 (<sup>81</sup>Br and <sup>35</sup>Cl, or <sup>79</sup>Br and <sup>37</sup>Cl), and 252 (<sup>81</sup>Br and <sup>37</sup>Cl). The ratio of molecular species 248, 250, and 252 by isotopic abundance was 1.0:1.6:0.6 calculated versus 1.0:1.4:0.4 measured from their relative mass signal intensities.

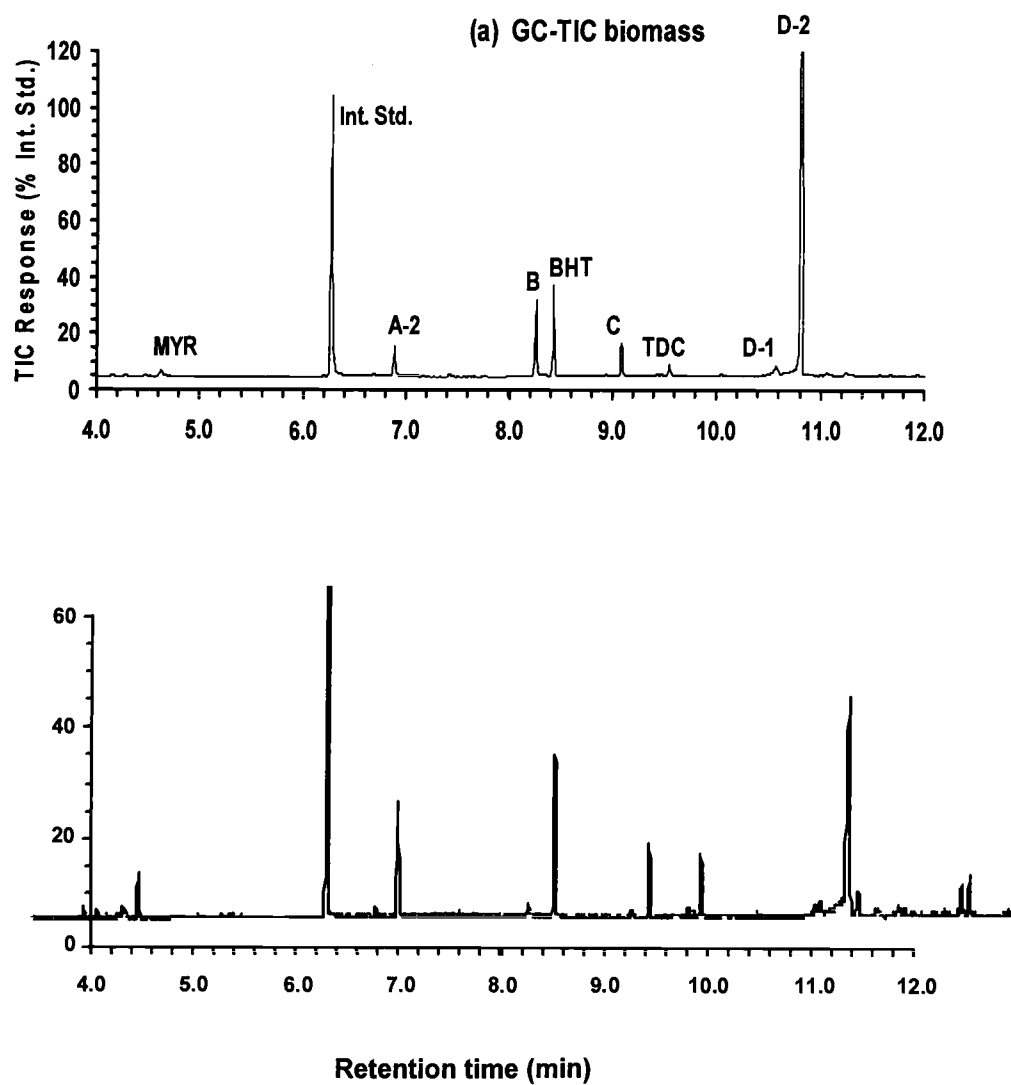
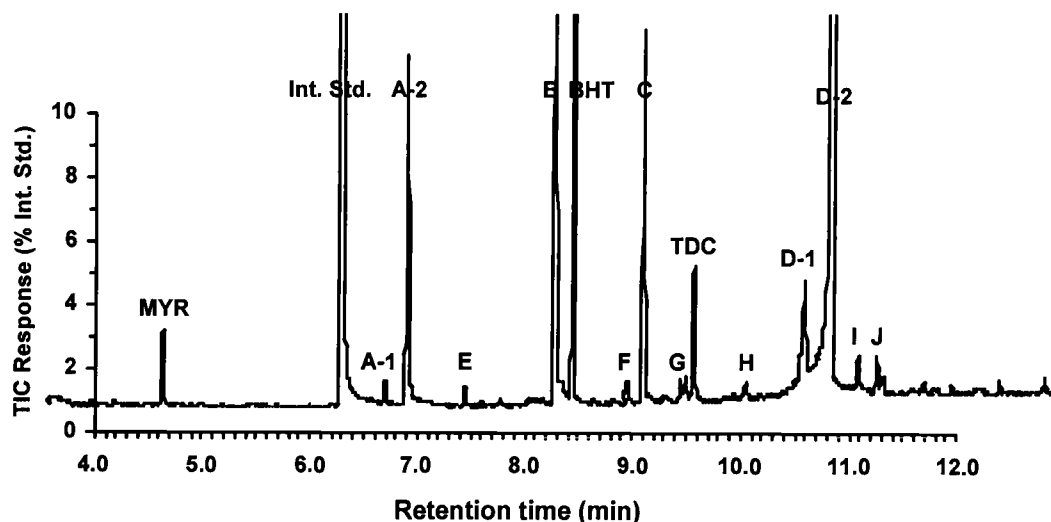


Figure 2-1. GC-TIC (a) and GC-FID (b) plots of DCM extracts of *Ochtodes secundiramea* microplantlets



**Figure 2-2. GC-TIC plots of DCM extracts of *Ochtodes secundiramea* microplantlets showing trace compounds E-J**

### 2.2.2. NMR Analysis

NMR analysis was performed on compounds B and D-2. Methods and results are presented in Barahona and Rorrer (2003). Briefly, the DCM crude extracts were profiled on a C18 reverse phase HPLC column at 22°C.  $^1\text{H}$  and  $^{13}\text{C}$  NMR spectra were obtained on a Bruker AM400 FT-NMR, with  $\text{CDCl}_3$  as the solvent.

### 2.2.3. Halogenated Monoterpene Structure Determination

All acyclic compounds were derived from the myrcene template, whereas all cyclic compounds were based on the ochtodane ring template, as shown in Figure 2-3.

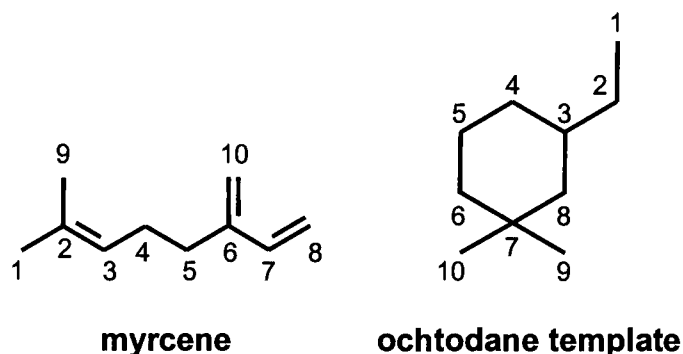


**Figure 2-3. Myrcene and ochtodane carbon backbone templates**

Several of the compounds shown in Table 2-1 from the photobioreactor cultured *O. secundiramea* plantlets had mass spectra consistent with halogenated monoterpenes previously reported in field collections of *Portieria hornemannii*. Both *Ochtodes* and *Portieria* are in the family of Rhizophyllidaceae. Compounds A-1 and A-2 are the *Z* and *E* stereoisomers of 10-bromomyrcene ( $C_{10}H_{15}Br$ ), respectively, found previously in *P. hornemannii*. The *Z* and *E* configurations are distinguished by characteristic differences in their relative signal intensities at  $m/z$  of 93, 135 and 171/173 (Ichikawa et al., 1974). Compound B is a BrCl product of myrcene, which possess characteristic mass fragments at  $m/z$  133, 169/171, and 248/250/252. Four BrCl isomers of myrcene were found previously in *P. hornemannii* (Ichikawa et al. 1974). NMR analysis of isolated compound B identified it as 3-chloro-10*E*-bromomyrcene; details of structural elucidation are provided by Barahona and Rorrer (2003). Compound C is most likely an isomer of dibromomyrcene, which has not been previously identified in field collections of either *Portieria* or *Ochtodes* species.

NMR analysis of isolated compound D-2 identified it as the cyclic monoterpene, Apakaochtodene B, 6(*S*<sup>\*</sup>)-bromo-1,4 (*S*<sup>\*</sup>),8(*R*<sup>\*</sup>)-trichloro-2(*E*)-

ochtodene; details of structural elucidation are provided by Barahona and Rorrer (2003). Interestingly, none of the halogenated monoterpenes shown in Table 2-1 matched any of those found in field-collected specimens of *Ochtodes secundiramea*, where the dominant compounds were cyclic halogenated monoterpenes based on the ochtodane ring template, including ochtodene, ochtodiol, chondrocole A (McConnel and Fenical, 1978), and 2-chloro-1,6,8-tribromo-3,8-ochtodene (Gerwick, 1984). Figure 2-4 presents the probable molecular structure for compounds A-D.

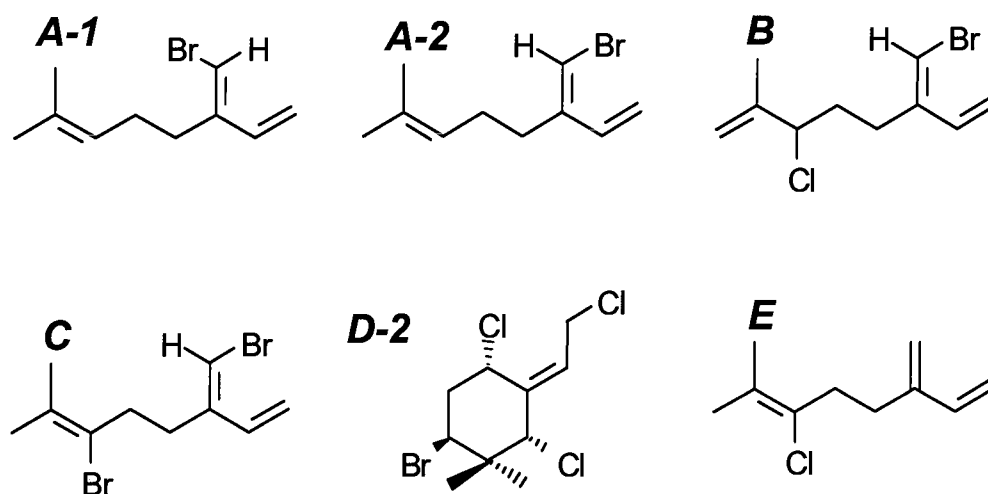


**Figure 2-4. Probable structures for dominate halogenated monoterpenes extracted from *Ochtodes secundiramea* microplantlets**

Halogenated monoterpenes labeled E-J were present in only trace amounts. Compound E is either chloromyrcene ( $C_{10}H_{15}Cl$ ) or its derivative  $C_{10}H_{16}Cl$ . Compound F is most likely Chondrocole A, found previously in *P. hornemannii* (Burreson et al., 1975) and *Ochtodes* species (McConnell and Fenical, 1978; Paul et al., 1980) with characteristic  $m/z$  at 185/187 and 149.

**Table 2-1. Dominant Halogenated Monoterpenes in Dichloromethane Extracts of Photobioreactor Cultivated *O. secundiramea* Microplantlets**

Label	Retention Time (min)		Characteristic Mass Signals ( <i>m/z</i> )				Mol. Formula (cyclization)	Mol. Weight
	TIC	FID (a)	100% peak	M-C <sub>3</sub> H <sub>7</sub> (43), M-CH <sub>3</sub> (15)	M-X	M+		
MYR	4.63	4.44	93	93(100) (Myr-43)		136(5)	C <sub>10</sub> H <sub>16</sub> (acyclic)	136.24
A-1	6.7	6.75	69	171(15), 173(19) (M-43) 93(25) (Myr-43)	135(23) X=Br	n.d.	C <sub>10</sub> H <sub>15</sub> Br (acyclic)	136.24
A-2	6.89	6.96	69	171(10), 173(10) (M-43) 93(70) (Myr-43)	135(36) X=Br	214(1) 216(1)	C <sub>10</sub> H <sub>15</sub> Br (acyclic)	215.13
B	8.28	8.5	133		133(100) X=Br+Cl+H 169(79), 171(27) X=Br 213(6), 215(6) X=Cl	248(10) 250(14) 252(4)	C <sub>10</sub> H <sub>14</sub> BrCl (acyclic)	249.58
C	9.09	9.41	133	171(2), 173(2) (M-Br-43+H) 197(12), 199(12) (M-Br-H-CH <sub>3</sub> ) 277(7), 279(12), 281(7) (M-CH <sub>3</sub> )	133(100), X=2Br+H 213(11), 215(12), X=Br	292(13) 294(26) 296(11)	C <sub>10</sub> H <sub>14</sub> Br <sub>2</sub> (acyclic)	294.03
D-1	10.6	11.1	203		167(69), 169(32) X=Br+2Cl	318(0.4) 320(1.1)	C <sub>10</sub> H <sub>14</sub> BrCl <sub>3</sub>	320.49
D-2	10.8	11.3			203(100), 205(64) X=Br+Cl+H 239(34), 241(32), 243(11) X=Br 283(5), 285(9), 287(4) X=Cl	322(0.7) (cyclic)		

(a)  $RT_{FID} = 1.113 \cdot RT_{TIC} - 0.709$

**Table 2-2. Trace Halogenated Monoterpenes in Dichloromethane Extracts of Photobioreactor Cultivated *O. secundiramea* Microplantlets**

Label	Retention		Characteristic Mass Signals ( <i>m/z</i> )					Mol. Formula	Mol. Weight
	Time (min)								
	TIC	FID	100% peak	M-C3H7 (43), M-CH <sub>3</sub> (15)	M-X	M+			
E	7.42	7.55	69	93(47) (Myr-43) 128(10) (M-43)	135(41), X = Cl	171(11) 173(8)	C <sub>10</sub> H <sub>15</sub> Cl or C <sub>10</sub> H <sub>16</sub> Cl	170.68 or 171.69	
F	8.94	9.24	229		149(20) X=Br+Cl+H 185(53), 187(22) X=Br 229(100), 231(98) X=Cl	264 (trace)	C <sub>10</sub> H <sub>14</sub> OBrCl	265.58	
G	9.48	9.84	69	93(38) (Myr-43)	133(80) X=2Br+Cl+2H 169 (42), 171(32) X=2Br+H 213(13), 215(19) X=Br+Cl+H 249(18), 251(26), 253(5) X = Br	328(4) 330(4)	C <sub>10</sub> H <sub>15</sub> Br <sub>2</sub> Cl	330.49	
H	10.1	10.5	203	239(33) (M-43)	167(65), 169(33) X=Br+Cl+H 203(100), 205(73) X=Br	284(12) 286(5)	C <sub>10</sub> H <sub>13</sub> Br Cl <sub>2</sub>	285.03	
I	11.1	11.6	249		167(90), 169(36) X=2Br+Cl+2H 203(33), 205(40) X=2Br+H 247(79), 249(100) X=Br+Cl+H 283(34), 285(44), 287(24) X=Br	362(6) 364(9) 366(5)	C <sub>10</sub> H <sub>14</sub> Br <sub>2</sub> Cl <sub>2</sub>	364.94	
J	11.3	11.8	91		211(36), 213(43) X=2Br+Cl+2H 247(47), 249(58) X=2Br+H 291(22), 293(39) X=Br+Cl+H 327(19), 329(31), 331(22) X=Br	408(11) 410(11)	C <sub>10</sub> H <sub>14</sub> Br <sub>3</sub> Cl	409.39	

### 2.3. REFERENCES

Barahona, L.F., and Rorrer, G.L. 2003. Isolation of halogenated monoterpenes from bioreactor-cultured microplantlets of the macrophytic red-algae *Ochtodes secundiramea* and *Portieria hornemannii*. *Journal of Natural Products* 66: 743-751.

Burreson, B.J., Woolard, F.X., and Moore, R.E. 1975. Evidence for the biogenesis of halogenated myrcenes from the red alga *Chondrococcus hornemannii*. *Chemistry Letters*: 1111-1114.

Gerwick, W.H. 1984. 2-Chloro-1,6(S\*),8-tribromo-3-(8)(Z)-ochtodene: a metabolite of the tropical red seaweed *Ochtodes secundiramea*. *Phytochemistry* **23**: 1323-1324.

Ichikawa, N., Naya, Y., and Enomoto, S. 1974. New halogenated monoterpenes from *Desmia (Chondrococcus) hornemanni*. *Chemistry Letters*: 1333-1336.

McConnell, O.J., and Fenical, W. 1978. Ochtodene and ochtodiol: novel polyhalogenated cyclic monoterpenes from the red seaweed *Ochtodes secundiramea*. *Journal of Organic Chemistry* **43**: 4238-4241.

Paul, V.J., McConnell, O.J., and Fenical, W. 1980. Cyclic monoterpenoid feeding deterrents from the red marine alga *Ochtodes crockeri*. *Journal of Organic Chemistry* **45**: 3401-3407.



### 3. NUTRIENT DELIVERY

Nutrient delivery cultivations were performed to evaluate the application of the growth-differentiation balance hypothesis to secondary metabolite production in *O. secundiramea* microplantlets. Forcing the cultivation conditions to low or high nutrient concentrations, while maintaining high levels of photosynthate, dictated the decisions for cultivation conditions. Efforts were made to maintain all cultivation parameters near or above saturation levels, so that the level of nutrients delivered could be isolated as the only independent variable. The nutrient concentrations varied from 5X to 0.05X stock cultivation conditions. Nitrate and phosphate levels were measured and oxygen evolution analysis was performed to assess the metabolic activity of the culture. The effects of nutrient delivery rate on the growth and halogenated monoterpene yield of *O. secundiramea* microplantlets were determined.

#### 3.1. MATERIALS AND METHODS

##### 3.1.1. Culture Maintenance

Plantlets of the macrophytic tropical red alga *Ochtodes secundiramea* (Montagne) Howe (Cryptonemiales, Rhizophyllidaceae) were established by callus induction and shoot tissue regeneration techniques developed in our previous work (Huang et al., 1998; Maliakal et al., 2001). The microplantlets were maintained on natural seawater (Hatfield Marine Science Center, Newport, Oregon) and supplemented with ESS nutrients (Kitade et al., 1996) adjusted to pH 8.0 with NaOH. Natural seawater was sterile filtered on a 0.2  $\mu\text{m}$  filter (cellulose acetate, Corning 430626), whereas 100X ESS nutrient stock solutions were autoclaved (121

°C and 15 psig for 30 min). The final composition of ESS nutrients in the natural seawater base medium used in this study was: 0.706 mM NaNO<sub>3</sub>; 0.037 mM K<sub>2</sub>HPO<sub>4</sub> · 3H<sub>2</sub>O; 0.0109 mM EDTA Fe-Na salt; 0.384 mM Na-HEPE buffer; 0.060 μM KI; 0.0032 μM ZnCl<sub>2</sub>; 0.0291 μM MnCl<sub>2</sub> · 4H<sub>2</sub>O; 0.00067 μM CoCl<sub>2</sub> · 6H<sub>2</sub>O; 0.00725 μM FeCl<sub>3</sub> · 6H<sub>2</sub>O; 0.0967 μM Na<sub>2</sub>EDTA · 2H<sub>2</sub>O; 0.738 μM H<sub>3</sub>BO<sub>3</sub>; 0.00074 μM vitamin B<sub>12</sub>; 0.00409 μM biotin (C<sub>10</sub>H<sub>16</sub>N<sub>2</sub>O<sub>3</sub>S); 0.296 μM thiamine-HCl; 0.812 μM nicotinic acid; 0.420 μM DL-pantothenic acid hemi Ca salt; 0.0729 μM *p*-aminobenzoic acid; 5.55 μM meso-inositol; 0.793 μM thymine. Bromine (as KBr) and vanadium (as Na<sub>3</sub>VO<sub>4</sub>) were not added to the ESS nutrients used for maintenance culture. However, they were present in natural seawater. The average concentration of bromine in seawater is 0.81 mM (Fenical, 1975). The concentration of soluble vanadium, phosphorous, and nitrogen in North Pacific Ocean waters is nominally 40 nM, 3 μM, and 40 μM, respectively (Butler, 1998a).

Microplantlet suspension cultures of *O. secundiramea* were maintained in 500 mL Erlenmeyer bubbler flasks. At inoculation, each flask contained 0.5 g fresh weight tissue in 450 mL of ESS-natural seawater liquid medium. Sterile-filtered air was bubbled into each flask through a 6 mm diameter glass tube at 750 mL min<sup>-1</sup>. Bubble flask cultures were grown under cool-white fluorescent light at 100 μE m<sup>-2</sup> · s<sup>-1</sup>, 14 h light/10 h dark photoperiod and a temperature of 26 °C within an illuminated incubator. Microplantlets were sub-cultured every four weeks, with medium exchange every two weeks. Prior to subculture, visibly healthy (e.g. dark red) microplantlet suspensions from three 28 day old flasks were pooled, sterile-filtered on 100 μm nylon mesh, and rinsed with ESS-natural seawater medium. The filtered, rinsed tissue was loaded into a 500 mL glass vessel containing 500 mL of fresh ESS-natural seawater medium. The vessel was fitted with an Osterizer blender assembly (Sunbeam-Oster corporation) consisting of four pitched, stainless-steel blades. The vessel assembly was mounted onto an Osterizer blender, and the microplantlet suspension within the vessel was chopped up on the "grind"

setting for approximately 2 seconds. The blended biomass suspension was sterile-filtered on 100  $\mu\text{m}$  nylon mesh. The filtered tissue was sterile transferred with forceps into eight 450 mL bubbler flasks (ca. 0.5 g fresh tissue per flask), with each flask containing 450 mL of ESS-natural seawater medium.

At inoculation, the plantlets were typically about 3-5 mm in diameter. When the plantlets were cultivated as an agitated suspension in the bubbler flasks, the morphology of the plantlets consisted of branched shoot tissues emanating from a central thallus. About four weeks after subculture, the plantlets ultimately assumed a symmetrical, spherical shape of nearly 10 mm diameter, where several tiny shoots lined each branch.

### 3.1.2. Photobioreactor Design and Operation

The airlift photobioreactor design shown in Figure 3-1 was used for all cultivation experiments. Three identical bioreactors were fabricated. Process conditions are detailed in Table 3-1. The glass vessel was 50 cm in height, 7.6 cm inner diameter, with working volume of 2100 mL. The draft tube length was 25.4 cm and the inner diameter was 3.2 cm. The vessel jacket was connected to a temperature-controlled water circulation bath maintained at 26 °C. The illumination stage was equipped with four vertically mounted 15 W cool-white fluorescent lamps surrounding the glass vessel. The lamps were positioned 1.0 cm from the vessel surface to provide a uniform incident light intensity of  $140 \mu\text{E m}^{-2} \text{s}^{-1}$  at all points along the vessel surface. A timer set the lamps to 14 h on and 10 h off per day (14:10 LD photoperiod). Carbon dioxide ( $\text{CO}_2$ ) in the aeration gas served as the sole carbon source for biomass growth. House air was metered to  $630 \text{ mL min}^{-1}$ , passed through a 0.2  $\mu\text{m}$  Gelman autoclaved filter, and then bubbled through a sterilized humidifier before being introduced into the vessel through a 4.0

cm diameter glass frit of 40-60  $\mu\text{m}$  pore size. Supplemental  $\text{CO}_2$  gas from a  $\text{CO}_2$  tank was metered to  $2.0 \text{ mL min}^{-1}$  and then mixed with the inlet air stream. Dissolved  $\text{CO}_2$  speciates to bicarbonate ion ( $\text{HCO}_3^-$ ) in seawater above pH 7. The pH of the liquid medium within the bioreactor was set to 8.0 using procedures described previously (Rorrer et al., 1996). For aerated ESS-natural seawater medium containing 10.7 mM  $\text{NaHCO}_3$  buffer, the equilibrium pH was 8.0 at 354 Pa  $\text{CO}_2$  partial pressure in the aeration gas (3500 ppm  $\text{CO}_2$ ). Fresh medium with composition detailed in Table 3-2 was pumped into the bottom of the vessel by a precision peristaltic pump (Buchler, model 426-2000) at  $30\text{-}32 \text{ mL h}^{-1}$  to provide up to  $450 \text{ mL day}^{-1}$  total fresh medium during the 14 hour light phase of the 24 hour photoperiod. The medium outlet port kept the culture volume constant at 2100 mL, and a 125  $\mu\text{m}$  nylon mesh mounted on the medium outlet port retained the biomass within the vessel.

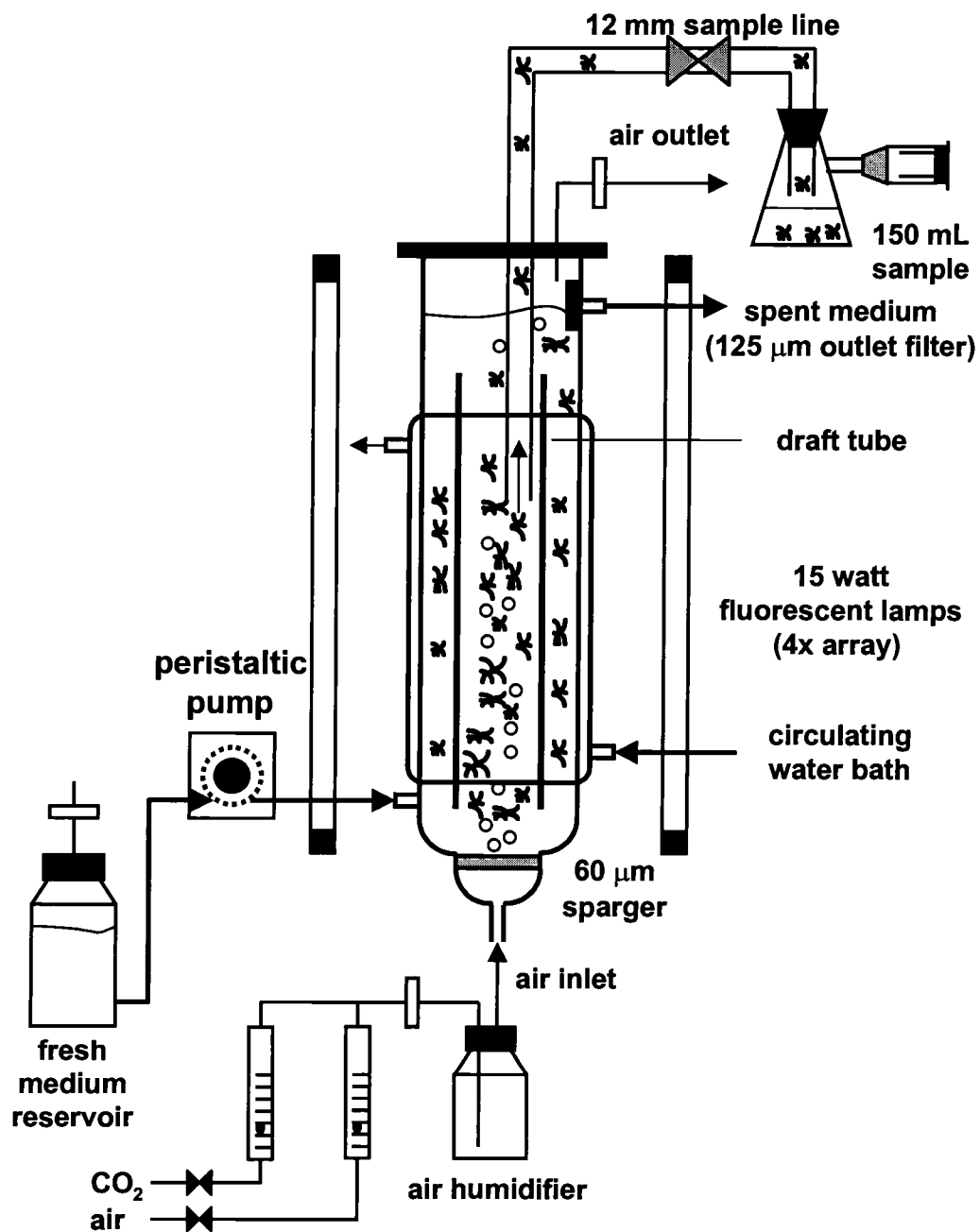


Figure 3-1. Schematic diagram of 2-L photobioreactor

The subculturing protocol described above was used to prepare the microplantlet tissue for bioreactor inoculation. The blended tissues were sterile-filtered, weighed under sterile conditions, and then re-suspended in 2100 mL of sterilized ESS-natural seawater medium and then loaded into the autoclaved vessel assembly (121 °C and 15 psig for 30 min) to provide a target inoculation density of 1.0 g FW L<sup>-1</sup>. The composition of the medium initially loaded into the bioreactor for a given cultivation experiment was identical to its perfusion medium composition detailed in Table 3-2. The microplantlet suspension was sampled at 2 to 5 day intervals, usually three hours into the light phase of the photoperiod. Culture samples were removed from the bioreactor suspension through a 13 mm inner diameter sampling tube (16 mm outer diameter) under sterile suction. The volume of each sample, typically 150 mL, was measured to precision of  $\pm 1$  mL.

**Table 3-1. Experimental Process Conditions for Nutrient Delivery Cultivations**

Process parameter	Nutrient Delivery Rate (mmol N L <sup>-1</sup> day <sup>-1</sup> )		
	0.735	0.0767	0.00628
Medium perfusion rate (mL day <sup>-1</sup> )	449	453	377
Working volume, $V$ (mL)	2121	2131	2100
Vessel inner diameter, $d_o$ (cm)	7.6	7.6	7.6
Draft tube inner diameter, $d_f$ (cm)	3.2	3.2	3.2
Aeration rate, $v_g$ (L min <sup>-1</sup> )	630	630	630
Aeration rate, $v_g / V$ (L air L <sup>-1</sup> min <sup>-1</sup> )	0.30	0.30	0.30
O <sub>2</sub> mass transfer, $k_L a$ (h <sup>-1</sup> )	66.3	33.9	33.9
CO <sub>2</sub> Partial pressure, (ppm)	3510	3510	3510
CO <sub>2</sub> -TR <sub>max</sub> (mmol CO <sub>2</sub> L <sup>-1</sup> h <sup>-1</sup> )	6.87	3.52	3.52
$n_{CO_2}$ (mmol CO <sub>2</sub> L <sup>-1</sup> h <sup>-1</sup> )	2.58	2.58	2.58
Setpoint pH	8.0	8.0	8.0
Average pH	8.0 ± 0.2	7.9 ± 0.2	7.8 ± 0.4
Culture removal rate, $v_f / V$ mL day <sup>-1</sup>	47.0	52.0	50.0
Incident light intensity, $I_o$ (μE m <sup>-2</sup> s <sup>-1</sup> )	143	138	138
Planes of illumination, $\alpha$	4	4	4
Photoperiod (h ON:h OFF LD)	14:10	14:10	14:10
Temperature (°C)	26	26	26
Final cultivation time (days)	30.0	29.0	36.0
Solids content (g DW g <sup>-1</sup> FW)			
Inoculation	22.70%	22.70%	21.50%
Final	34.50%	29.20%	35.10%
Initial plantlet density, $X_0$ (g DW L <sup>-1</sup> )	0.23	0.23	0.91
Final plantlet density, $X_0$ (g DW L <sup>-1</sup> )	9.68	4.67	1.55

**Table 3-2. Medium Composition for Nutrient Delivery Cultivations**

Parameter	Nutrient Delivery Rate (mmol N L <sup>-1</sup> day <sup>-1</sup> )		
	0.735	0.0767	0.00628
Inlet medium flowrate (mL day <sup>-1</sup> )	449	453	377
Perfusion rate (% per day)	21	21	18
ESS Nitrate (NaNO <sub>3</sub> ) conc. (mM) <sup>(a)</sup>	3.47	0.361	0.035
ESS Phosphate (K <sub>2</sub> HPO <sub>4</sub> ) conc. (μM) <sup>(a)</sup>	183	19	1.85
N:P (mol N: mol P)	19:1	19:1	19:1
ESS Bromide (KBr) conc. (mM) <sup>(a)</sup>	0.94	0.94	1.0
ESS Vanadate (Na <sub>3</sub> VO <sub>4</sub> ) conc. (μM) <sup>(a)</sup>	0.248	0.026	0.025
NaHCO <sub>3</sub> conc. (mM) <sup>(b)</sup>	10.7	10.7	10.7
ESS Micronutrient conc. (x base medium)	5	0.5	0.05

(a) Does not include levels present in natural seawater: 40 μM N, 3 μM P, 0.81 mM Br, 40 nM V

(b) The perfusion medium did not contain 0.384 mM Na-HEPE buffer

### 3.1.3. Cell Biomass, Nitrate and Phosphate

The suspension culture sample was vacuum-filtered on a 80 mL Buchner funnel. Microplantlets were gently blotted with a paper towel, transferred with forceps onto pre-weighed paper, and then weighed to precision of ± 1.0 mg to determine the fresh weight (FW). The plantlets were then transferred to a glass Petri dish, oven-dried at 80 °C for 24 h within a closed petri dish, and weighed again to precision of ± 0.1 mg to determine the dry weight (DW). The dried solids content was the ratio of dry weight to fresh weight. Total soluble nitrogen (as nitrate NO<sub>3</sub><sup>-</sup> and nitrite NO<sub>2</sub><sup>-</sup>) in the liquid sample was assayed spectrophotometrically at 530 nm with a LaMotte nitrate test kit (model NCR



3110). Free phosphate ( $\text{PO}_4^{-3}$ ) was assayed spectrophotometrically at 605 nm with a LaMotte standard phosphorous test kit (model VM-12 4408) after a color development time of 30 minutes. All nitrate and phosphate assays were performed in duplicate.

#### 3.1.4. GC-FID Analysis

DCM extracts were analyzed on a Hewlett Packard Model 5890 Series II gas chromatograph equipped with a FID detector. Compounds were profiled on a 30 m by 0.25 mm DB-5 capillary column (J&W Scientific, 5% phenyl-95% methyl silicone film, 0.25  $\mu\text{m}$  thickness) under the following temperature program: injector temperature 250 °C, column temperature 50 °C initial, 20 °C  $\text{min}^{-1}$  ramp to 300 °C, 1.0 min hold at 300 °C, 40 °C  $\text{min}^{-1}$  ramp to 320 °C, 7.0 min hold at 320 °C. The He carrier gas flowrate was 1.3  $\text{mL min}^{-1}$  and column head pressure of 16 psig. Sample injection volume was 2.0  $\mu\text{L}$ . The yield of a given compound ( $Y_i$ ) was calculated, by the internal standard method

$$Y_i = \frac{A_i R_{f,IS} m_{IS}}{A_{IS} R_{f,i} m_{DW}} \quad (3-1)$$

where  $A_i$  is the peak area of the compound,  $A_{IS}$  is the peak area of the internal standard,  $R_{f,i}$  is the response factor of the compound,  $R_{f,IS}$  is the response factor for the internal standard,  $m_{IS}$  is the mass of the internal standard,  $m_{DW}$  is the mass of dry tissue that was originally extracted.

The GC-FID response factors for halogenated monoterpenes were based on the myrcene response factor using well-established effective carbon number methods detailed by Grob (1995). The presence of halogen moieties did not have

significant effect on the GC-FID response factor for a given halogenated monoterpene, as demonstrated in Table 3-3 using decane, 1-bromodecane, and 1,10-dibromodecane as model C<sub>10</sub> compounds.

**Table 3-3. GC-FID Response Factors for Model C<sub>10</sub> Brominated Compounds**

Compound	Formula	Retention Time (min)	$R_{F,I} / R_{F,IS}$ $\pm 1.0$ s.e.
Napthalene	$C_{10}H_8$	6.28	1
Myrcene	$C_{10}H_{16}$	4.44	$0.947 \pm 0.017$
Decane	$C_{10}H_{22}$	4.54	$1.046 \pm 0.017$
1-bromodecane	$C_{10}H_{23}Br$	7.49	$0.996 \pm 0.025$
1,10-dibromodecane	$C_{10}H_{22}Br_2$	10.19	$0.986 \pm 0.025$

Aqueous samples were also extracted to determine if any compounds were released to the culture medium. Specifically, 10 mL of aqueous culture sample was extracted with 40 mL DCM at room temperature for 24 hours. The extract was blown down to dryness on ice under flowing  $N_2$ , and then re-suspended in 40  $\mu$ L DCM containing 50  $\mu$ g  $mL^{-1}$  naphthalene (250-fold concentration).

### 3.1.5. Specific Oxygen Evolution Rate

Measurements of the photosynthetic oxygen evolution rate (OER) for microplantlet samples obtained from the photobioreactor were performed using the apparatus and procedures described by Huang et al. (1998). The specific oxygen evolution rate ( $P_o$ ) was the OER normalized to the amount of equivalent dry

biomass loaded into the D.O. test cell. For a given microplantlet sample, the OER was measured at 26 °C with increasing incident light intensity ranging 0 to 400  $\mu\text{E m}^{-2} \text{s}^{-1}$ . OER values were expressed as net photosynthetic  $\text{O}_2$  evolution, accounting for dark phase  $\text{O}_2$  respiration.

### 3.1.6. Volumetric Oxygen Mass Transfer and $\text{CO}_2$ -TR

The volumetric mass transfer coefficient ( $k_La$ ) for interphase mass transfer of oxygen into 2100 mL of natural seawater liquid medium within the airlift photobioreactor vessel was determined by the dynamic gassing-in method at 26 °C. The tip of the YSI model 5750 D.O. electrode was placed 5 cm below the liquid surface. Dissolved oxygen in the liquid medium was removed by sparging with  $\text{N}_2$  through the sparger at a constant rate of 630  $\text{mL min}^{-1}$ . When the D.O. concentration reached 10% of air saturation, air was re-introduced through the sparger at 630  $\text{mL min}^{-1}$ . The value for  $k_La$  was estimated from the least-squares slope of the D.O. concentration vs. re-aeration time data on a semi-log scale. The  $k_La$  values were corrected for the D.O. electrode response time constant (5.2 sec). The maximum possible  $\text{CO}_2$  delivery was calculated in two ways. The interphase mass transfer rate of  $\text{CO}_2$ , defined by

$$\text{CO}_2 - \text{TR}_{\max} = k_La \sqrt{\frac{D_{\text{CO}_2}}{D_{\text{O}_2}}} \frac{P_{\text{CO}_2}}{H} \quad (3-2)$$

was determined, where  $H$  is Henry's law constant for  $\text{CO}_2$  in 35 ppt seawater at 25 °C (0.0339 atm  $\text{mM}^{-1}$ ),  $P_{\text{CO}_2}$  is the partial pressure of  $\text{CO}_2$  in the aeration gas (3500 ppm), and  $D_{\text{CO}_2} / D_{\text{O}_2}$  is the ratio of  $\text{CO}_2$  and  $\text{O}_2$  diffusion coefficients in seawater, equal to 0.93 (Raven, 1984). The  $\text{CO}_2$  delivered by the aeration gas, defined by

$$R_{CO_2} = CO_2 - TR_{\max} = \frac{v_g}{V} \frac{P_{CO_2}}{RT} \quad (3-3)$$

was also determined, where  $R$  is the gas constant,  $T$  is the temperature of the aeration gas,  $v_g$  is the volumetric flowrate of the aeration gas, and  $V$  is the culture volume. The  $CO_2$  delivery is typically limited by  $R_{CO_2}$  if the  $k_La$  is relatively high,  $v_g$  is relatively low, and the pH is above 8.0 where absorption of  $CO_2$  is enhanced by the speciation of  $CO_2$  to bicarbonate.

## 3.2. RESULTS AND DISCUSSION

### 3.2.1. Growth Data

Process conditions for cultivation of the *Ochtodes secundiramea* microplantlet suspension within the airlift photobioreactor are detailed in Table 3-1. Airlift operation was required to keep the microplantlets uniformly suspended within the vessel. All cultivations were carried out under continuous nutrient perfusion at the conditions detailed in Table 3-2. The concentration of nutrients in the perfusion medium was the manipulated variable. The volumetric flow rate was constant at 0.20 L medium L<sup>-1</sup> suspension day<sup>-1</sup>, and the N:P molar ratio in the perfusion medium was fixed at 19:1, which reflects the relative N and P content within red macroalgae (Atkinson and Smith, 1983). The perfusion medium was also supplemented with 1.0 mM Br<sup>-</sup> and 0.25 μM vanadate (VO<sub>4</sub><sup>-3</sup>) to flood the microplantlet suspension with bromination reagent and co-factor for vanadium-dependent bromoperoxidase, the putative bromination catalyst.

Biomass density profiles for cultivation of the *O. secundiramea* microplantlets in the perfusion airlift photobioreactor are presented in Figure 3-2. The nitrate and phosphate concentration profiles in the perfusion medium effluent are presented in Figures 3-3 and 3-4. Increasing the nutrient delivery rate from 0.0063 to 0.74 mmol N L<sup>-1</sup> day<sup>-1</sup> significantly enhanced biomass productivity. At a nutrient delivery rate of 0.74 mmol N L<sup>-1</sup> day<sup>-1</sup>, a plantlet mass density of 9.7 g DW L<sup>-1</sup> was obtained after 30 days of cultivation (Table 3-1).

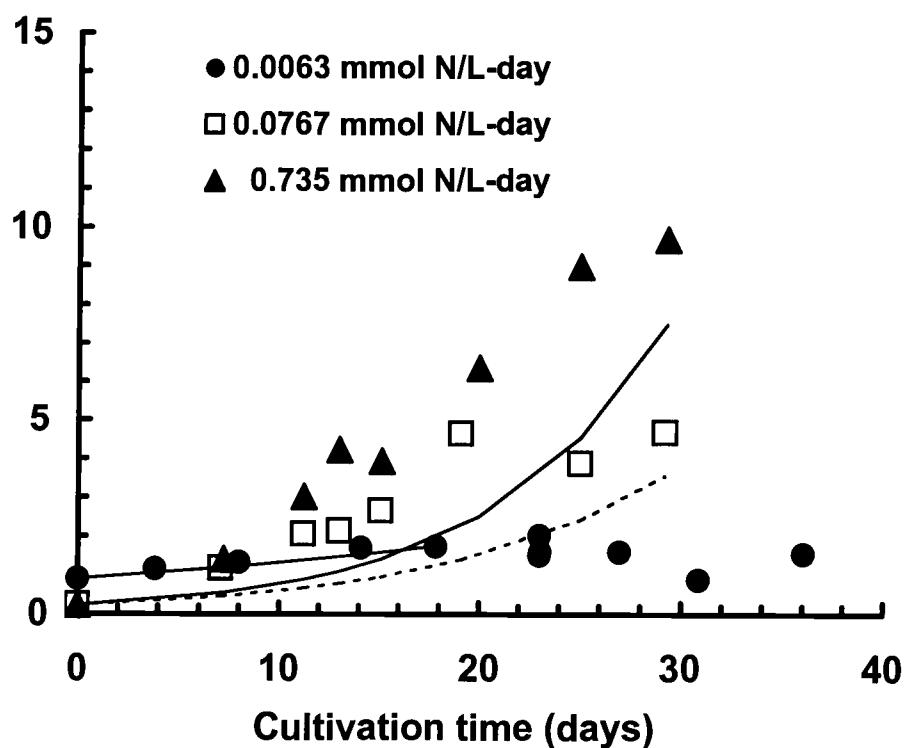


**Figure 3-2. Experimental and estimated biomass density profiles for nutrient delivery cultivations. Solid lines represent the biomass density profiles using a specific growth rate estimated from a least squares fit of the experimental biomass density data.**

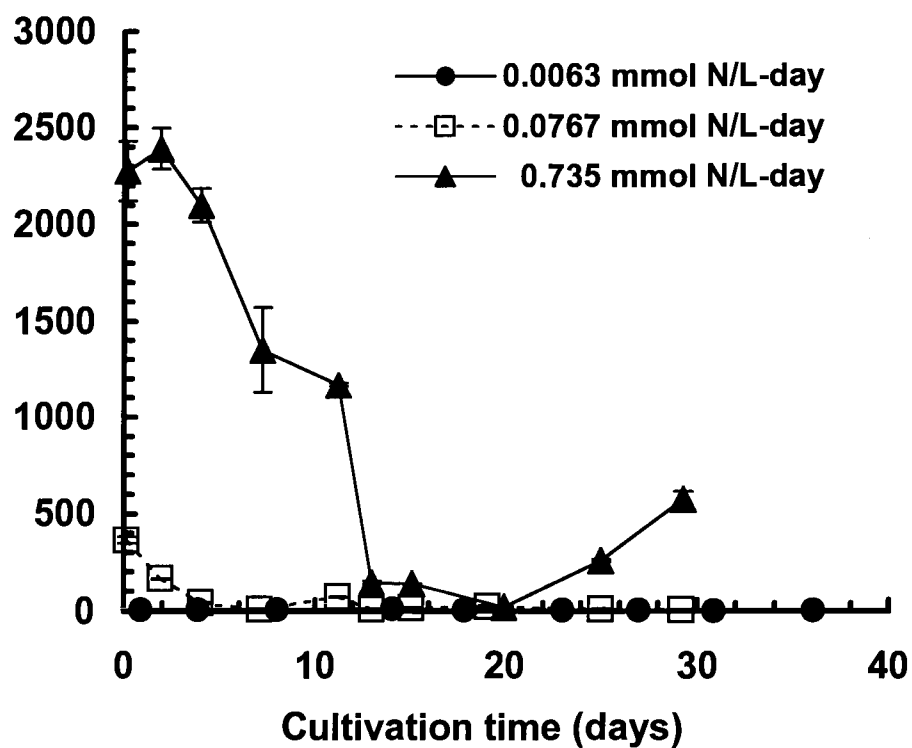


**Figure 3-3. Photobioreactor medium nitrate concentration profiles for nutrient delivery cultivations**



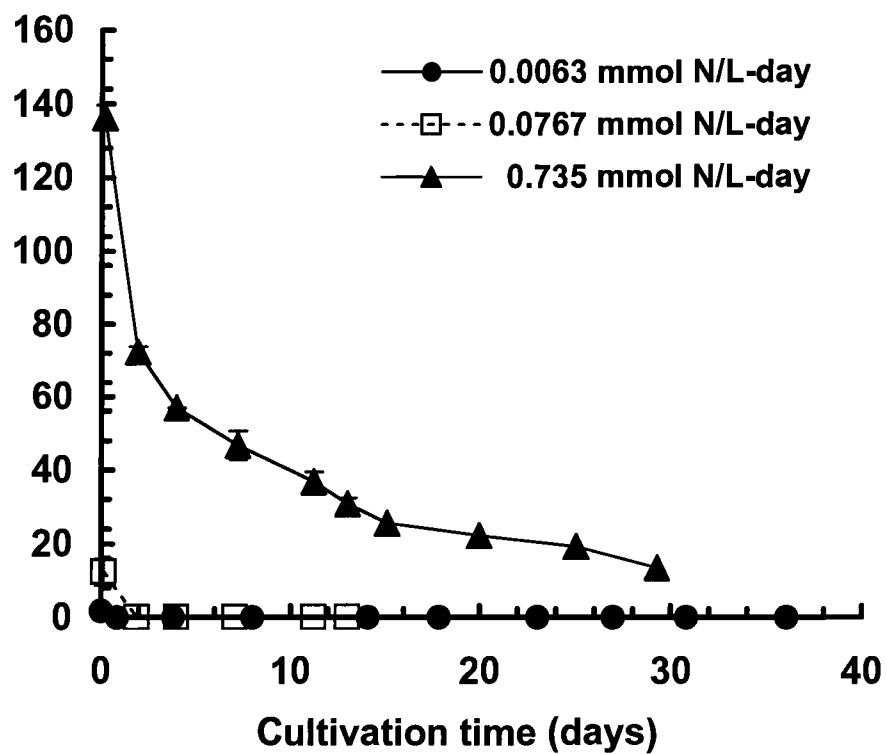


**Figure 3-4. Photobioreactor medium Phosphate Concentration Profiles for nutrient delivery cultivations**

The leveling off in plantlet density with time was due to microplantlet removal during sampling, which worked to dilute out the suspension during medium perfusion at a fixed 2100 mL culture volume. The volumetric suspension culture removal rate by sampling was nominally 50 mL per day (Table 3-1).

Biomass production rates were ultimately limited by the nutrient delivery rate. The nitrate and phosphate concentrations in the exiting medium went to zero as plantlet mass density increased. For the high nutrient delivery rate of  $0.74 \text{ mmol N L}^{-1} \text{ day}^{-1}$ , the culture growth was not nitrate limited until after 20 days of cultivation. However, at lower nutrient delivery rates, culture growth was macronutrient limited within the first seven days.

In red algae, significant amounts of nitrate are funneled into nitrogen-bearing photosynthetic pigments, including chlorophyll *a*, phycoerythrins and phycocyanins (South and Whittick, 1987). Furthermore, photosynthesis and nitrogen metabolism are integrally coupled (Turpin, 1991). Consequently, the photosynthetic oxygen evolution rate ( $P_o$ ,  $\text{mmol O}_2 \text{ g}^{-1} \text{ DW h}^{-1}$ ) of the microplantlets during photobioreactor cultivation was measured as function of nutrient delivery rate. Representative *P-I* curves of *O. secundiramea* microplantlets cultivated in the airlift photobioreactor at the high nutrient delivery rate of  $0.74 \text{ mmol N L}^{-1} \text{ day}^{-1}$  are presented in Figure 3-5, and the maximum photosynthetic rate at light saturation ( $P_{o,max}$ ) at nutrient delivery rates of 0.077 and  $0.74 \text{ mmol N L}^{-1} \text{ day}^{-1}$  are presented in Table 3-4. As expected,  $P_{o,max}$  decreased in response to the decrease in nutrient delivery rate. Furthermore,  $P_{o,max}$  decreased with increasing cultivation time, suggesting a decrease in the overall rate of primary metabolism as the microplantlet tissues increased in size.

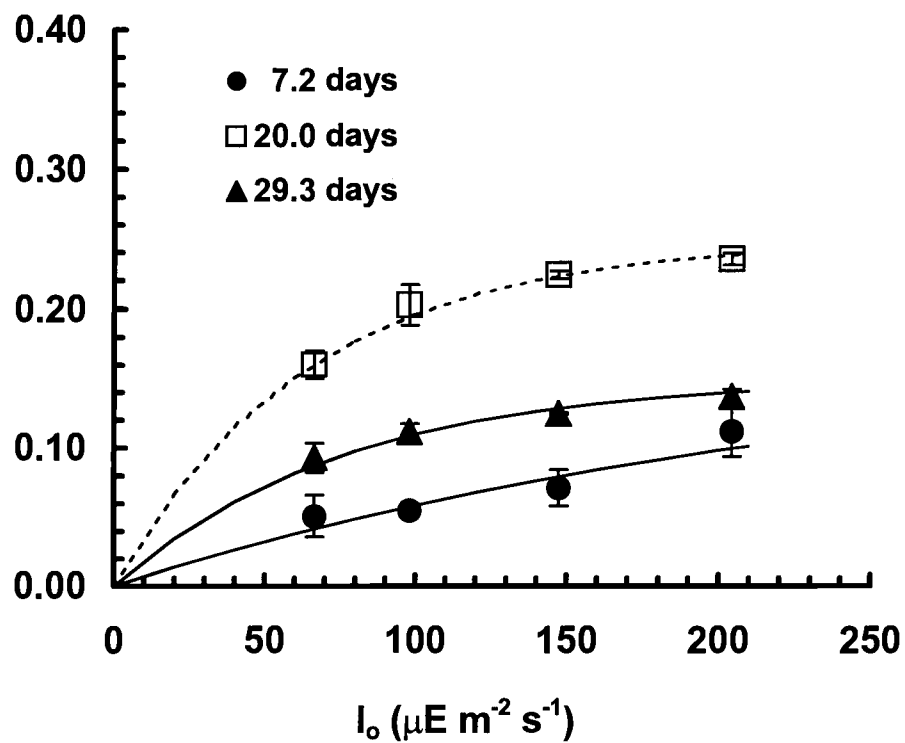


Figure 3-5. Net photosynthetic oxygen evolution rate vs. light intensity curves for nutrient delivery cultivation at  $0.74 \text{ mmol N L}^{-1} \text{day}^{-1}$

**Table 3-4. Photosynthetic Growth Parameters for Nutrient Delivery Cultivations** (all errors  $\pm 1$  s.e.)

Nutrient Delivery (mmol N L <sup>-1</sup> day <sup>-1</sup> )	Cultivation Time (days)	Plantlet Density, $X_{DW}$ (g DCW L <sup>-1</sup> )	$P_{o,max}$ (mmol O <sub>2</sub> g <sup>-1</sup> DCW h <sup>-1</sup> )	$Q_{CO_2}$ (mmol CO <sub>2</sub> L <sup>-1</sup> h <sup>-1</sup> )	$\mu'$ (day <sup>-1</sup> )
0.735	7.2	1.4	0.088 $\pm$ 0.0085	0.123	0.063
	20	6.34	0.242 $\pm$ 0.0073	1.537	0.175
	29.3	9.68	0.139 $\pm$ 0.0058	1.343	0.1
0.0767	7.1	1.18	0.055 $\pm$ 0.013	0.065	0.04
	19.1	4.63	0.026 $\pm$ 0.0041	0.119	0.018
	29.2	4.68	0.026 $\pm$ 0.0031	0.119	0.018
0.0063	23	1.55	0.0068 $\pm$ 0.0021	0.011	0.0049

The solids content of microplantlet tissue also increased during cultivation (Table 3-1), indicating that biomass production was moving from cell division to photosynthate accumulation. All of these observations suggest that the structured growth characteristics of the nonfriable microplantlet will ultimately limit the growth rate even if all other limiting factors are minimized.

The maximum specific growth rate during illumination ( $\mu'$ ) was estimated from the maximum oxygen evolution rate by

$$\mu' = P_{o,max} \cdot Y_{X/O_2} \quad (3-4)$$

where  $P_{o,max}$  is the specific  $O_2$  evolution rate at light saturation, and  $Y_{x/o_2}$  is the biomass yield coefficient based on  $O_2$  evolution, equal to 30 g DW mol<sup>-1</sup>  $O_2$  evolved. The highest observed  $\mu'$  was 0.175 day<sup>-1</sup> (Table 3-4).

The  $CO_2$  supplied by the aeration gas was the sole carbon source for photosynthetic biomass production. The potential for  $CO_2$  delivery limitations was addressed by comparing  $CO_2$ -TR<sub>max</sub> and  $R_{CO_2}$  to the volumetric  $CO_2$  consumption rate. A conservative estimate for the volumetric  $CO_2$  demand is given by

$$Q_{CO_2} = P_{o,max} \cdot X_{DW} \frac{v_{CO_2}}{v_{O_2}} \quad (3-5)$$

Assuming Calvin  $CO_2$  fixation stoichiometry,  $\frac{v_{CO_2}}{v_{O_2}}$  is equal to 1.0. Estimates for

$Q_{CO_2}$  shown in Table 3-4 were always less than the  $CO_2$ -TR<sub>max</sub> or  $R_{CO_2}$  values in Table 3-1, demonstrating that cultivation of the *O. secundiramea* microplantlets in the airlift photobioreactor was not limited by  $CO_2$  delivery. Light transfer limitations to growth resulting from absorption and scattering of photons through the suspension at high plantlet density were not quantitatively assessed by this study. However, as shown in Table 3-1, the incident light intensity to the photobioreactor vessel surface was set to 140  $\mu E\ m^{-2}\ s^{-1}$ , and light from four lamps was directed into the vessel.  $P$ - $I$  curves (Figure 3-5) show that growth was near the light saturation condition at this light intensity.

### 3.2.2. Halogenated Monoterpene Kinetic Data

Halogenated monoterpene content vs. cultivation time profiles in the photobioreactor cultivated *Ochtodes secundiramea* microplantlets are presented in Figures 3-6 to 3-11. Specific concentrations of myrcene and halogenated monoterpenes A-D were expressed as  $\mu\text{mole}$  of product in the dichloromethane extract per gram of equivalent dry cell mass extracted. In all experiments, compounds E-J were present in amounts too small for accurate quantification by GC-FID.

The nutrient delivery rate had a complex effect on the patterns of halogenated monoterpene production. Increasing the nutrient delivery rate from  $0.0063 \text{ mmol N L}^{-1} \text{ day}^{-1}$  to  $0.74 \text{ mmol N L}^{-1} \text{ day}^{-1}$  greatly increased the transient accumulation of myrcene and 10(*E*)-bromomyrcene. At a nutrient delivery rate of  $0.74 \text{ mmol N L}^{-1} \text{ day}^{-1}$ , the specific concentration of 10(*E*)-bromomyrcene peaked after 15 days of cultivation. The acyclic dihalogenated products,  $\text{C}_{10}\text{H}_{14}\text{BrCl}$  and  $\text{C}_{10}\text{H}_{14}\text{Br}_2$ , also peaked at this time. In contrast, at a lower nutrient delivery rate of  $0.077 \text{ mmol N L}^{-1} \text{ day}^{-1}$ , no significant accumulation of myrcene and 10(*E*)-bromomyrcene was observed, and the yield vs. time profiles of  $\text{C}_{10}\text{H}_{14}\text{BrCl}$  and  $\text{C}_{10}\text{H}_{14}\text{Br}_2$  paralleled those at the nutrient delivery rate of  $0.74 \text{ mmol N L}^{-1} \text{ day}^{-1}$ . Decreasing the nutrient delivery rate to  $0.0063 \text{ mmol N L}^{-1} \text{ day}^{-1}$  further decreased the specific concentration of all products. This cultivation was nutrient delivery limited during the 35 day cultivation period, and the yields of all compounds were essentially constant with time. The specific concentration vs. time profile for the cyclic halogenated monoterpene ( $\text{C}_{10}\text{H}_{14}\text{BrCl}_3$ ) apakaochtodene B, was maximized at the nutrient delivery rate of  $0.077 \text{ mmol N L}^{-1} \text{ day}^{-1}$ .

In all perfusion photobioreactor cultivation experiments, the Br and vanadate addition to the suspension culture was in significant stoichiometric excess

relative to the Br consumed by halogenated monoterpenes and the vanadate consumed by incorporation into bromoperoxidase.

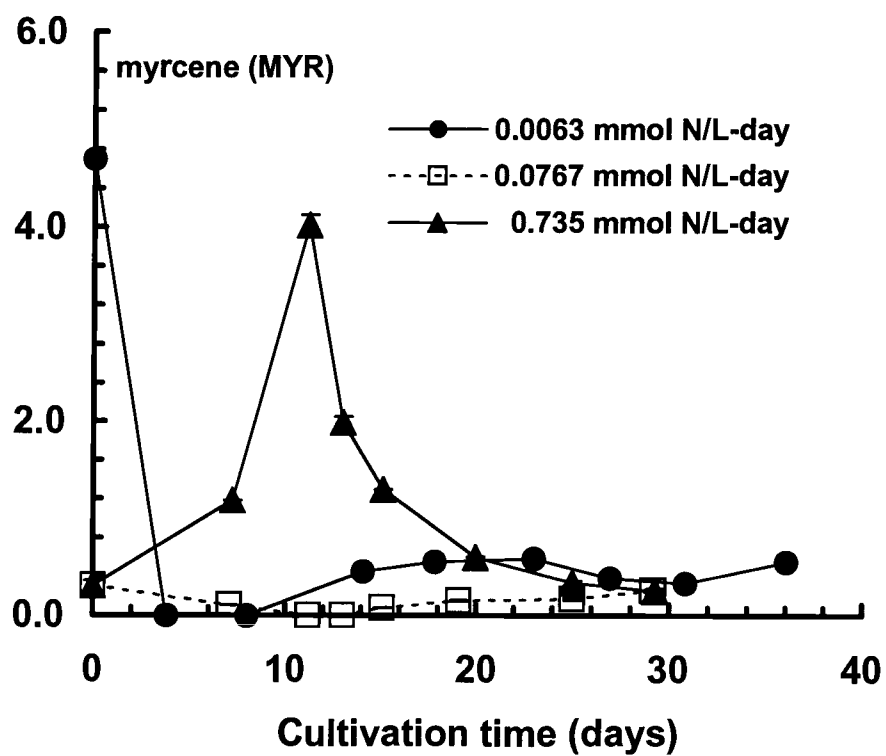


Figure 3-6. Myrcene profiles for nutrient delivery cultivations

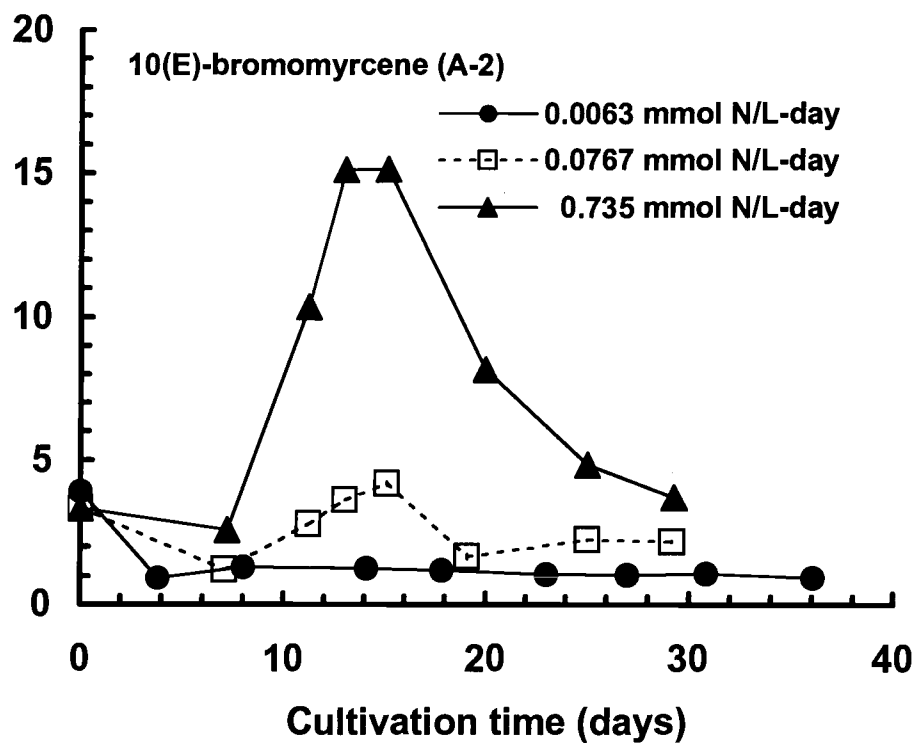
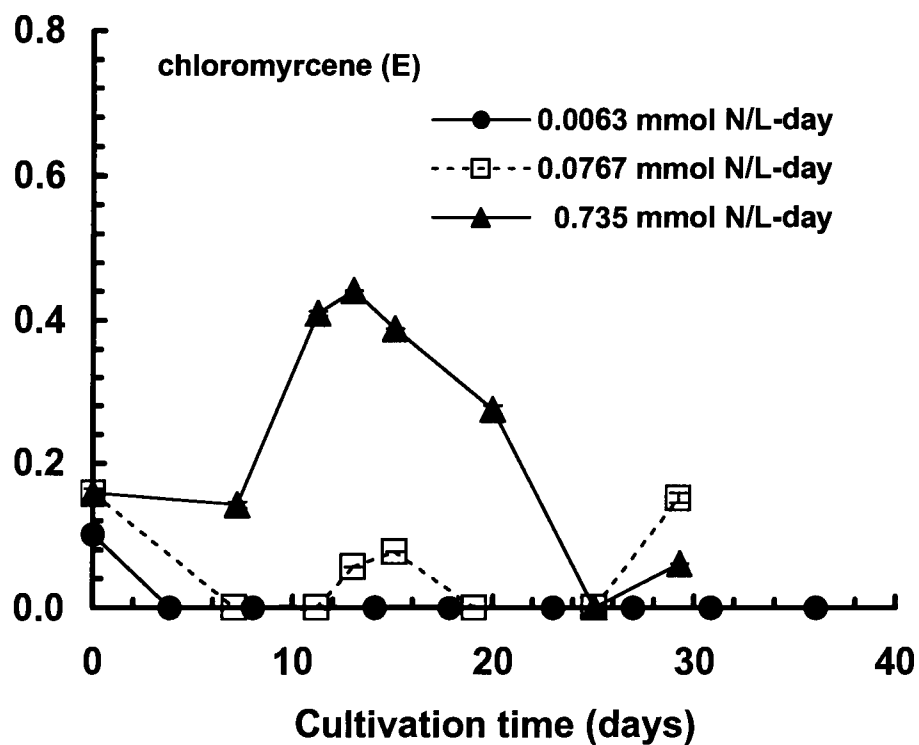
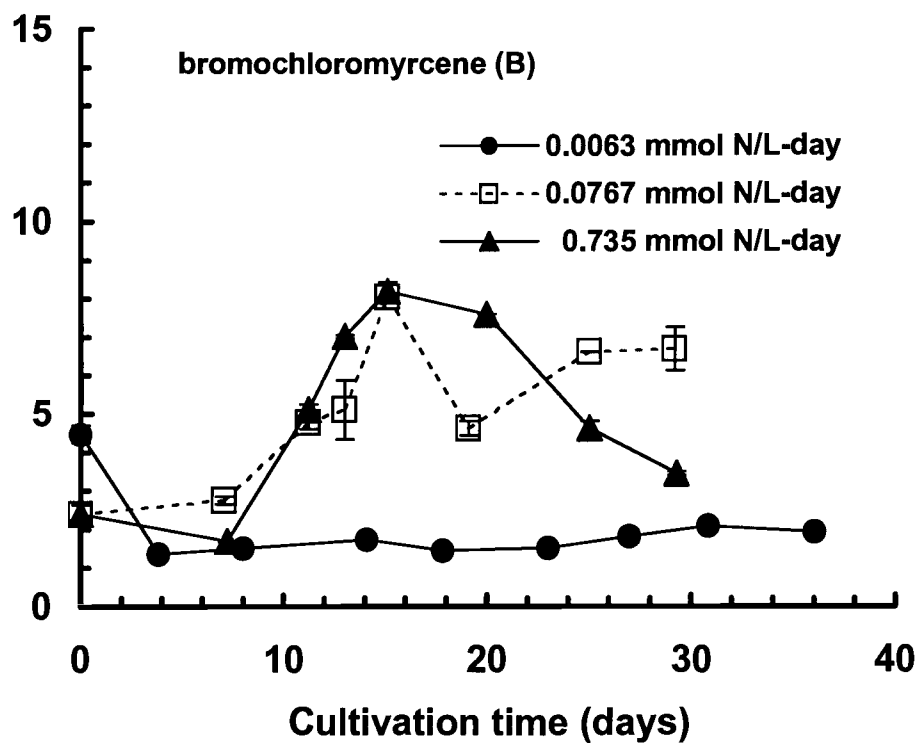


Figure 3-7. Compound A-2 (10(E)-bromomyrcene) profiles for nutrient delivery cultivations





**Figure 3-8. Compound E (chloromyrcene) profiles for nutrient delivery cultivations**



**Figure 3-9. Compound B (bromochloromyrcene) profiles for nutrient delivery cultivations**

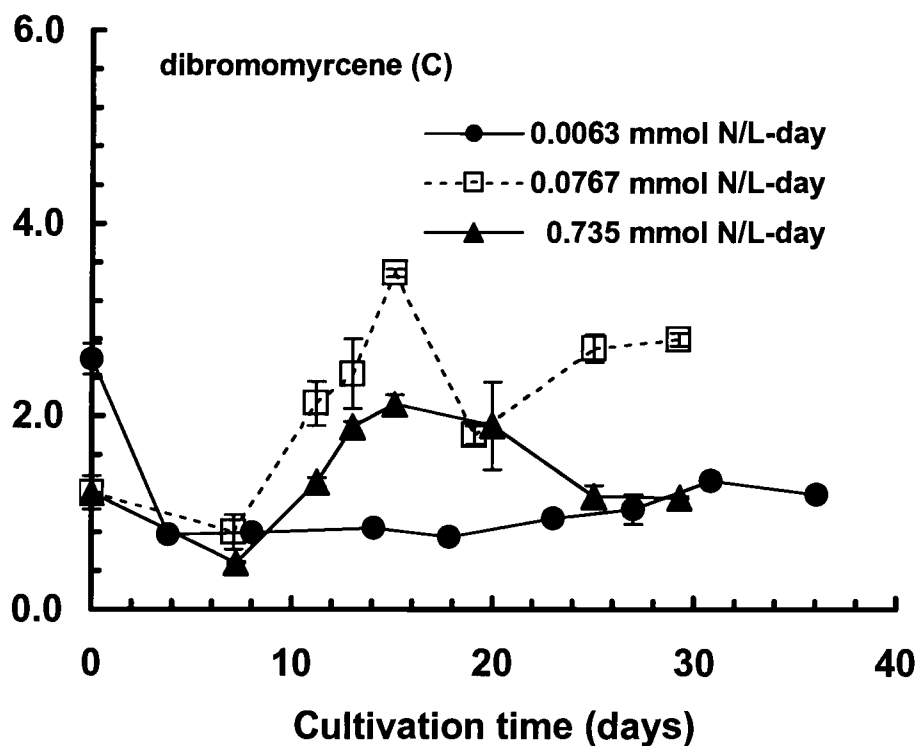
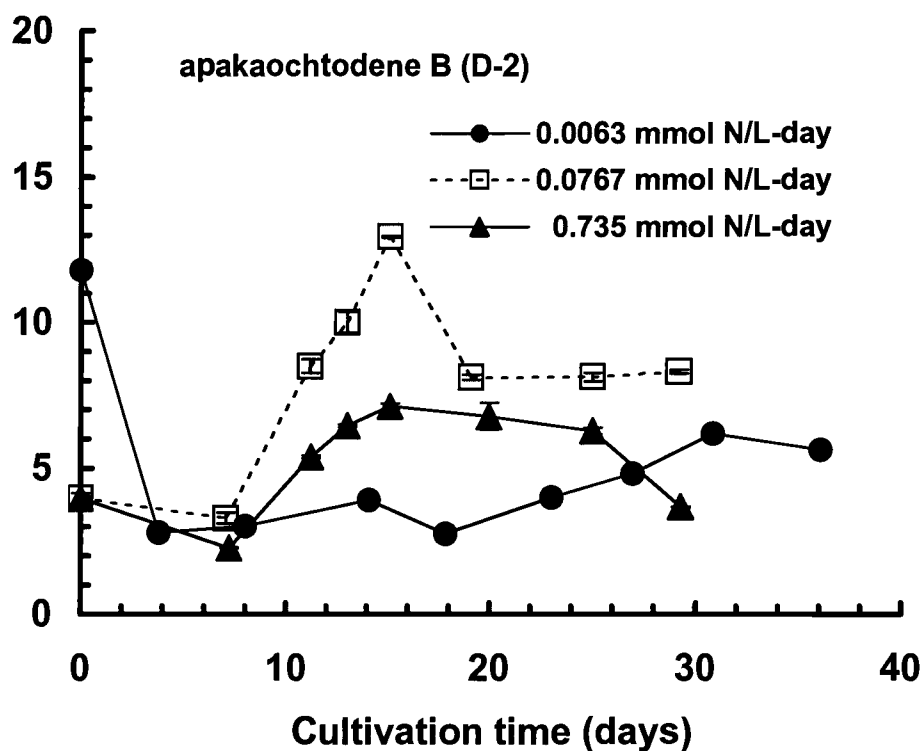


Figure 3-10. Compound C (dibromomyrcene) profiles for nutrient delivery cultivations



**Figure 3-11. Compound D-2 (apakauchtodene B) profiles for nutrient delivery cultivations**

### 3.2.3. Dynamic Growth Model

A growth model was developed which predicts biomass, nitrate and phosphate profiles of photobioreactor cultivated *Ochtophysa secundiramea* microplantlets under medium perfusion. A comparison will be made between predicted profiles and experimental data.

The differential balance on biomass is given by equation 3-6 subject to the following constraints:

1. Constant vessel volume
2. Well mixed liquid
3. Uniform biomass suspension
4. Culture growth not limited by CO<sub>2</sub> input
5. Isothermal process
6. Specific growth rate includes photoperiod

$$\mu X = \frac{dX}{dt} \quad (3-6)$$

where  $\mu$  (days<sup>-1</sup>) is the specific biomass growth rate, and  $X$  (g dry biomass L<sup>-1</sup>) is the biomass concentration. The differential balance on nitrate is

$$(C_{N,o} - C_N) \frac{\nu}{V} - \frac{\mu X}{Y_{X/N}} = \frac{dC_N}{dt} \quad (3-7)$$

where  $C_N$  (mmol N L<sup>-1</sup>) is the medium nitrate concentration,  $C_{N,o}$  is the inlet perfusion medium nitrate concentration,  $\nu$  (mL day<sup>-1</sup>) is the perfusion rate,  $V$  (L) is the vessel volume and  $Y_{X/N}$  (g dry biomass mmol N<sup>-1</sup>) is the yield coefficient of biomass on nitrate. The differential balance on phosphate is

$$(C_{P,o} - C_P) \frac{\nu}{V} - \frac{\mu X}{Y_{X/P}} = \frac{dC_P}{dt} \quad (3-8)$$

where  $C_p$  (mmol P L<sup>-1</sup>) is the medium phosphate concentration,  $C_{p,o}$  is the inlet perfusion medium phosphate concentration and  $Y_{x/p}$  (g dry biomass mmol P<sup>-1</sup>) is the yield coefficient of biomass on phosphate.

The specific growth rate is presumed to following a Monod model with respect to nutrient concentrations

$$\mu = \mu_{\max} \frac{C_N}{K_N + C_N} \frac{C_P}{K_P + C_P} \frac{I_m}{I_k + I_m} \quad (3-9)$$

where  $\mu_{\max}$  (days<sup>-1</sup>) is the maximum specific growth rate that would occur if all nutrients were above saturation levels,  $K_N$  (mmol N L<sup>-1</sup>) is the half saturation constant for nitrate,  $K_P$  (mmol P L<sup>-1</sup>) is the half saturation constant for phosphate,  $I_m$  (μE m<sup>-2</sup> s<sup>-1</sup>) is the mean light intensity, and  $I_k$  is the half saturation constant for light. The mean light intensity is given by

$$I_m = \frac{\alpha I_o}{k'd} (1 - e^{-k'd}) \quad (3-10)$$

where  $\alpha$  is the number of planes of light delivery,  $I_o$  (μE m<sup>-2</sup> s<sup>-1</sup>) is the light intensity incident to the vessel wall,  $d$  (m) is the diameter of the vessel and  $k'$  (m<sup>-1</sup>) is the light attenuation constant. The light attenuation constant quantifies the scattering and absorption effects that occur as light passes through the base medium containing biomass, and it is a linear function of biomass given by

$$k' = k_o + k_c X \quad (3-11)$$

where  $k_o$  ( $m^{-1}$ ) is the attenuation due to the cell free media and  $k_c$  ( $m^{-1}$  g dry biomass $^{-1}$ ) is the attenuation caused by the biomass.

Equations 3-6 to 3-11 were solved numerically by 4<sup>th</sup>-order Runge-Kutta integration using the parameters given in Table 3-5. The values for the biomass yield on nitrate,  $Y_{X/N}$ , was found by performing flask cultivation experiments in which the initial nitrate concentration was varied at excess phosphate concentration. The slope of a least squares linear fit of the biomass generated versus mass of nitrate consumed was used to calculate the yield. Experiments were not performed to estimate the biomass yield on phosphate,  $Y_{X/P}$ , rather the nitrate yield was multiplied by the N:P ratio of 19 for the seawater medium to determine the phosphate yield. The half saturation light intensity,  $I_k$ , was determined from a non-linear regression of P-I data presented in Figure 3-5 to Equation 5-5. The cell free attenuation,  $k_o$ , and the attenuation caused by biomass,  $k_c$ , were determined using the procedures of Huang and Rorrer (2002) and are described in section 5.1.3. The maximum specific growth rate,  $\mu_{max}$  was the highest value obtained from Equation 3-4 as detailed above in section 3.2.1. The profiles are presented in Figures 3-12 to 3-14.

**Table 3-5. Dynamic Model Estimation Parameters**

Model parameter	Value
Initial plantlet density, $X_0$ (g DW L <sup>-1</sup> )	0.23
Initial nitrate concentration, $C_{N,0}$ (mmol N L <sup>-1</sup> )	3.47
Initial phosphate concentration, $C_{P,0}$ (mmol P L <sup>-1</sup> )	0.183
Inlet nitrate concentration, $C_{N,i}$ (mmol N L <sup>-1</sup> )	3.47
Inlet phosphate concentration, $C_{P,i}$ (mmol P L <sup>-1</sup> )	0.183
Half saturation nitrate concentration, $C_{N,0}$ (mmol N L <sup>-1</sup> )	0.05
Half saturation phosphate concentration, $C_{P,0}$ (mmol P L <sup>-1</sup> )	0.01
Biomass yield on nitrate, $Y_{X/N}$ (g DW mmol N <sup>-1</sup> )	1.28
Biomass yield on phosphate, $Y_{X/P}$ (g DW mmol P <sup>-1</sup> )	25
Biomass yield on oxygen, $Y_{X/O_2}$ (g DW mmol O <sub>2</sub> <sup>-1</sup> )	30.6
Maximum specific growth rate, $\mu_{\max}$ (day <sup>-1</sup> )	0.18
Medium perfusion rate (mL day <sup>-1</sup> )	435
Working volume, $V$ (mL)	2121
Vessel inner diameter, $d_o$ (cm)	7.6
Incident light intensity, $I_o$ ( $\mu\text{E m}^{-2} \text{s}^{-1}$ )	143
Half saturation light intensity, $I_k$ ( $\mu\text{E m}^{-2} \text{s}^{-1}$ )	70
Planes of illumination, $\alpha$	4
Light attenuation of cell free media, $k_o$ (cm <sup>-1</sup> )	0
Light attenuation of biomass, $k_c$ (L g DW <sup>-1</sup> cm <sup>-1</sup> )	0.06
Photoperiod (h ON:h OFF LD)	14:10



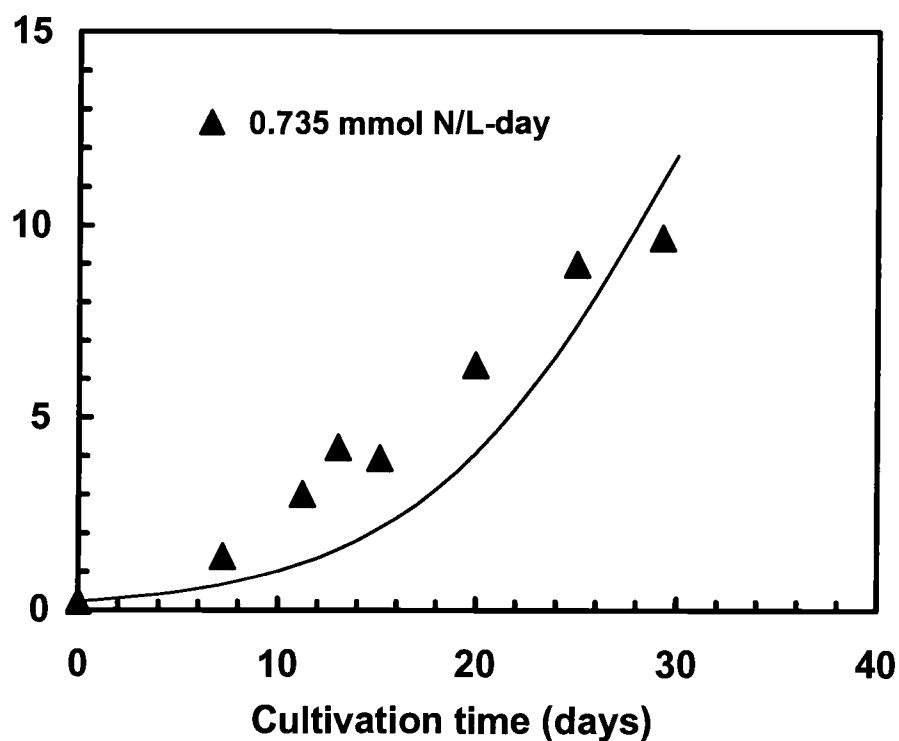


**Figure 3-12. Dynamic model prediction (solid line) and experimental data of biomass density for nutrient delivery cultivation at  $0.74 \text{ mmol N L}^{-1} \text{ day}^{-1}$**

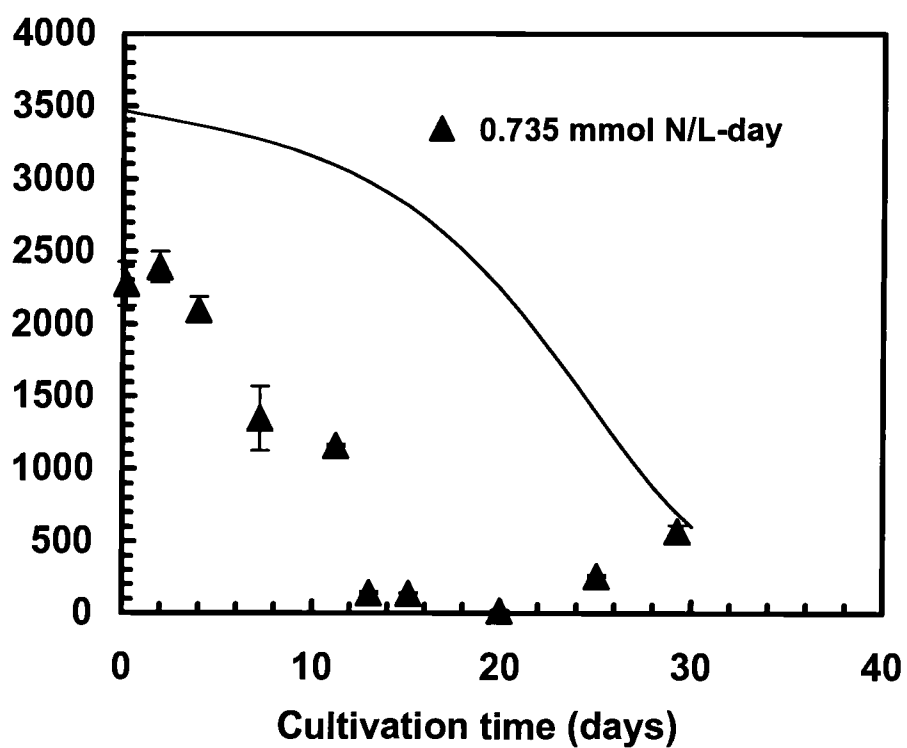


**Figure 3-13. Dynamic model prediction (solid line) and experimental data of nitrate concentration for nutrient delivery cultivation at  $0.74 \text{ mmol N L}^{-1} \text{ day}^{-1}$**

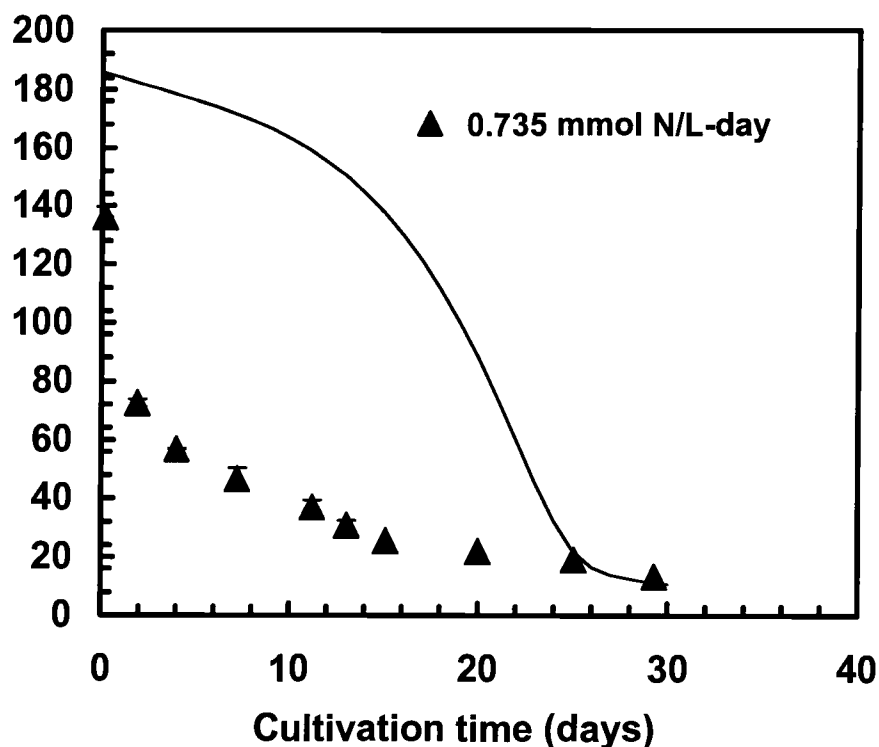


**Figure 3-14. Dynamic model prediction (solid line) and experimental data of phosphate concentration for nutrient delivery cultivation at  $0.74 \text{ mmol N L}^{-1} \text{ day}^{-1}$**

Figure 3-12 shows a good correlation for biomass between experimental data and the model prediction developed from first principles. Figures 3-13 and 3-14 show the dynamic model cannot predict the rate of consumption of nitrate or phosphate, but does predict the final concentrations of these compounds. The simplicity of the model, which assumes a constant nitrate and phosphate uptake rate proportional to the growth rate, is the likely cause for deviations from experimental data. Likely, *Ochthodes secundiramea* does not uptake nitrate and phosphate at a constant rate scaled to the biomass growth rate, but rather uptakes it at a faster rate and incorporates them into storage compounds such as photosynthetic pigments to be utilized when the medium concentration goes down (Chopin et al., 1990).

### 3.3. REFERENCES

- Atkinson, M.J., Smith, S.V. 1983. C:N:P ratios of benthic marine plants. *Limnol Oceanogr* **28**: 568-574.
- Butler, A. 1998. Acquisition and utilization of transition metal ions by marine organisms. *Science* **281**: 207-210.
- Chopin, T., Hanisk, M.D., Koehn, F.E., Mollion, J., and Moreau, S. 1990. Studies on carrageenans and effects of seawater phosphorous concentration on carrageenan content and growth of *Agardhiella subulata* (C. Agardh) Kraft and Wynne (Rhodophyceae, Solieriaceae). *Journal of Applied Phycology* **2**: 3-16.
- Fenical, W. 1975. Halogenation in the rhodophyta—a review. *Journal of Phycology* **11**: 245-259.
- Grob, R.L. 1995. Modern practice of gas chromatography, 3<sup>rd</sup> ed. New York: Wiley-Interscience.
- Huang, Y.M., Maliakal, S., Cheney, D.P., and Rorrer, G.L. 1998. Comparison of development and photosynthetic growth for filament clump and regenerated microplantlet cultures of *Agardhiella subulata* (Rhodophyta, Gigartinales). *Journal of Phycology* **34**: 893-901.
- Huang, Y.M., and Rorrer, G.L. 2002. Dynamics of oxygen evolution and biomass production during cultivation of *Agardhiella subulata* microplantlets in a bubble-column photobioreactor under medium perfusion. *Biotechnology Progress* **18**: 62-71.
- Kitade, Y., Yamazaki, S., Saga, N. 1996. A method of high molecular weight DNA from the macroalga *Porphyra yezoensis* (Rhodophyta). *Journal of Phycology* **32**: 496-498.
- Maliakal, S., Cheney, D.P., and Rorrer, G.L. 2001. Halogenated monoterpene production in regenerated plantlet cultures of *Ochtodes secundiramea*. *Journal of Phycology* **37**: 1010-1019.
- Rorrer, G.L., Polne-Fuller, M., and Zhi, C. 1996. Development and bioreactor cultivation of a novel semi-differentiated tissue suspension derived from the marine plant *Acrosiphonia coalita*. *Biotechnology and Bioengineering* **49**: 559-567.

South, G.R., Whittick, A. 1987. Introduction to phycology. Oxford: Blackwell Scientific Publications.

Turpin, D.H. 1991. Effects of inorganic N availability on algal photosynthesis and carbon metabolism. *Journal of Phycology* **27**: 14-20.

#### 4. BROMIDE AND VANADIUM DELIVERY

The effects of bromide and vanadium delivery on the growth and halogenated monoterpene yield of *O. secundiramea* microplantlets were determined. Semi-continuous and fed batch delivery experiments were conducted in which the concentrations of bromide were varied from 0.0 to 1.40 mM bromide, and vanadium concentrations were varied from 0.0 to 515 nM. Semi-continuous bromide delivery experiments were conducted to determine if the halogenated monoterpene pathway could be altered by different medium bromide concentrations, and to determine the minimum concentration of bromide required to initiate halogenated monoterpene production. Fed-batch bromide delivery experiments were conducted to determine the effect of total mass of bromide present in the culture medium on the halogenated monoterpene pathway, and determine if a bromide limitation to halogenated monoterpene production could be reached. Zero vanadium delivery experiments were designed to test whether the brominating ability of *O. secundiramea* could be shut down or significantly altered.

For semi-continuous cultivation experiments, the production rate of each halogenated monoterpene (HMT) was estimated. From the HMT production rate data, the fluxes to and from each compound in a proposed halogenation pathway were estimated. Flux analysis gave insights to the effect of bromide and vanadium delivery rate on the pathway, and also illuminated any control aspects of the halogenation reactions.

## 4.1. MATERIALS AND METHODS

### 4.1.1. Culture Maintenance

Plantlets of the macrophytic tropical red alga *Ochtodes secundiramea* (Montagne) Howe (Cryptonemiales, Rhizophyllidaceae) were established by callus induction and shoot tissue regeneration techniques developed in our previous work (Huang et al., 1998; Maliakal et al., 2001). The microplantlets used in this study were derived from the original stock developed in our previous work (Huang et al., 1998; Maliakal et al., 2001), and maintained in the same manner as described in Chapter 3 except they were maintained on bromide and vanadium free artificial seawater supplemented with ESS nutrients (Kitade et al., 1996). For the study of bromide and vanadium delivery effects on halogenated monoterpene production, it was critical to know the exact concentrations of bromide and vanadium in the culture medium. Since natural seawater contains approximately 0.81 mM bromine (Fenical, 1975) and 40 nM vanadium, natural seawater could not be used as the cultivation medium and an artificial medium was developed that contains less than 0.01 mM bromine.

Artificial seawater and 200X ESS nutrient stock solutions were autoclaved at 121 °C and 15 psig for 30 min. The final composition of the artificial base medium was: 460 mM NaCl; 27.7 mM MgSO<sub>4</sub> · 7H<sub>2</sub>O; 26.5 mM MgCl<sub>2</sub> · 6H<sub>2</sub>O; 9.93 mM CaCl<sub>2</sub>; 10.3 mM KCl; 3.14 mM NaHCO<sub>3</sub>; 0.52 mM H<sub>3</sub>BO<sub>3</sub>; 0.098 mM SrCl<sub>2</sub> · 6H<sub>2</sub>O. The final composition for the ESS nutrients in the artificial seawater base medium used in this study was: 1.41 mM NaNO<sub>3</sub>; 0.074 mM K<sub>2</sub>HPO<sub>4</sub> · 3H<sub>2</sub>O; 0.0218 mM EDTA Fe-Na salt; 0.768 mM Na-HEPE buffer; 0.787 mM KI; 0.428 mM ZnCl<sub>2</sub>; 0.364 mM MnCl<sub>2</sub> · 4H<sub>2</sub>O; 0.0034 mM CoCl<sub>2</sub> · 6H<sub>2</sub>O; 0.0145 μM FeCl<sub>3</sub> · 6H<sub>2</sub>O; 0.193 μM Na<sub>2</sub>EDTA · 2H<sub>2</sub>O; 1.48 μM H<sub>3</sub>BO<sub>3</sub>; 0.00148 μM vitamin B<sub>12</sub>; 0.00818 μM biotin (C<sub>10</sub>H<sub>16</sub>N<sub>2</sub>O<sub>3</sub>S); 0.592 μM thiamine-HCl; 1.62 μM

nicotinic acid; 0.840  $\mu\text{M}$  DL-pantothenic acid hemi Ca salt; 0.146  $\mu\text{M}$  *p*-aminobenzoic acid; 11.1  $\mu\text{M}$  meso-inositol; 1.59  $\mu\text{M}$  thymine. Bromine (as KBr) and vanadium (as  $\text{Na}_3\text{VO}_4$ ) were not added to the ESS nutrients used for maintenance culture.

#### 4.1.2. Photobioreactor Design and Operation

##### 4.1.2.1. Semi-Continuous Cultivations

The airlift photobioreactor shown in Figure 3-1 was used for all semi-continuous bromide and vanadium delivery experiments. Inoculation and sampling were performed as described in Chapter 3. Process conditions and initial medium compositions for semi-continuous bromide and vanadium delivery experiments are detailed in Tables 4-1 to 4-4. Operating in semi-continuous mode was designed to provide the culture with a constant nutrient delivery, and maintain the liquid medium bromide and vanadium levels at a set value. It was the setpoint concentration of bromide and vanadium that was the manipulated variable in semi-continuous cultivations.

To achieve constant nutrient delivery, and maintain the bromide and vanadium setpoint concentrations, 1 L of spent medium was removed every 4 days, and 1 L of fresh medium with composition detailed in Tables 4-3 and 4-4 was added. Initially, the replacement medium contained no added bromide or vanadium, and a step change to a new bromide and vanadium concentration setpoint was made to initiate the experiment. Concentrations of all other species in the replacement medium, aside from bromide and vanadium, were constant, equal to the inoculum concentration. Sterile fresh medium was added to the culture by



gravity feed from a 1 L medium replacement bottle connected via 3/8 in tubing to an inlet port above the cultivation medium level.

**Table 4-1. Experimental Process Conditions for Semi-continuous Bromide Delivery Cultivations**

Process parameter	Bromide Delivery Rate (mmol Br L <sup>-1</sup> day <sup>-1</sup> )			
	0.0	0.0074	0.013	0.13
Bromide conc. (mmol Br L <sup>-1</sup> )	0.0	0.05	0.10	1.0
Vanadium delivery rate (nmol V L <sup>-1</sup> day <sup>-1</sup> )	6.60	7.35	6.38	6.38
Vanadium conc. (nmol V L <sup>-1</sup> )	50.0	50.0	50.0	50.0
Medium perfusion rate (mL day <sup>-1</sup> )	243	272	236	236
Working volume, $V$ (mL)	1850	1850	1850	1850
Vessel inner diameter, $d_o$ (cm)	7.6	7.6	7.6	7.6
Draft tube inner diameter, $d_i$ (cm)	3.2	3.2	3.2	3.2
Aeration rate, $v_g$ (L min <sup>-1</sup> )	630	630	630	630
Aeration rate, $v_g / V$ (L air L <sup>-1</sup> min <sup>-1</sup> )	0.34	0.34	0.34	0.34
O <sub>2</sub> mass transfer, $k_L a$ (h <sup>-1</sup> )	66.3	66.3	66.3	33.9
CO <sub>2</sub> Partial pressure, (ppm)	350	350	350	350
CO <sub>2</sub> - $TR_{max}$ (mmol CO <sub>2</sub> L <sup>-1</sup> h <sup>-1</sup> )	0.68	0.68	0.68	0.35
$n_{CO_2}$ (mmol CO <sub>2</sub> L <sup>-1</sup> h <sup>-1</sup> )	0.29	0.29	0.29	0.29
Setpoint pH	8.0	8.0	8.0	8.0
Average pH	8.4 ± 0.3	8.5 ± 0.2	8.6 ± 0.2	8.7 ± 0.3
Culture removal rate, $v_f / V$ mL day <sup>-1</sup>	30.9	40.2	40.1	37.4
Incident light intensity, $I_o$ (μE m <sup>-2</sup> s <sup>-1</sup> )	143	143	143	143
Planes of illumination, $\alpha$	2	2	2	2
Photoperiod (h ON:h OFF LD)	14:10	14:10	14:10	14:10
Temperature (°C)	26	26	26	26
Final cultivation time (days)	51.8	48.0	48.0	47.94
Solids content (g DW g <sup>-1</sup> FW)				
Inoculation	25.96%	22.97%	34.38%	34.38%
Final	24.50%	32.77%	25.17%	25.08%
Initial plantlet density, $X_0$ (g DW L <sup>-1</sup> )	1.28	1.11	1.68	1.69
Final plantlet density, $X_0$ (g DW L <sup>-1</sup> )	2.49	2.39	1.78	3.10

**Table 4-2. Experimental Process Conditions for Semi-continuous Vanadium Delivery Cultivations**

Process parameter	Vanadium Delivery Rate (nmol V L <sup>-1</sup> day <sup>-1</sup> )	
	0.0	6.38
Vanadium conc. (nmol V L <sup>-1</sup> )	0.0	50.0
Bromide conc. (mmol Br L <sup>-1</sup> )	1.0	1.0
Bromide delivery rate (mmol Br L <sup>-1</sup> day <sup>-1</sup> )	0.13	0.13
Medium perfusion rate (mL day <sup>-1</sup> )	273	236
Working volume, <i>V</i> (mL)	1850	1850
Vessel inner diameter, <i>d<sub>o</sub></i> (cm)	7.6	7.6
Draft tube inner diameter, <i>d<sub>i</sub></i> (cm)	3.2	3.2
Aeration rate, <i>v<sub>g</sub></i> (L min <sup>-1</sup> )	630	630
Aeration rate, <i>v<sub>g</sub></i> / <i>V</i> (L air L <sup>-1</sup> min <sup>-1</sup> )	0.34	0.34
O <sub>2</sub> mass transfer, <i>k<sub>L</sub>a</i> (h <sup>-1</sup> )	33.9	33.9
CO <sub>2</sub> Partial pressure, (ppm)	350	350
CO <sub>2</sub> - <i>TR<sub>max</sub></i> (mmol CO <sub>2</sub> L <sup>-1</sup> h <sup>-1</sup> )	0.35	0.35
<i>n<sub>CO2</sub></i> (mmol CO <sub>2</sub> L <sup>-1</sup> h <sup>-1</sup> )	0.29	0.29
Setpoint pH	8.0	8.0
Average pH	8.7 ± 0.3	8.7 ± 0.3
Culture removal rate, <i>v<sub>f</sub></i> / <i>V</i> mL day <sup>-1</sup>	41.5	37.4
Incident light intensity, <i>I<sub>o</sub></i> (μE m <sup>-2</sup> s <sup>-1</sup> )	143	143
Planes of illumination, <i>α</i>	2	2
Photoperiod (h ON:h OFF LD)	14:10	14:10
Temperature (°C)	26	26
Final cultivation time (days)	48.00	47.94
Solids content (g DW g <sup>-1</sup> FW)		
Inoculation	22.97%	34.38%
Final	30.00%	25.08%
Initial plantlet density, <i>X<sub>0</sub></i> (g DW L <sup>-1</sup> )	1.12	1.69
Final plantlet density, <i>X<sub>0</sub></i> (g DW L <sup>-1</sup> )	3.02	3.10

**Table 4-3. Medium Composition for Semi-continuous Bromide Delivery Cultivations**

Parameter	Bromide Delivery Rate (mmol Br L <sup>-1</sup> day <sup>-1</sup> )			
	0.0	0.0074	0.013	0.13
Initial perfusion medium composition				
Cultivation time (days)	0-16	0-16	0-16	0-16
Bromide conc. (mmol Br L <sup>-1</sup> )	0.0	0.0	0.0	0.0
Vanadium conc. (nmol V L <sup>-1</sup> )	0.0	0.0	0.0	0.0
Nitrate conc. (μmol N L <sup>-1</sup> )	1400	1400	1400	1400
Phosphate conc. (μmol P L <sup>-1</sup> )	74	74	74	74
Micronutrient conc. (x base medium)	2	2	2	2
Final perfusion medium composition				
Cultivation time (days)	16-52	16-48	16-48	16-48
Bromide conc. (mmol Br L <sup>-1</sup> )	0.0	0.05	0.10	1.0
Vanadium conc. (nmol V L <sup>-1</sup> )	50.0	50.0	50.0	50.0
Nitrate conc. (μmol N L <sup>-1</sup> )	1400	1400	1400	1400
Phosphate conc. (μmol P L <sup>-1</sup> )	74	74	74	74
Micronutrient conc. (x base medium)	2	2	2	2

**Table 4-4. Medium Composition for Semi-continuous Vanadium Delivery Cultivations**

Parameter	Vanadium Delivery Rate (nmol V L <sup>-1</sup> day <sup>-1</sup> )	
	0.0	6.38
Initial perfusion medium composition		
Cultivation time (days)	0-16	0-16
Bromide conc. (mmol Br L <sup>-1</sup> )	0.0	0.0
Vanadium conc. (nmol V L <sup>-1</sup> )	0.0	0.0
Nitrate conc. (μmol N L <sup>-1</sup> )	1400	1400
Phosphate conc. (μmol P L <sup>-1</sup> )	74	74
Micronutrient conc. (x base medium)	2	2
Final perfusion medium composition		
Cultivation time (days)	16-48	16-48
Bromide conc. (mmol Br L <sup>-1</sup> )	1.0	1.0
Vanadium conc. (nmol V L <sup>-1</sup> )	0.0	50.0
Nitrate conc. (μmol N L <sup>-1</sup> )	1400	1400
Phosphate conc. (μmol P L <sup>-1</sup> )	74	74
Micronutrient conc. (x base medium)	2	2

**Table 4-5. Experimental Process Conditions for Fed-batch Bromide Delivery Cultivations**

Process parameter	Bromide conc. (mmol Br L <sup>-1</sup> )			
	0.0	0.038	0.128	1.40
Initial volume, $V_i$ (mL)	2250	2000	2000	2000
Final volume, $V_f$ (mL)	1290	1140	625	626
Vessel inner diameter, $d_o$ (cm)	7.0	10	7.6	7.6
Aeration rate, $v_g$ (L min <sup>-1</sup> )	630	630	438	438
Aeration rate, $v_g / V$ (L air L <sup>-1</sup> min <sup>-1</sup> )	0.34	0.32	0.22	0.22
O <sub>2</sub> mass transfer, $k_L a$ (h <sup>-1</sup> )	132.1	25.3	18.2	17.7
CO <sub>2</sub> Partial pressure, (ppm)	350	350	350	350
CO <sub>2</sub> -TR <sub>max</sub> (mmol CO <sub>2</sub> L <sup>-1</sup> h <sup>-1</sup> )	1.36	0.26	0.19	0.18
$n_{CO_2}$ (mmol CO <sub>2</sub> L <sup>-1</sup> h <sup>-1</sup> )	0.24	0.27	0.19	0.19
Setpoint pH	8.0	8.0	8.0	8.0
Average pH	8.2 ± 0.1	8.4 ± 0.2	8.6 ± 0.2	8.4 ± 0.2
Culture removal rate, $v_f / V$ mL day <sup>-1</sup>	32.4	47.7	42.0	41.0
Incident light intensity, $I_o$ (μE m <sup>-2</sup> s <sup>-1</sup> )	143	143	143	143
Planes of illumination, $\alpha$	2	2	2	2
Photoperiod (h ON:h OFF LD)	14:10	14:10	14:10	14:10
Temperature (°C)	26	26	26	26
Final cultivation time (days)	36.0	20.0	37.8	37.8
Solids content (g DW g <sup>-1</sup> FW)				
Inoculation	26.55%	29.79%	24.48%	24.48%
Final	22.61%	31.44%	28.57%	34.53%
Initial plantlet density, $X_o$ (g DW L <sup>-1</sup> )	1.06	1.34	1.19	1.23
Final plantlet density, $X_o$ (g DW L <sup>-1</sup> )	1.25	2.16	1.17	2.77

**Table 4-6. Experimental Process Conditions for Fed-batch Vanadium Delivery Cultivations**

Process parameter	Vanadium Conc. (nmol V L <sup>-1</sup> )	
	0.0	515
Initial volume, $V_i$ (mL)	1900	2000
Final volume, $V_f$ (mL)	770	626
Vessel inner diameter, $d_o$ (cm)	7.6	7.6
Aeration rate, $v_a$ (L min <sup>-1</sup> )	438	438
Aeration rate, $v_a / V$ (L air L <sup>-1</sup> min <sup>-1</sup> )	0.23	0.22
O <sub>2</sub> mass transfer, $k_L a$ (h <sup>-1</sup> )	18.2	17.7
CO <sub>2</sub> Partial pressure, (ppm)	350	350
CO <sub>2</sub> -TR <sub>max</sub> (mmol CO <sub>2</sub> L <sup>-1</sup> h <sup>-1</sup> )	0.19	0.18
$n_{CO_2}$ (mmol CO <sub>2</sub> L <sup>-1</sup> h <sup>-1</sup> )	0.20	0.19
Setpoint pH	8.0	8.0
Average pH	8.5 ± 0.1	8.4 ± 0.2
Culture removal rate, $v_r / V$ mL day <sup>-1</sup>	42.2	41.0
Incident light intensity, $I_o$ (μE m <sup>-2</sup> s <sup>-1</sup> )	143	143
Planes of illumination, $\alpha$	2	2
Photoperiod (h ON:h OFF LD)	13:10	14:10
Temperature (°C)	26	26
Final cultivation time (days)	33.8	37.8
Solids content (g DW g <sup>-1</sup> FW)		
Inoculation	25.07%	24.48%
Final	33.23%	34.53%
Initial plantlet density, $X_o$ (g DW L <sup>-1</sup> )	0.85	1.23
Final plantlet density, $X_o$ (g DW L <sup>-1</sup> )	2.30	2.77

**Table 4-7. Medium Composition for Fed-batch Bromide Delivery Cultivations**

Parameter	Bromide conc. (mmol Br L <sup>-1</sup> )			
	0.0	0.038	0.128	1.40
Initial medium composition				
Bromide conc. (mmol Br L <sup>-1</sup> )	0.0	0.0	0.0	0.0
Vanadium conc. (nmol V L <sup>-1</sup> )	0.0	0.0	0.0	0.0
Nitrate conc. (μmol N L <sup>-1</sup> )	1400	1400	1400	1400
Phosphate conc. (μmol P L <sup>-1</sup> )	74	74	74	74
Micronutrient conc. (x base medium)	2	2	2	2
Pulse composition				
Pulse time (days)	16	0	16	16
Bromide mass (mmol Br)	0.0	0.075	0.195	2.134
Vanadium mass (nmol V)	958	831	784	763
Medium composition after pulse				
Reactor volume at pulse (mL)	1840	2000	1524	1524
Bromide conc. (mmol Br L <sup>-1</sup> )	0.0	0.038	0.128	1.40
Vanadium conc. (nmol V L <sup>-1</sup> )	520	416	500	515
Nutrient addition composition				
Nutrient delivery rate (mL day <sup>-1</sup> )	1.95	2.44	3.67	3.68
Nitrate conc. (μmol N L <sup>-1</sup> )	140000	140000	140000	140000
Phosphate conc. (μmol P L <sup>-1</sup> )	7400	7400	7400	7400
Micronutrient conc. (x base medium)	200	200	200	200



**Table 4-8. Medium Composition for Fed-batch Vanadium Delivery Cultivations**

Parameter	Vanadium Conc. (nmol V L <sup>-1</sup> )	
	0.0	515
Initial medium composition		
Bromide conc. (mmol Br L <sup>-1</sup> )	0.0	0.0
Vanadium conc. (nmol V L <sup>-1</sup> )	0.0	0.0
Nitrate conc. (μmol N L <sup>-1</sup> )	1400	1400
Phosphate conc. (μmol P L <sup>-1</sup> )	74	74
Micronutrient conc. (x base medium)	2	2
Pulse composition		
Pulse time (days)	16	16
Bromide mass (mmol Br)	1.550	2.134
Vanadium mass (nmol V)	0	763
Medium composition after pulse		
Reactor volume at pulse (mL)	1415	1524
Bromide conc. (mmol Br L <sup>-1</sup> )	1.10	1.40
Vanadium conc. (nmol V L <sup>-1</sup> )	0.0	515
Nutrient addition composition		
Nutrient delivery rate (mL day <sup>-1</sup> )	2.94	3.68
Nitrate conc. (μmol N L <sup>-1</sup> )	140000	140000
Phosphate conc. (μmol P L <sup>-1</sup> )	7400	7400
Micronutrient conc. (x base medium)	200	200

#### 4.1.2.2. Fed-Batch Cultivations

The photobioreactor shown in Figure 3-1 was used without the draft tube for all fed-batch bromide and vanadium delivery experiments. Inoculation and sampling were performed as described in Chapter 3. Process conditions and initial medium compositions for fed-batch bromide and vanadium delivery experiments are detailed in Tables 4-5 to 4-8. No base medium was added to the culture following inoculation, instead concentrated 200x ESS nutrient stock with composition described in Tables 4-7, 4-8 was added at a rate described in Tables 4-7, 4-8. Operating in fed-batch mode was designed to provide the culture with a constant nutrient delivery, but limit bromide and vanadium addition to a one-time pulse addition. The experiment was initiated by adding a one-time pulse of a known amount of bromide and vanadium, without any further addition of bromide or vanadium. The masses of bromide and vanadium pulsed into the culture and the resultant reactor medium concentrations of bromide and vanadium were the manipulated variables in the fed-batch cultivation experiments. Since artificial seawater has up to  $0.02 \text{ mmol Br L}^{-1}$ , replacing medium with artificial seawater without added bromide would still deliver a significant amount of bromide over the course of the cultivation.

#### 4.1.3. Bromide

The bromide concentration was determined by the phenol red colorimetric method (APHA, 1992) in 20 mL glass scintillation vials. Specifically, 0.4 mL acetate buffer solution ( $90 \text{ g L}^{-1} \text{ NaCl}$ ,  $68 \text{ g L}^{-1} \text{ NaC}_2\text{H}_3\text{O}_2 \cdot 3\text{H}_2\text{O}$ ,  $1.5 \text{ mL L}^{-1}$  glacial acetic acid), 0.4 mL phenol red indicator solution ( $210 \text{ mg L}^{-1}$  phenolsulfonephthalein sodium salt), and 0.1 mL chloramines-T solution ( $5 \text{ g L}^{-1}$  chloramine-T, sodium p-toluenesulfonchloramide) were added to 10 mL of sample

diluted to a bromide concentration within 0.1-1.0 mg L<sup>-1</sup>. Twenty minutes after adding chloramine-T solution, 0.1 mL sodium thiosulfate solution (496 g L<sup>-1</sup> Na<sub>2</sub>S<sub>2</sub>O<sub>3</sub>·5H<sub>2</sub>O) was added, and the absorbance at 590 nm was measured. All bromide assays were performed in duplicate.

#### 4.1.4. Estimation of Specific Growth Rate

The specific growth rates for semi-continuous and fed-batch cultivations are determined by performing a mass balance within the vessel, subject to the following assumptions:

1. Constant biomass removal rate,  $m_s$
2. Constant biomass growth rate,  $\mu$

The differential balance on the biomass is

$$\mu M - m_s = \frac{dM}{dt} \quad (4-1)$$

where  $m_s$  (g DW day<sup>-1</sup>) is the rate of biomass removed from the vessel by sampling,  $M$  (g DW) is the amount of biomass in the vessel at any time  $t$  (days) and  $\mu$  (day<sup>-1</sup>) is the specific growth rate. The biomass removal rate is estimated by the least squares fit of the sum of all biomass removed by sampling up to time,  $t$ , vs time,  $t$  given by

$$m_{s,total} = m_s t \quad (4-2)$$

where  $m_{s,total}$  (g DW) is the total mass of samples collected up to time,  $t$ .

Integration of equation 4-1 at constant  $m_s$  yields

$$M(t) = \frac{r_s}{\mu} + \frac{M_o - \frac{r_s}{\mu}}{e^{-\mu t}} \quad (4-3)$$

where  $M_o$  (g DW) is the inoculum mass. Solving equation 4-3 for the shutdown mass gives

$$M_f = \frac{r_s}{\mu} + \frac{M_o - \frac{r_s}{\mu}}{e^{-\mu t_f}} \quad (4-4)$$

where  $M_f$  (g DW) is the final biomass. Since all variables in equation 4-4 are known, except  $\mu$ , we can use a solver routine to estimate the value of the specific biomass growth rate.

#### 4.1.5. Compound Production Rate Estimation

The compound production rate is estimated from a material balance over the cultivation time, subject to the following assumptions

1. Constant biomass removal rate,  $r_s$
2. Constant biomass growth rate,  $\mu$

The differential balance on compound  $i$ , is given by

$$-r_s C_i + r_i M = \frac{d(C_i M)}{dt} \quad (4-5)$$

where  $r_i$  ( $\mu\text{mol compound g DW}^{-1} \text{ day}^{-1}$ ) is the production of compound  $i$ ,  $C_i$  ( $\mu\text{mol compound g DW}^{-1}$ ) is the concentration of compound  $i$  at time  $t$  (days). Separating the two terms on the right hand side of equation 4-5 and dividing by  $M$  gives

$$\frac{-r_s}{M} C_i + r_i = \frac{dC_i}{dt} + \frac{C_i}{M} \frac{dM}{dt} \quad (4-6)$$

Recall that

$$\mu M - r_s = \frac{dM}{dt} \quad (4-1)$$

therefore

$$\frac{-r_s}{M} C_i + r_i = \frac{dC_i}{dt} + \frac{C_i}{M} (\mu M - r_s) \quad (4-7)$$

which is simplified to

$$\frac{dC_i}{dt} + C_i \mu = r_i \quad (4-8)$$

Integration of equation 4-8 at constant  $r_i$  and  $\mu$  yields

$$C_i = \frac{r_i}{\mu} + e^{\mu(t_0 - t)} \left( C_{i,0} - \frac{r_i}{\mu} \right) \quad (4-9)$$

where  $C_{i,o}$  ( $\mu\text{mol compound g DW}^{-1}$ ) is the initial concentration of compound  $i$  at time  $t_o$  (days). Equation 4-9 is used to perform a least squares non-linear regression on  $C_i$  vs  $t$  data to estimate  $r_i$ .

## 4.2. RESULTS AND DISCUSSION

### 4.2.1. Semi-Continuous Cultivations

#### 4.2.1.1. Growth Data

Cultivations performed under semi-continuous bromide and vanadium delivery addition were designed to maintain the culture at a steady metabolic condition. Light and  $\text{CO}_2$  delivery rates are detailed in Tables 4-1 and 4-2. Growth rate was not optimized, and the culture did not grow at significant rates. The specific growth rate is presented in Table 4-9.

The nitrate and phosphate concentrations of the liquid medium were measured over the cultivation time. These results are presented in Figures 4-1, 4-2, 4-3 and 4-4. Nitrate concentrations for all cultivations reach zero at approximately 20 days, and phosphate concentrations for all cultivations reach zero after 4 or 8 days. The metabolic activity was therefore limited by the rate of phosphate and nitrate delivery for all cultivations. Phosphate and nitrate delivery rates were set to an N:P ratio of 19:1 as determined by Atkinson and Smith (1983) for balanced growth of red marine algae. An increase in the ratio of phosphate to nitrate would be required to increase the day of phosphate limitation from 4 or 8 days to 20 days. For the current study the N:P ratio was set to ensure consistency with earlier studies.

**Table 4-9. Estimated Specific Growth Rates for Semi-continuous Bromide and Vanadium Delivery Cultivations** (all errors  $\pm 1$  s.e.)

	Bromide Delivery Rate <sup>(a)</sup> (mmol Br L <sup>-1</sup> day <sup>-1</sup> )				Vanadium Delivery Rate <sup>(b)</sup> (nmol V L <sup>-1</sup> day <sup>-1</sup> )	
	0.0	0.0074	0.013	0.13	0.0	6.4
M <sub>0</sub> (g)	2.36	2.04	3.12	3.12	2.07	3.12
M <sub>f</sub> (g)	4.61	4.48	3.3	5.73	5.61	5.73
t <sub>0</sub> (day)	0	0	0	0	0	0
t <sub>f</sub> (day)	52	52	48	48	48	48
m <sub>s</sub> (g/day)	0.13 $\pm$ 0.0044	0.11 $\pm$ 0.0063	0.12 $\pm$ 0.0048	0.14 $\pm$ 0.0078	0.14 $\pm$ 0.0088	0.14 $\pm$ 0.0078
$\mu$ (day <sup>-1</sup> )	0.057	0.057	0.038	0.050	0.071	0.050

(a) Vanadium delivery rate = 6.38 nmol V L<sup>-1</sup> day<sup>-1</sup>

(b) Bromide deliver rate = 0.13 mmol Br L<sup>-1</sup> day<sup>-1</sup>

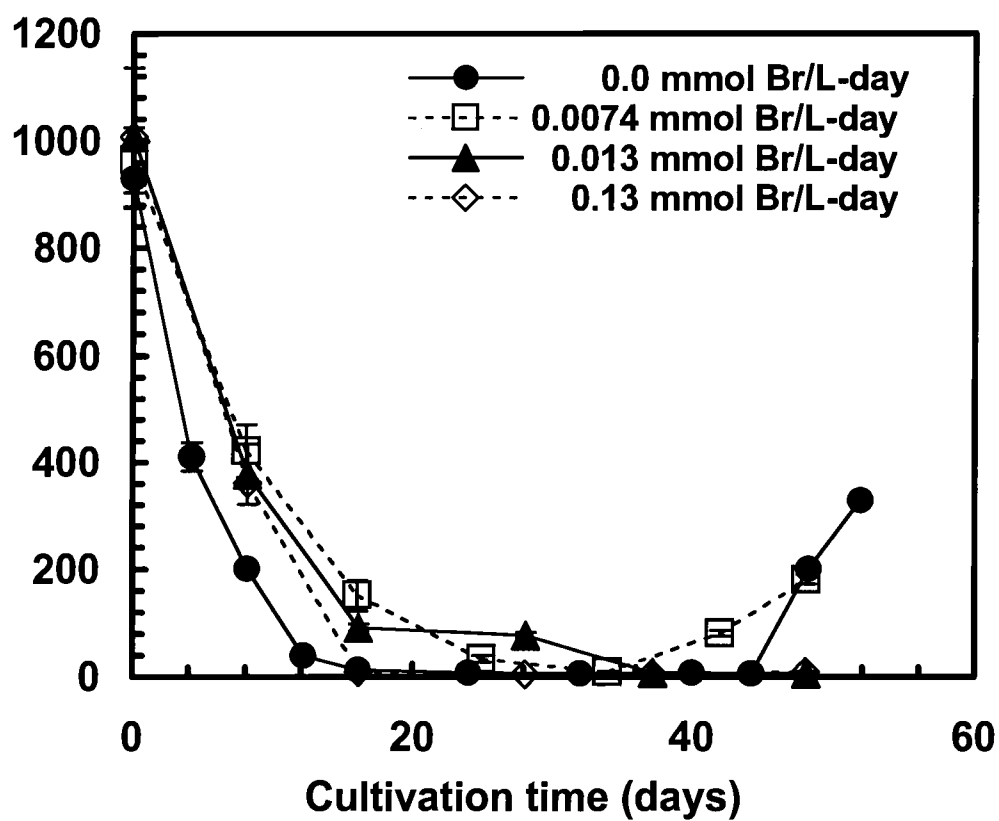


**Figure 4-1. Photobioreactor medium nitrate concentration profiles for semi-continuous bromide delivery cultivations**



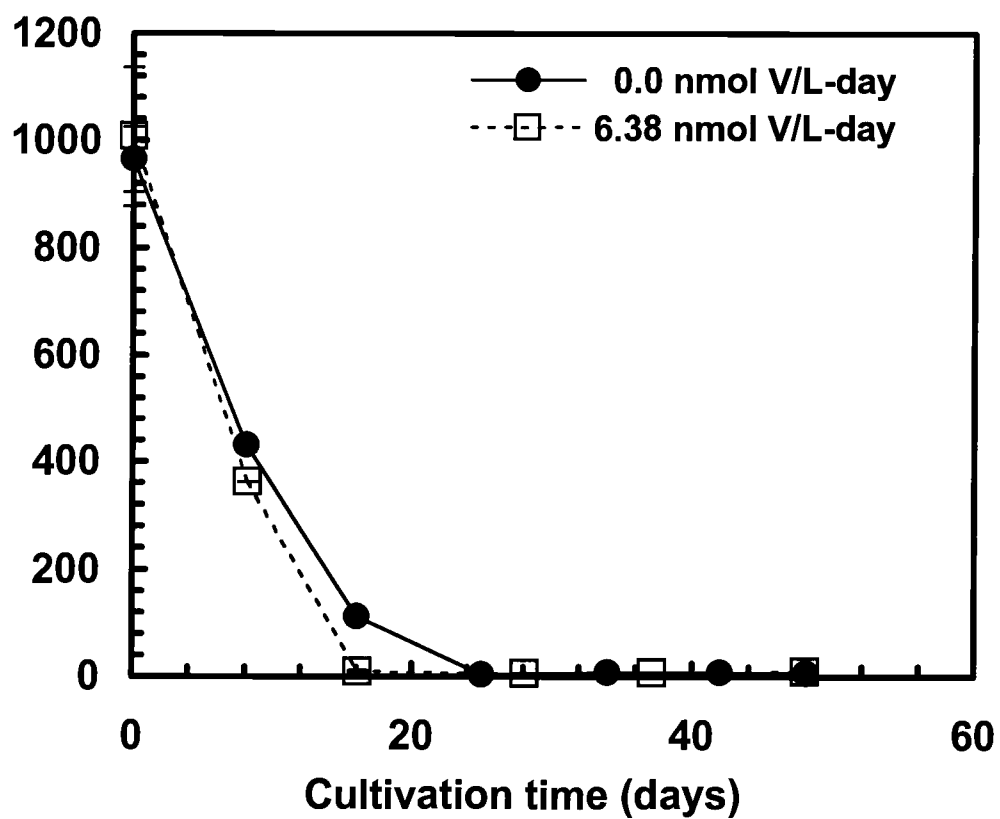


**Figure 4-2. Photobioreactor medium nitrate concentration profiles for semi-continuous vanadium delivery cultivations**

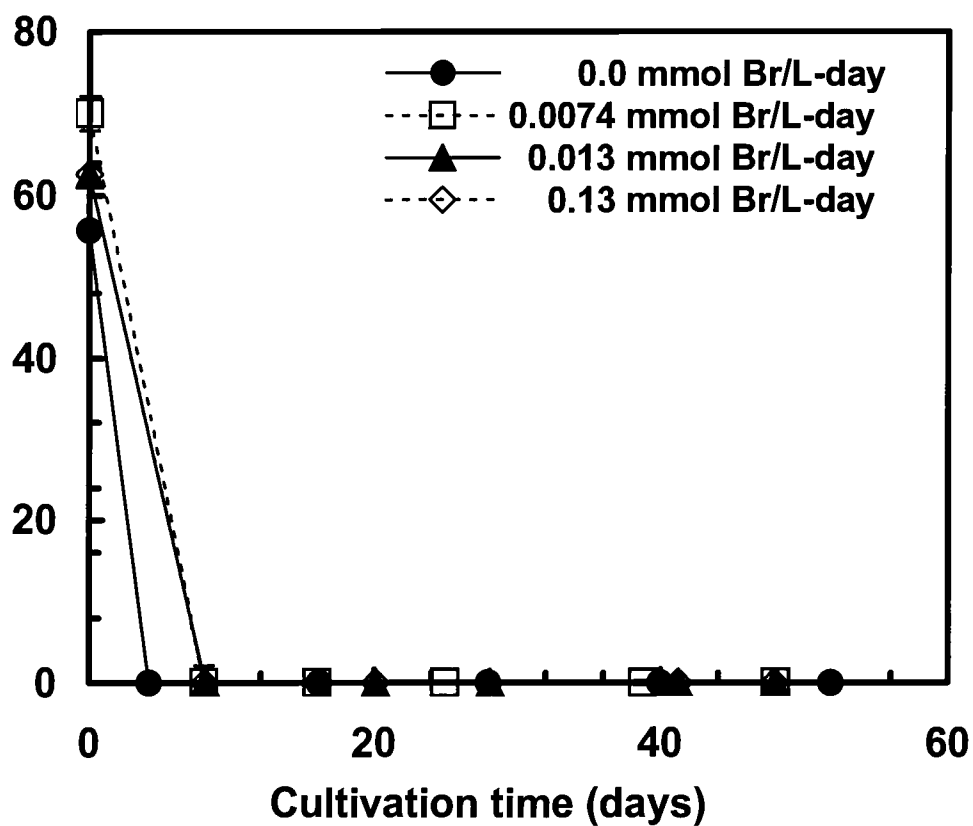


**Figure 4-3. Photobioreactor medium phosphate concentration profiles for semi-continuous bromide delivery cultivations**

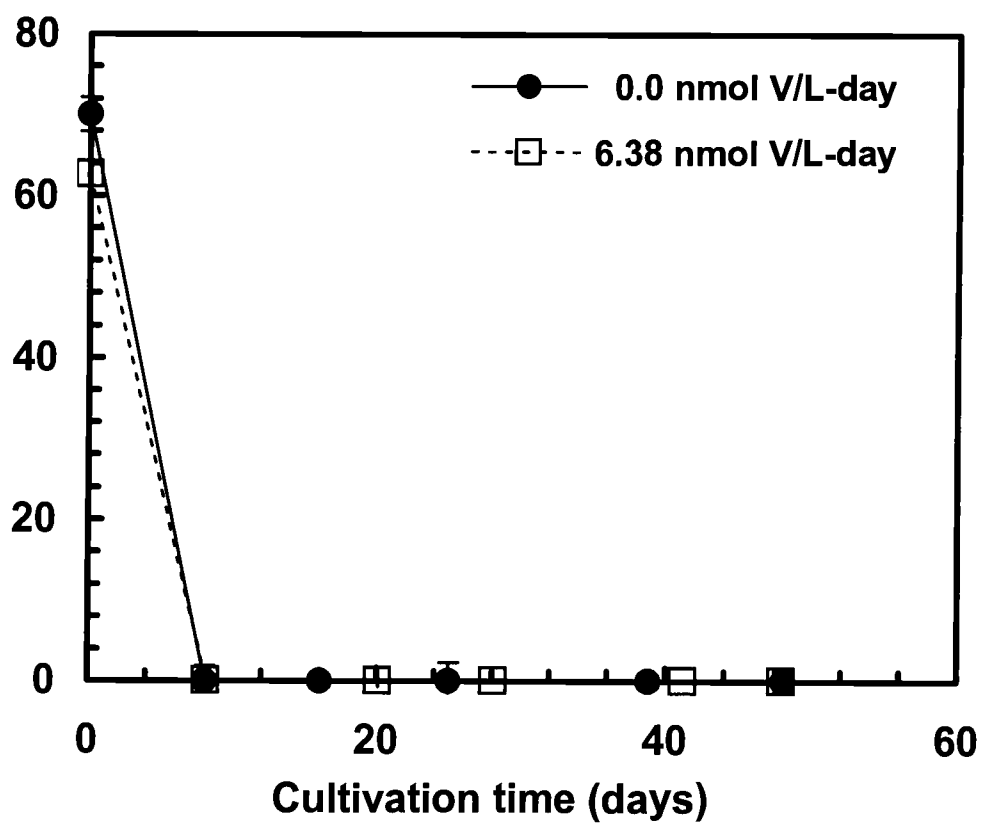


**Figure 4-4. Photobioreactor medium phosphate concentration profiles for semi-continuous vanadium delivery cultivations**

Light delivery was set to  $143 \mu\text{E m}^{-2} \text{s}^{-1}$  for all cultivations. Figure 4-5 shows the P-I curve for microplantlets cultivated in bromide and vanadium free artificial medium. The curve shows that the incident light intensity is above saturation levels. Therefore, differences in metabolic activity cannot be attributed to light delivery.

CO<sub>2</sub> delivery was kept constant for all cultivations (Tables 4-1 and 4-2). In all cultivations the calculation of the maximum transfer rate of CO<sub>2</sub> into the culture medium from the aeration gas is greater than the actual molar flow rate of CO<sub>2</sub> into the reactor as illustrated in Tables 4-1 and 4-2. For all cultivations this molar flow rate is equal to  $0.29 \text{ mmol CO}_2 \text{ L}^{-1} \text{ h}^{-1}$ . CO<sub>2</sub> delivery was the same for all cultivations; therefore, differences in metabolic activity cannot be attributed to CO<sub>2</sub> delivery.

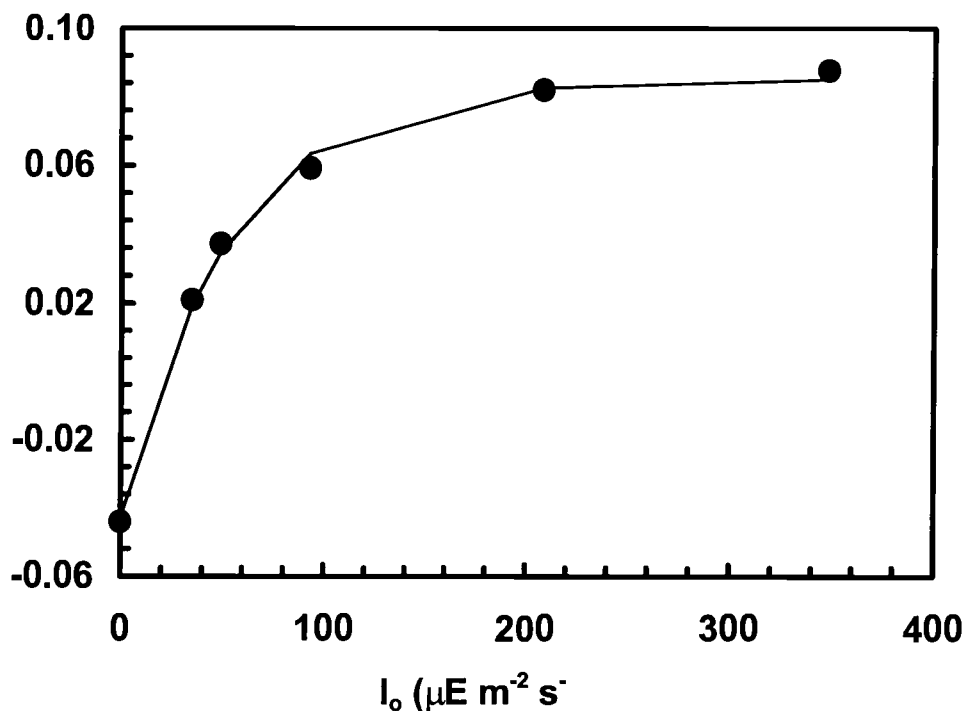


**Figure 4-5. Photosynthetic oxygen evolution rate vs incident light intensity (PI) curve for *Ochtodes secundiramea* microplantlets**

Table 4-9 illustrates that the estimated growth rates for all cultivations are very nearly equal to each other, supporting the conclusion that the metabolic activity of all cultivations was constant. Any differences in secondary metabolism can therefore be attributed to changing the bromide or vanadium delivery.

#### 4.2.1.2. Bromide Kinetic Data

Medium bromide concentration profiles are presented in Figures 4-6, 4-7 and 4-8. Figures 4-6 and 4-7 show cultivations carried out under vanadium delivery rates between 6.39 and 7.35  $\text{nmol L}^{-1} \text{day}^{-1}$ , while Figure 4-8 shows two different vanadium delivery rates of zero and 6.38  $\text{nmol L}^{-1} \text{day}^{-1}$ .

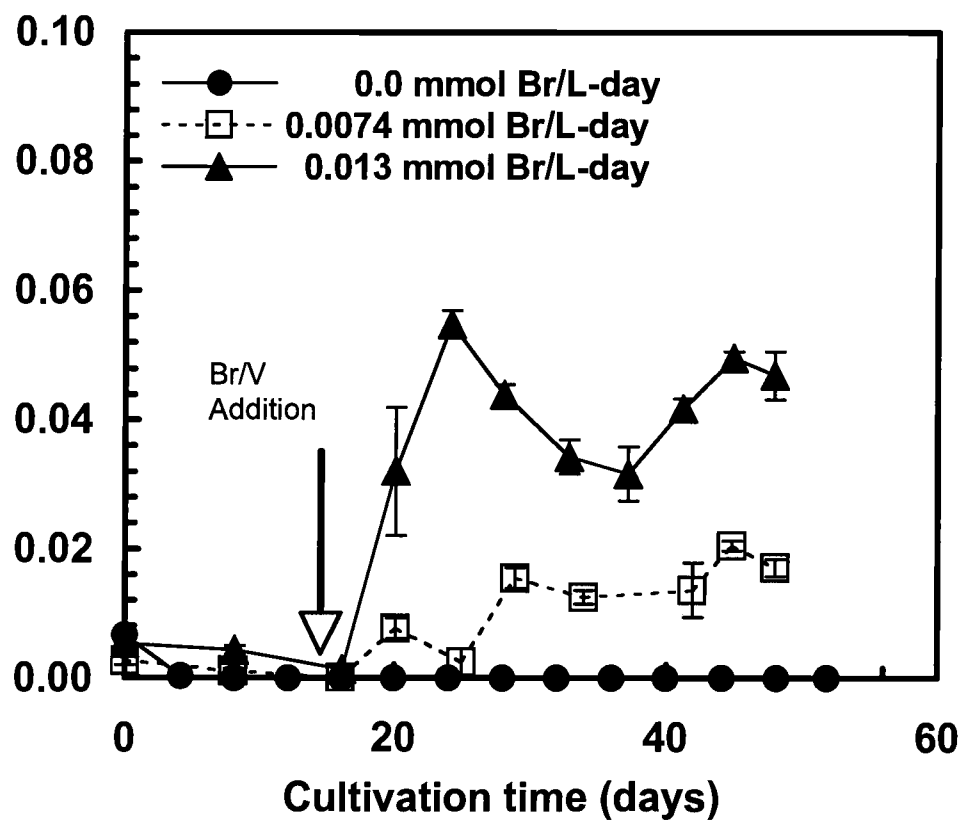


**Figure 4-6. Photobioreactor medium bromide concentration profiles for semi-continuous bromide delivery cultivations**

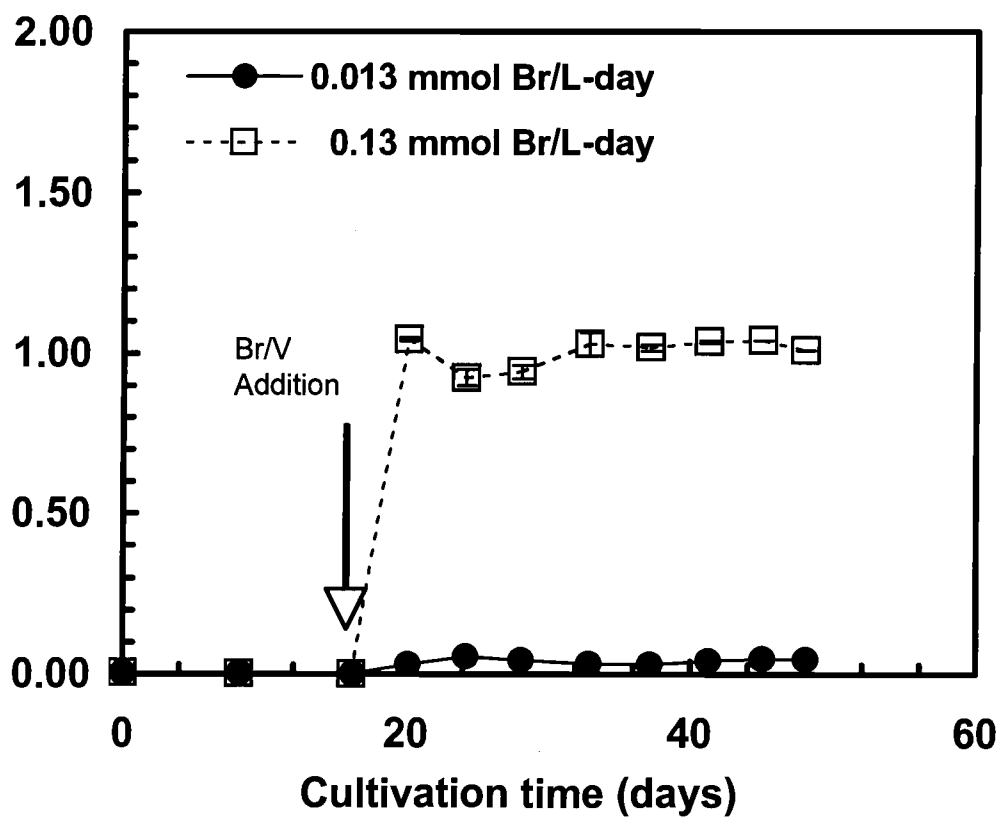


**Figure 4-7. Photobioreactor medium bromide concentration profiles for semi-continuous bromide delivery cultivations**

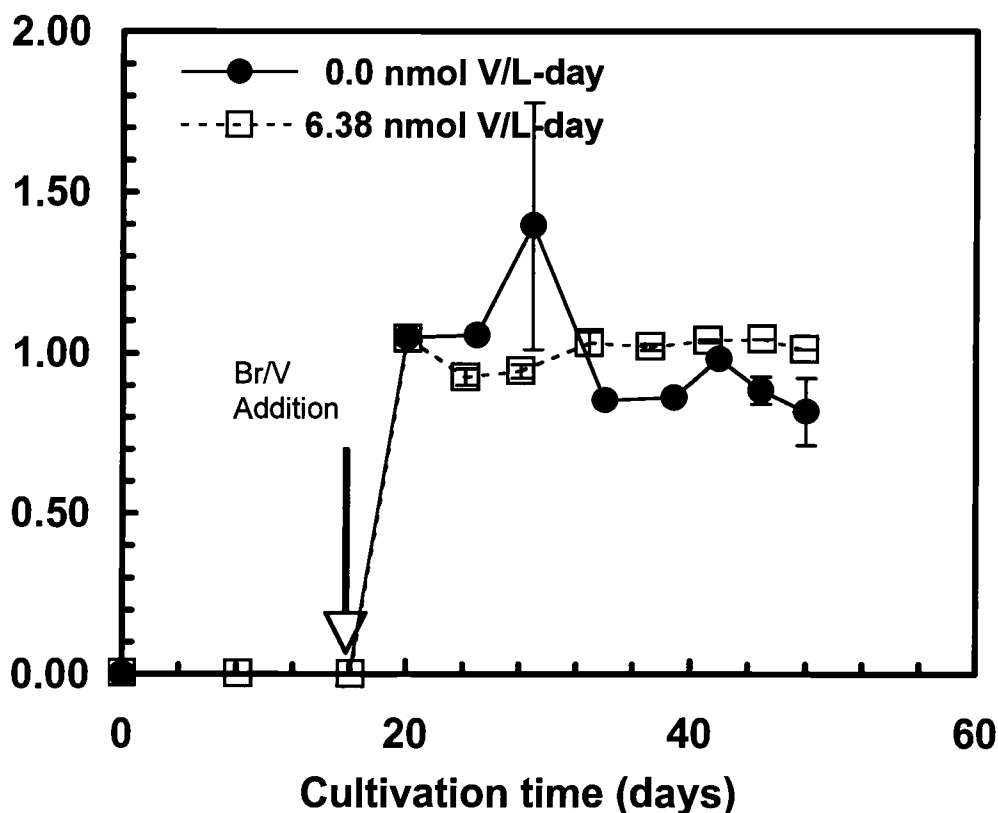


**Figure 4-8. Photobioreactor medium bromide concentration profiles for semi-continuous vanadium delivery cultivations**

Figures 4-6, 4-7 and 4-8 show that by replacing 1 L of medium with different bromide concentrations every 4 days, the concentration of bromide within the reactor could be maintained at different levels. For vanadium delivery experiments the bromide level was desired to be constant between cultivations, but vanadium delivery was to vary between zero and  $6.38 \text{ nmol V L}^{-1} \text{ day}^{-1}$ . No assay was used to determine the vanadium concentrations in the liquid medium. The concentration of bromide and vanadium to which the culture was constantly exposed was the manipulated variable for this study.



#### 4.2.1.3. Halogenated Monoterpene Kinetic Data

Profiles of the key halogenated monoterpenes identified in section 2.2 are presented in Figures 4-9 to 4-20. Figures 4-9 to 4-14 present the information for cultivations varying bromide delivery rate from 0.0 to 0.13 mmol Br L<sup>-1</sup> day<sup>-1</sup>, with a vanadium delivery rate between 6.39 and 7.35 nmol V L<sup>-1</sup> day<sup>-1</sup>. Figures 4-15 to 4-20 present the information for cultivations varying vanadium delivery rate between 0.0 and 6.38 nmol V L<sup>-1</sup> day<sup>-1</sup>, with a bromide delivery rate of 0.13 to 0.15 mmol Br L<sup>-1</sup> day<sup>-1</sup>.

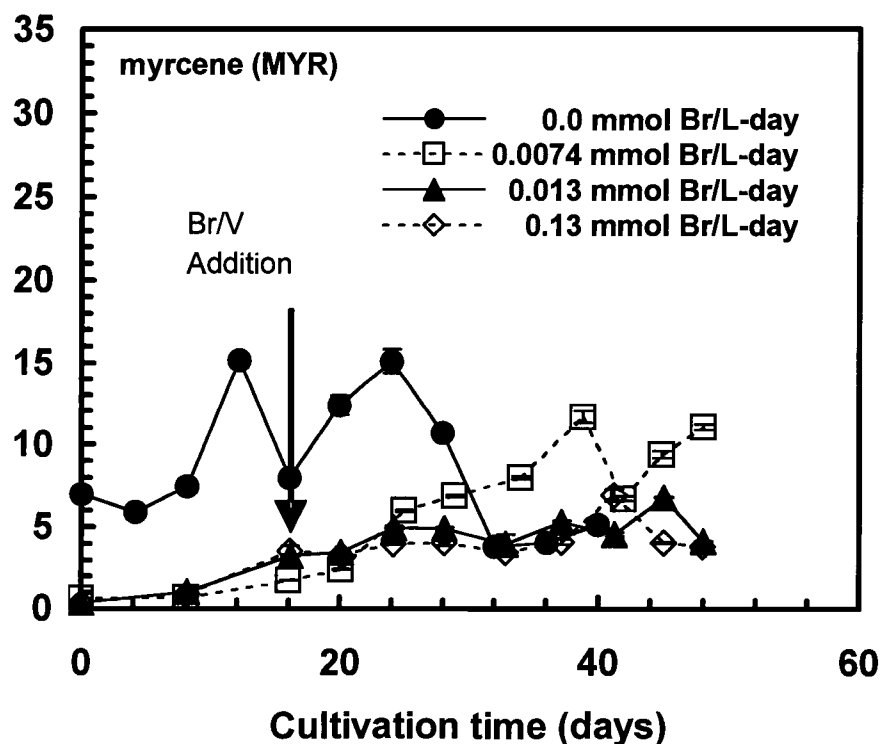


**Figure 4-9. Myrcene profiles for semi-continuous bromide delivery cultivations**

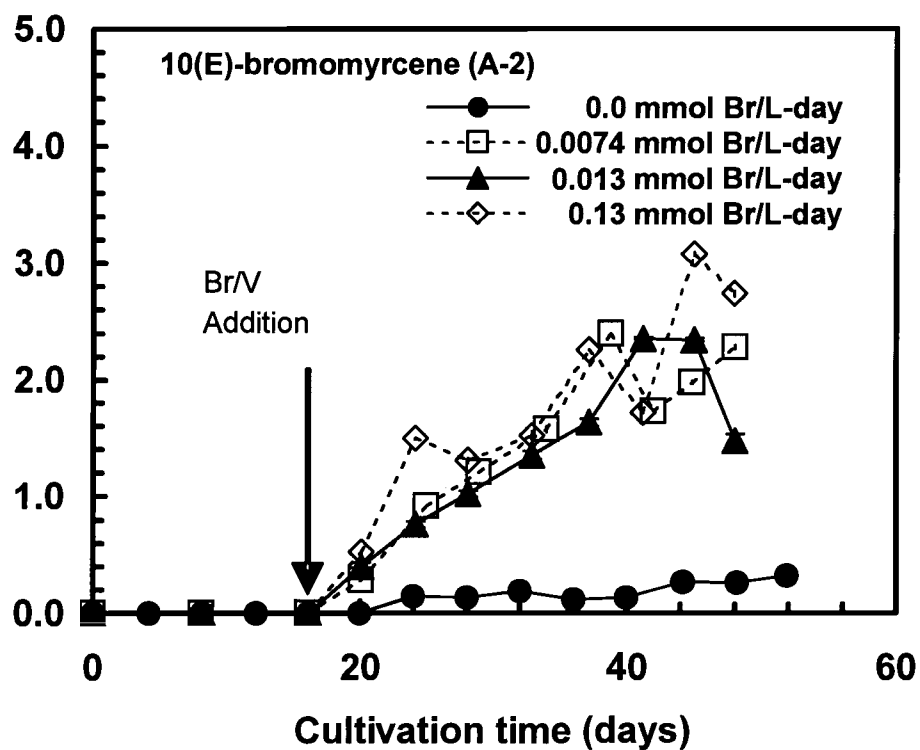


Figure 4-10. Compound A-2 (10(E)-bromomyrcene) profiles for semi-continuous bromide delivery cultivations

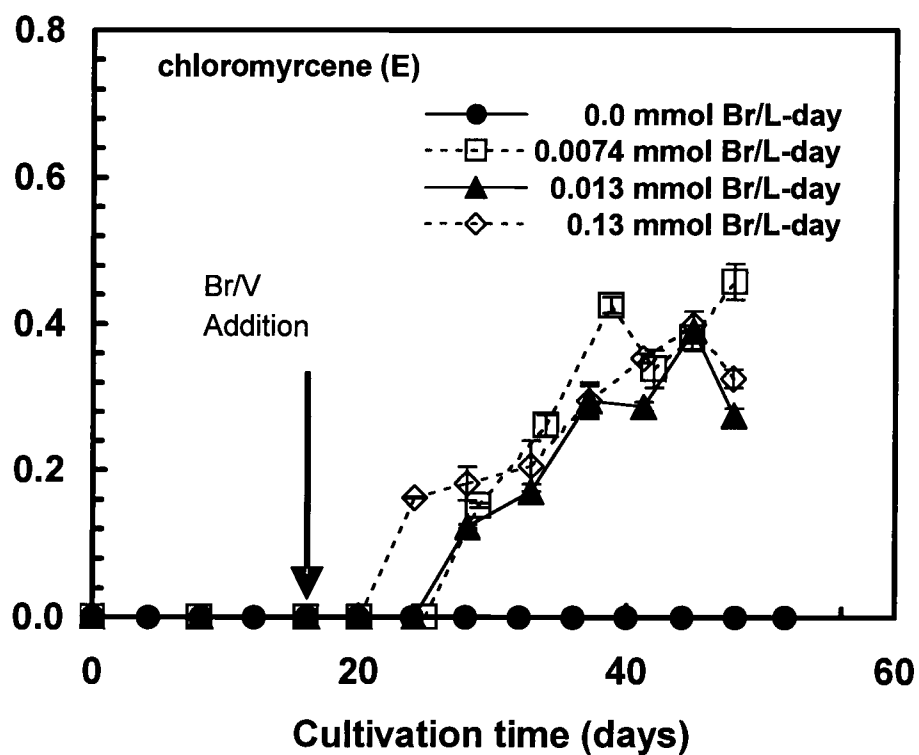
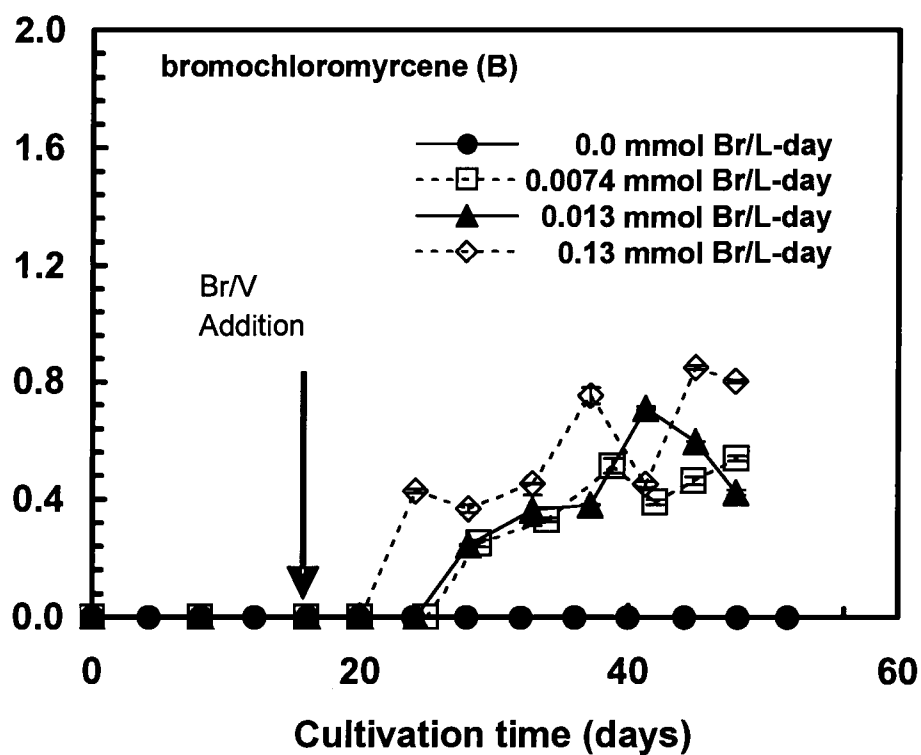


Figure 4-11. Compound E (chloromyrcene) profiles for semi-continuous bromide delivery cultivations



**Figure 4-12.** Compound B (bromochloromycene) profiles for semi-continuous bromide delivery cultivations

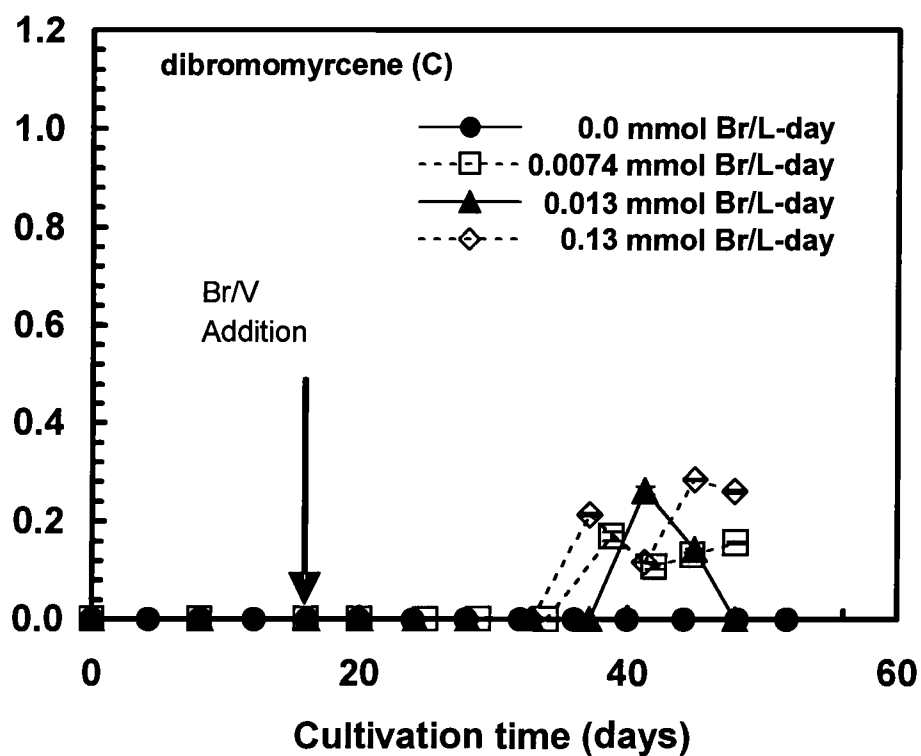


Figure 4-13. Compound C (dibromomyrcene) profiles for semi-continuous bromide delivery cultivations

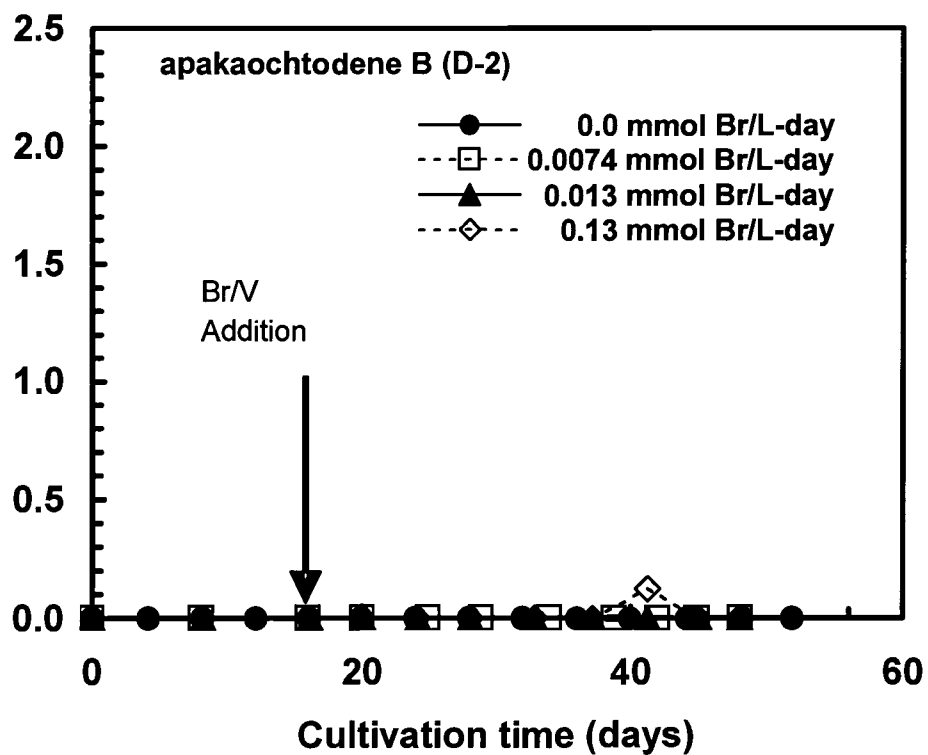


Figure 4-14. Compound D-2 (apakaochtodene B) profiles for semi-continuous bromide delivery cultivations

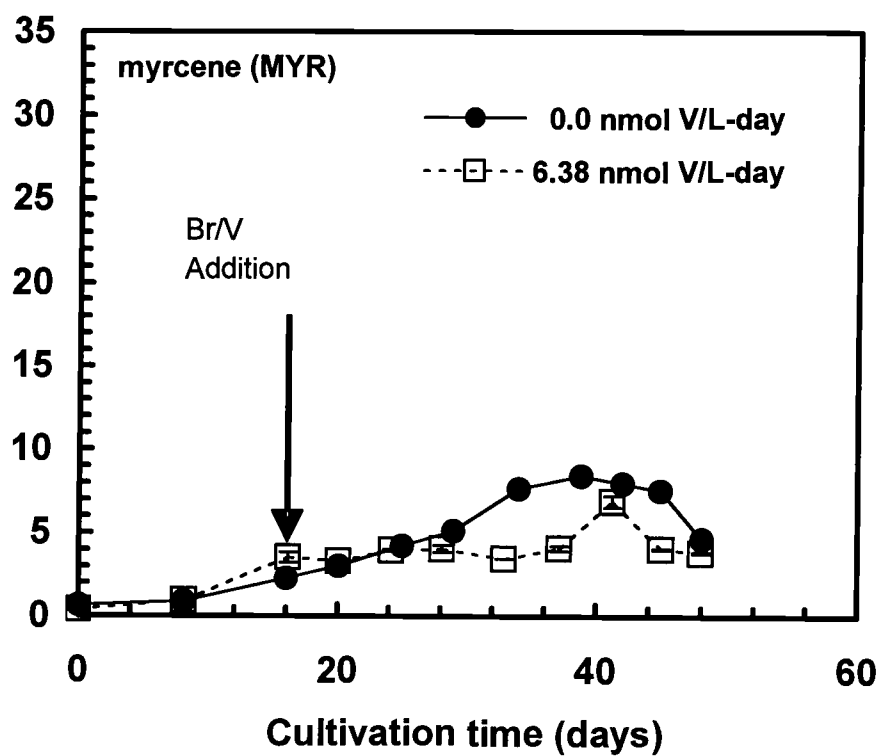


Figure 4-15. Myrcene profiles for semi-continuous vanadium delivery cultivations

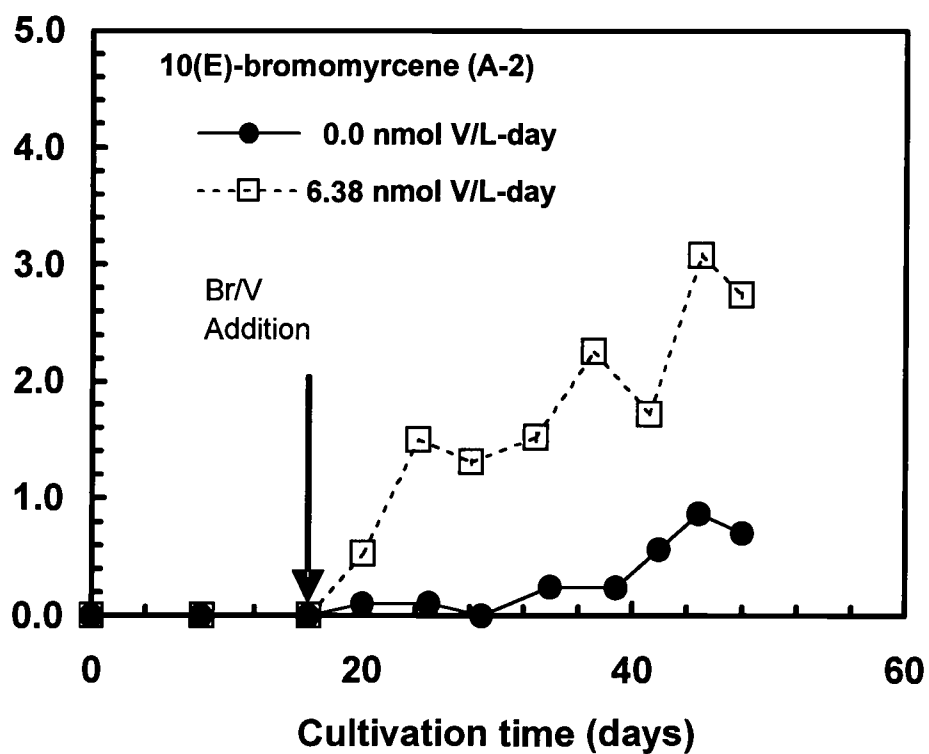
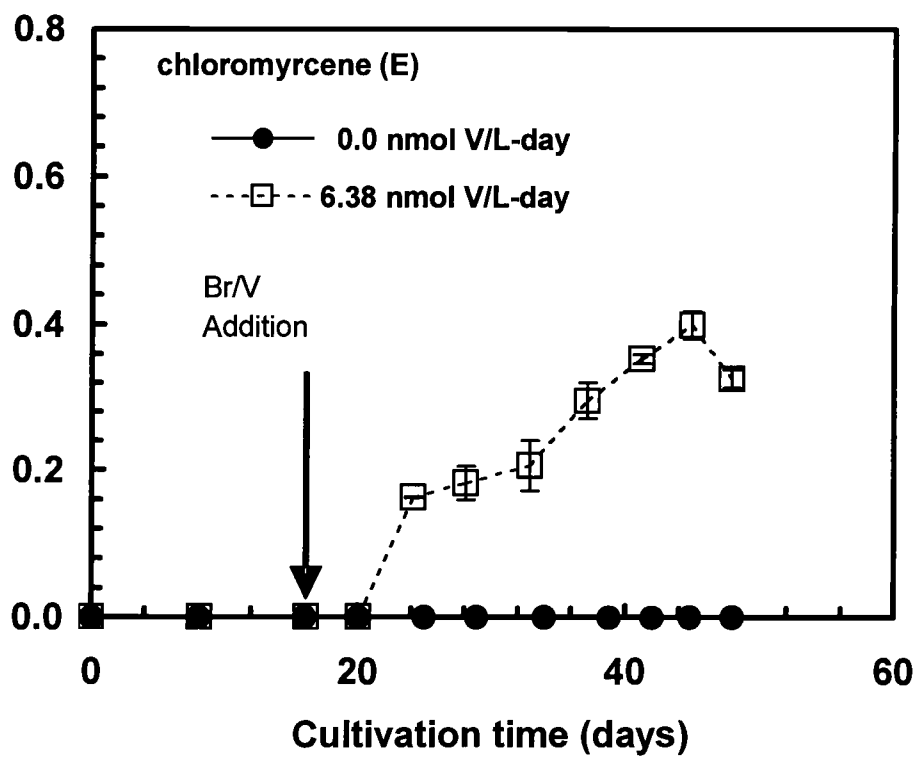
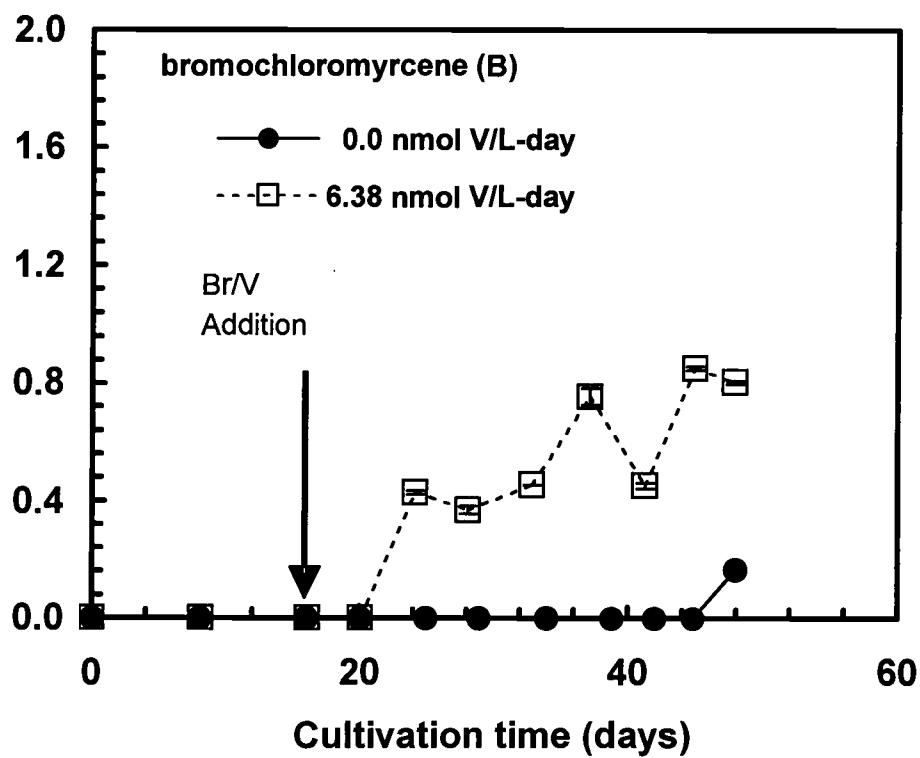


Figure 4-16. Compound A-2 (10(E)-bromomyrcene) profiles for semi-continuous vanadium delivery cultivations





**Figure 4-17. Compound E (chloromyrcene) profiles for semi-continuous vanadium delivery cultivations**



**Figure 4-18. Compound B (bromochloromyrcene) profiles for semi-continuous vanadium delivery cultivations**

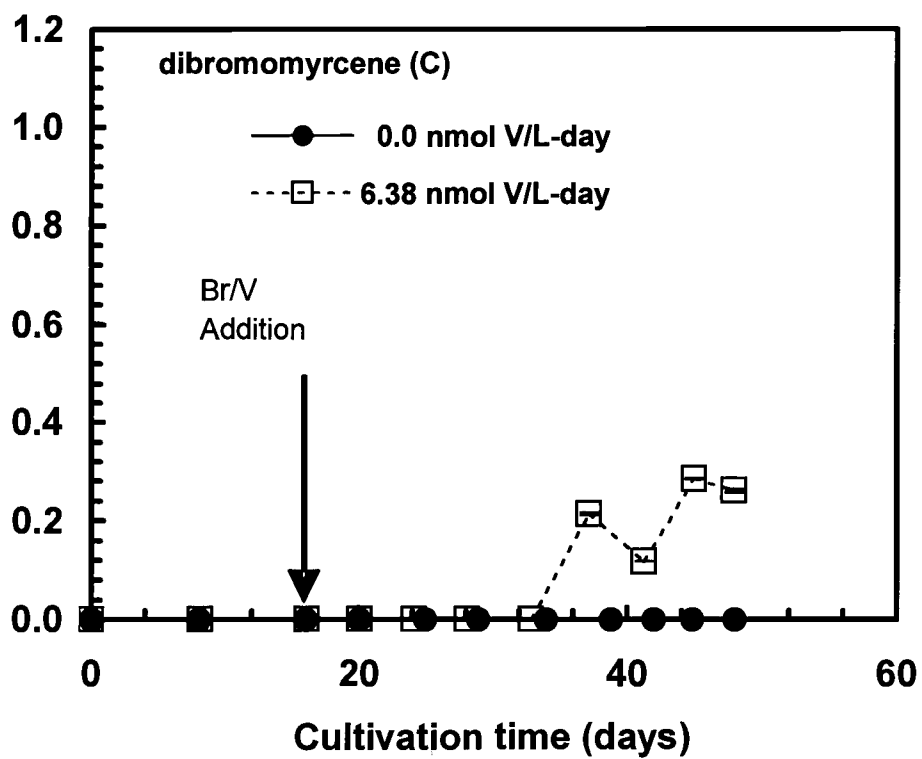


**Figure 4-19. Compound C (dibromomycene) profiles for semi-continuous vanadium delivery cultivations**

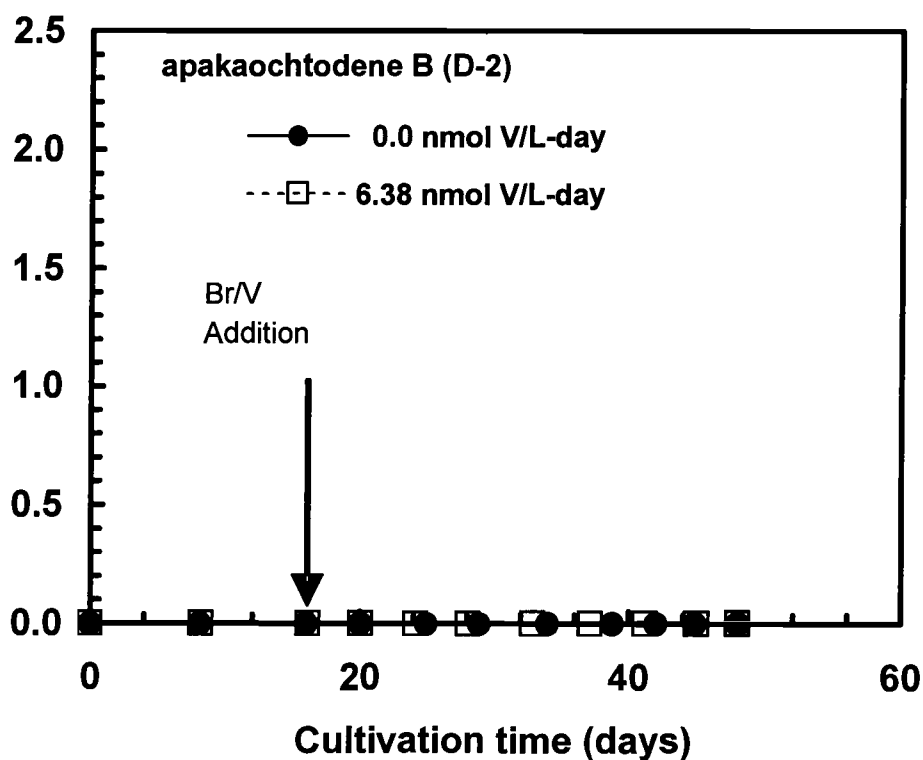


**Figure 4-20. Compound D-2 (apakaochtodene B) profiles for semi-continuous vanadium delivery cultivations**

There are no significant differences in halogenated monoterpene yields for cultivations varying bromide delivery between 0.0074 and 0.13 mmol Br L<sup>-1</sup> day<sup>-1</sup> for all products. There is a significant difference in yield between 0.0 and 0.0074 mmol Br L<sup>-1</sup> day<sup>-1</sup>, with 0.0 mmol Br L<sup>-1</sup> day<sup>-1</sup> only producing one compound, 10(*E*)-bromomyrcene (A-2). Myrcene profiles of bromide delivery between 0.0 and 0.13 mmol Br L<sup>-1</sup> day<sup>-1</sup> show similar yields.

There is a significant difference in yield between 0.0 and 6.38 nmol V L<sup>-1</sup> day<sup>-1</sup>, with 0.0 nmol V L<sup>-1</sup> day<sup>-1</sup> only producing one compound, 10(*E*)-bromomyrcene (A-2), at a much lower yield than for 6.38 nmol V L<sup>-1</sup> day<sup>-1</sup>.

Myrcene profiles of vanadium delivery between 0.0 and 6.38 nmol V L<sup>-1</sup> day<sup>-1</sup> show similar yields.

#### 4.2.2. Fed-Batch Cultivations

##### 4.2.2.1. Growth Data

Cultivations performed under pulsed bromide and vanadium delivery addition were designed to maintain the culture at a steady metabolic condition. Light and CO<sub>2</sub> delivery rates are detailed in Tables 4-3 and 4-4, and the specific growth rate is presented in Table 4-10.

The nitrate and phosphate concentrations of the liquid medium were measured over the cultivation time. These results are presented in Figures 4-26 to 4-29. Nitrate concentrations for all cultivations continue to increase throughout the cultivation and never reach zero. All cultivations have similar values at each sampling point. The phosphate concentration for all cultivations reach zero after 8 or 12 days. The metabolic activity was therefore limited by phosphate delivery rate for all cultivations. Phosphate and nitrate delivery rates were set to an N:P ratio of 19:1 as determined by Atkinson and Smith (1983) for balanced growth of red marine algae. An increase in the ratio of phosphate to nitrate would be required to prevent phosphate limitation. For the current study the N:P ratio was set to ensure consistency with earlier studies.

**Table 4-10. Estimated Specific Growth Rates for Fed-batch Bromide and Vanadium Delivery Cultivations** (all errors  $\pm 1$  s.e.)

	Bromide Conc. <sup>(a)</sup> (mmol Br L <sup>-1</sup> )				Vanadium Conc. <sup>(b)</sup> (nmol V L <sup>-1</sup> )	
	0.0	0.038	0.128	1.4	0.0	515
$M_0$ (g)	2.39	2.68	2.37	2.46	1.39	1.62
$M_f$ (g)	1.62	2.46	0.732	1.73	1.58	1.77
$t_0$ (day)	0	0	0	0	0	0
$t_f$ (day)	36	20	38	38	34	34
$r_s$ (g/day)	0.053 $\pm$ 0.0058	0.055 $\pm$ 0.0041	0.10 $\pm$ 0.0084	0.092 $\pm$ 0.0030	0.070 $\pm$ 0.0085	0.074 $\pm$ 0.0050
$\mu$ (day <sup>-1</sup> )	0.0160	0.0170	0.0330	0.0340	0.0520	0.0470

(a) Vanadium conc. = 515 nmol V L<sup>-1</sup>

(b) Bromide conc. = 1.4 mmol Br L<sup>-1</sup>

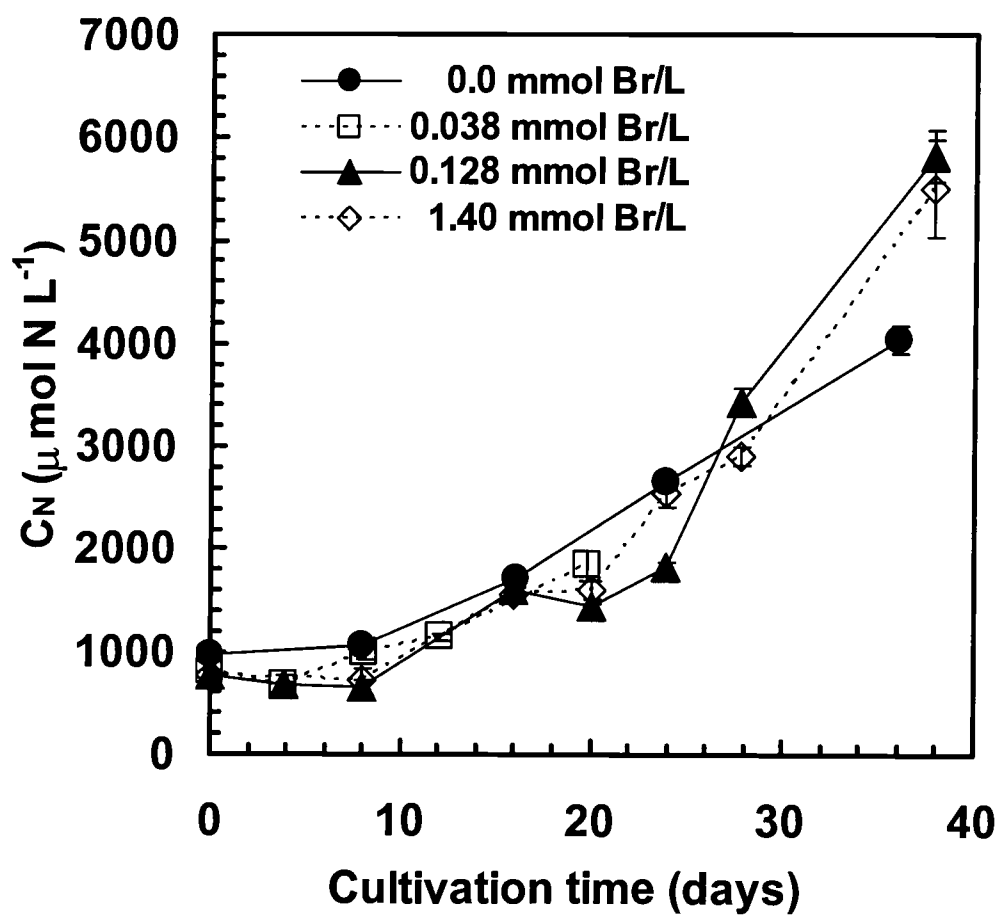
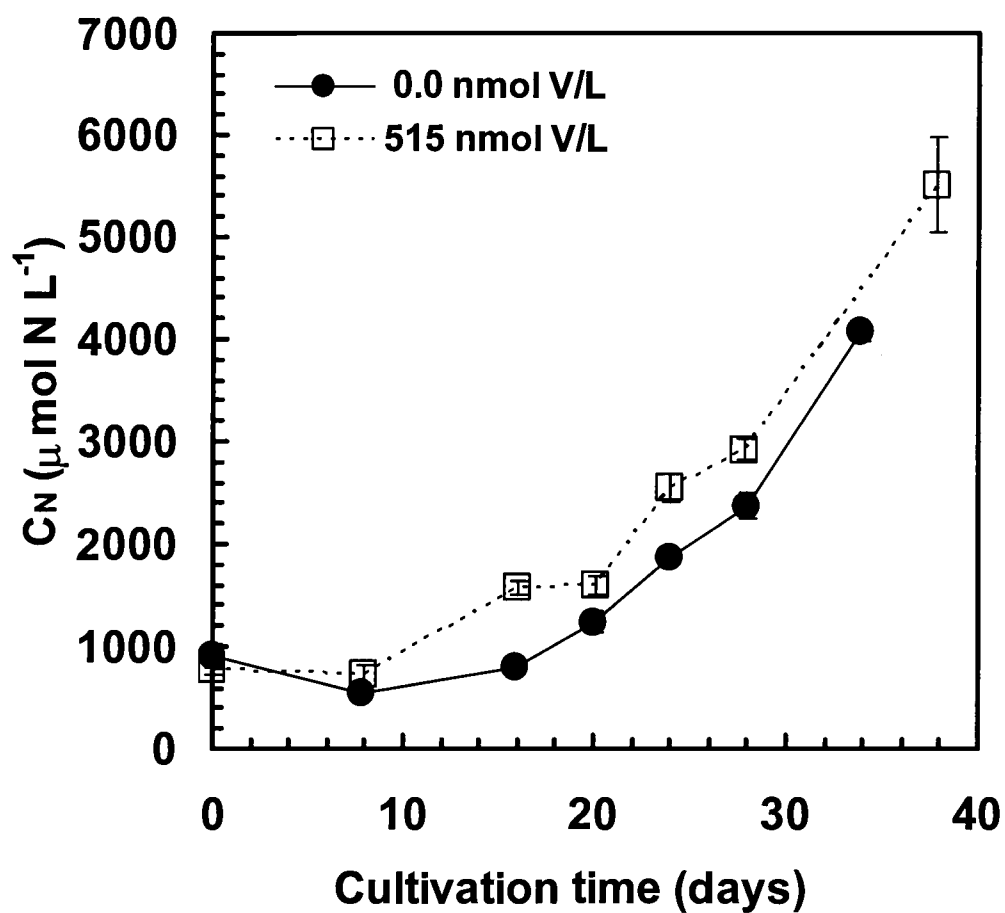


Figure 4-21. Photobioreactor medium nitrate concentration profiles for fed-batch bromide delivery cultivations



**Figure 4-22. Photobioreactor medium nitrate concentration profiles for fed-batch vanadium delivery cultivations**



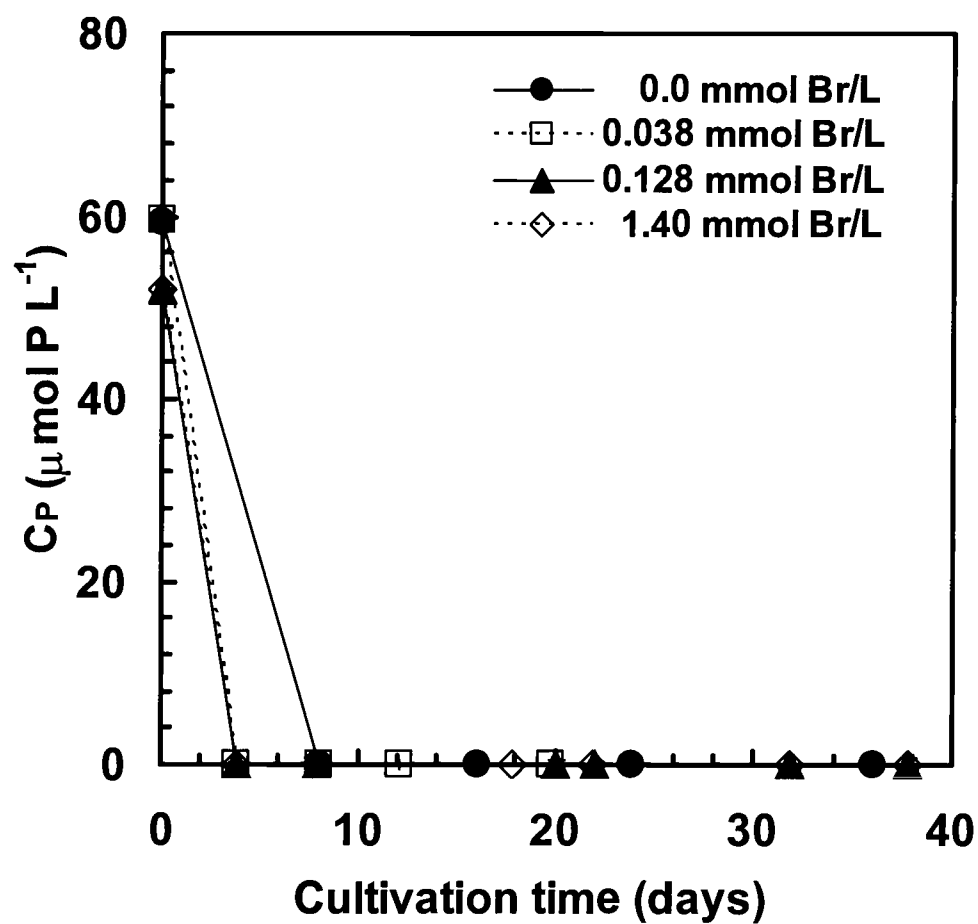
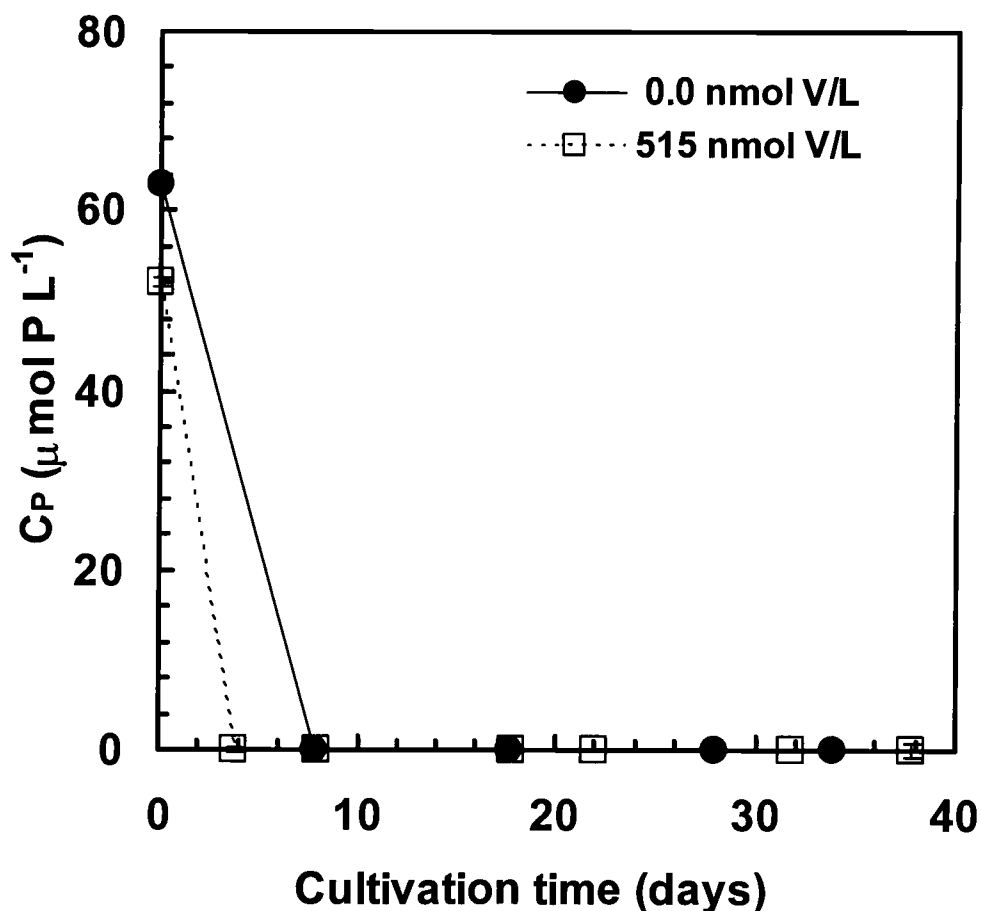


Figure 4-23. Photobioreactor medium phosphate concentration profiles for fed-batch bromide delivery cultivations



**Figure 4-24. Photobioreactor medium phosphate concentration profiles for fed-batch vanadium delivery cultivations**

Light delivery was set to  $143 \mu\text{E m}^{-2} \text{s}^{-1}$  for all cultivations. Figure 4-5 shows the P-I curve for microplantlets cultivated in bromide and vanadium free artificial medium. The curve shows that the incident light intensity is above saturation levels. Therefore, differences in metabolic activity cannot be attributed to light delivery.

CO<sub>2</sub> delivery was at two levels. (Tables 4-3 and 4-4) In all cultivations the calculation of the maximum transfer rate of CO<sub>2</sub> into the culture medium from the

aeration gas is greater than or approximately equal to the actual molar flow rate of  $\text{CO}_2$  into the reactor as illustrated in Tables 4-3 and 4-4. For all cultivations this molar flow rate is equal to  $0.20 \text{ mmol CO}_2 \text{ L}^{-1} \text{ h}^{-1}$  or  $0.29 \text{ mmol CO}_2 \text{ L}^{-1} \text{ h}^{-1}$ .

Table 4-10 illustrates that the estimated growth rates for cultivations at bromide concentrations of  $0.0$  and  $0.38 \text{ mmol Br L}^{-1}$  are approximately half that of bromide concentrations of  $0.128$  and  $1.4 \text{ mmol Br L}^{-1}$ . Growth rates for vanadium delivery cultivations are nearly equal to each other, but are greater than the growth rate for the bromide delivery cultivations. Given that the nitrate and phosphate profiles are identical for all cultivations, it seems likely that the differences in growth rate are not a result of differences in bromide or vanadium concentrations, but are a result of the difficulty in sampling the discrete units of *Ochtodes secundiramea* microplantlets. The method of calculating growth rate based solely on initial and final biomass values, which was utilized given the difficulty in obtaining representative biomass per volume samples, is likely the source of the differences. Any differences in secondary metabolism can therefore be attributed to the manipulated variable of bromide or vanadium delivery.

#### 4.2.2.2. Bromide Kinetic Data

Medium bromide concentration profiles are presented in Figures 4-25 to 4-27. Figures 4-25 and 4-26 show cultivations carried out under a vanadium concentration of  $416$  to  $515 \text{ nmol V L}^{-1}$ , while Figure 4-27 shows two different vanadium concentrations of zero and  $515 \text{ nmol L}^{-1}$ .

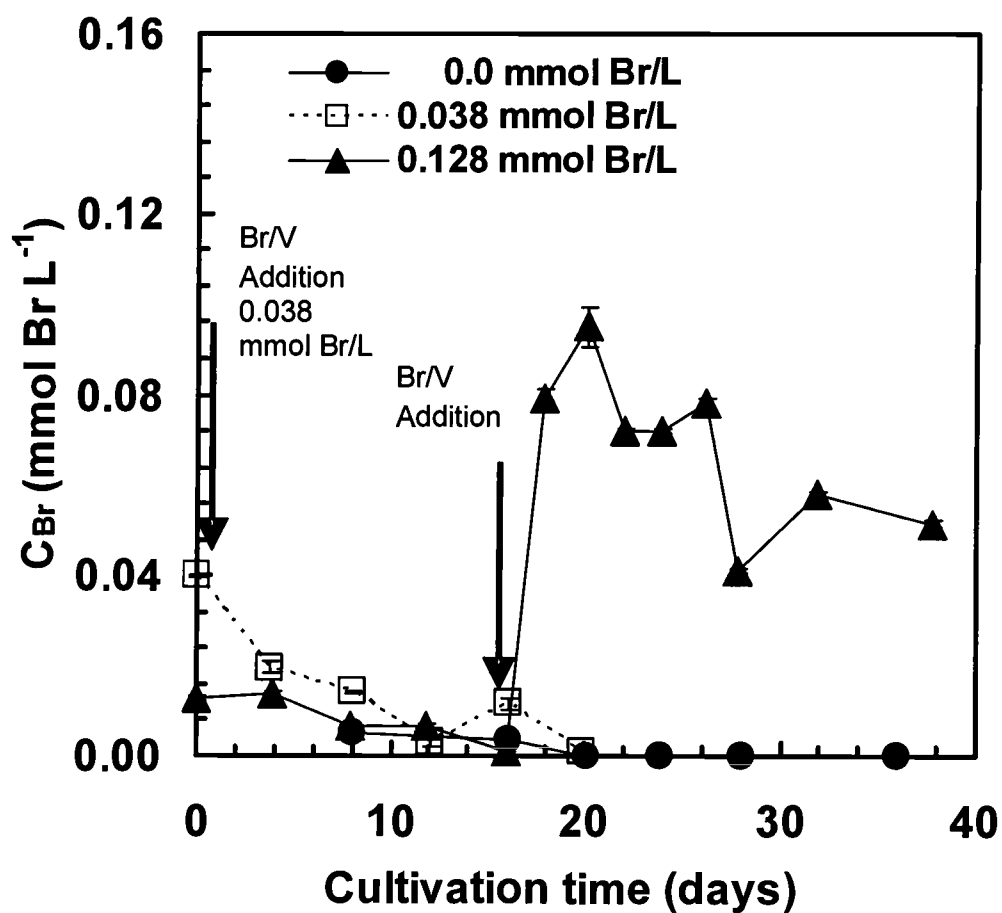


Figure 4-25. Photobioreactor medium bromide concentration profiles for fed-batch bromide delivery cultivations

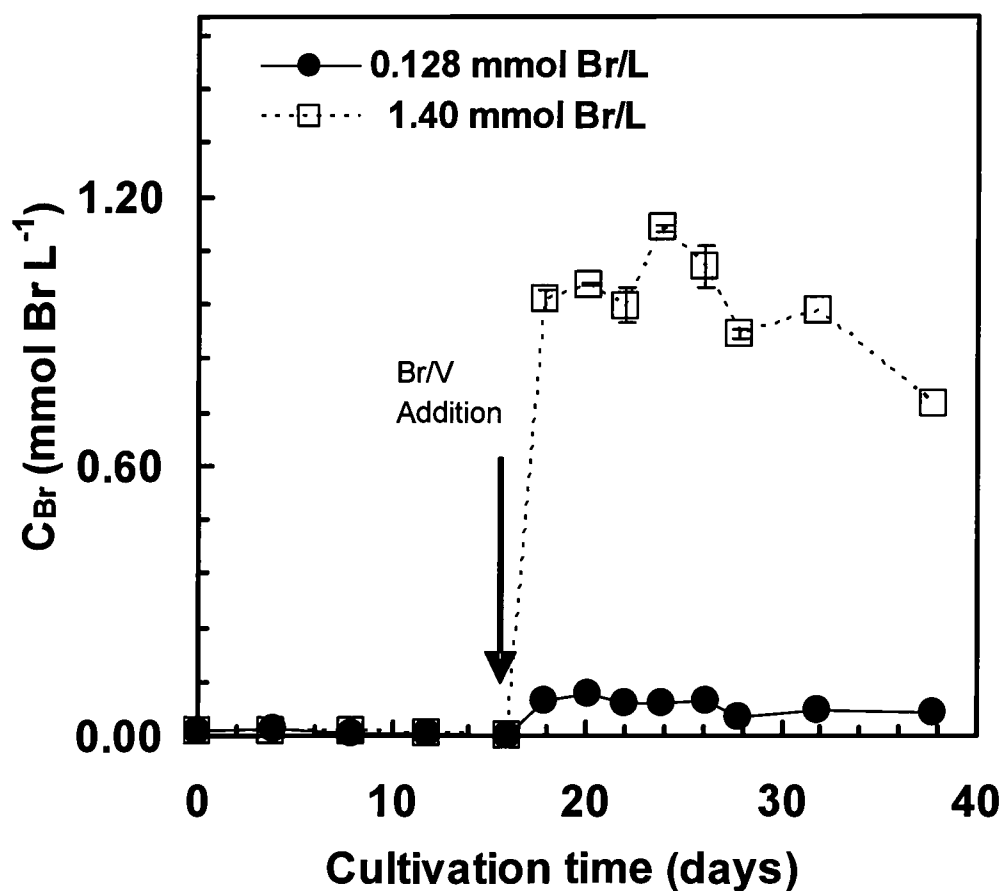
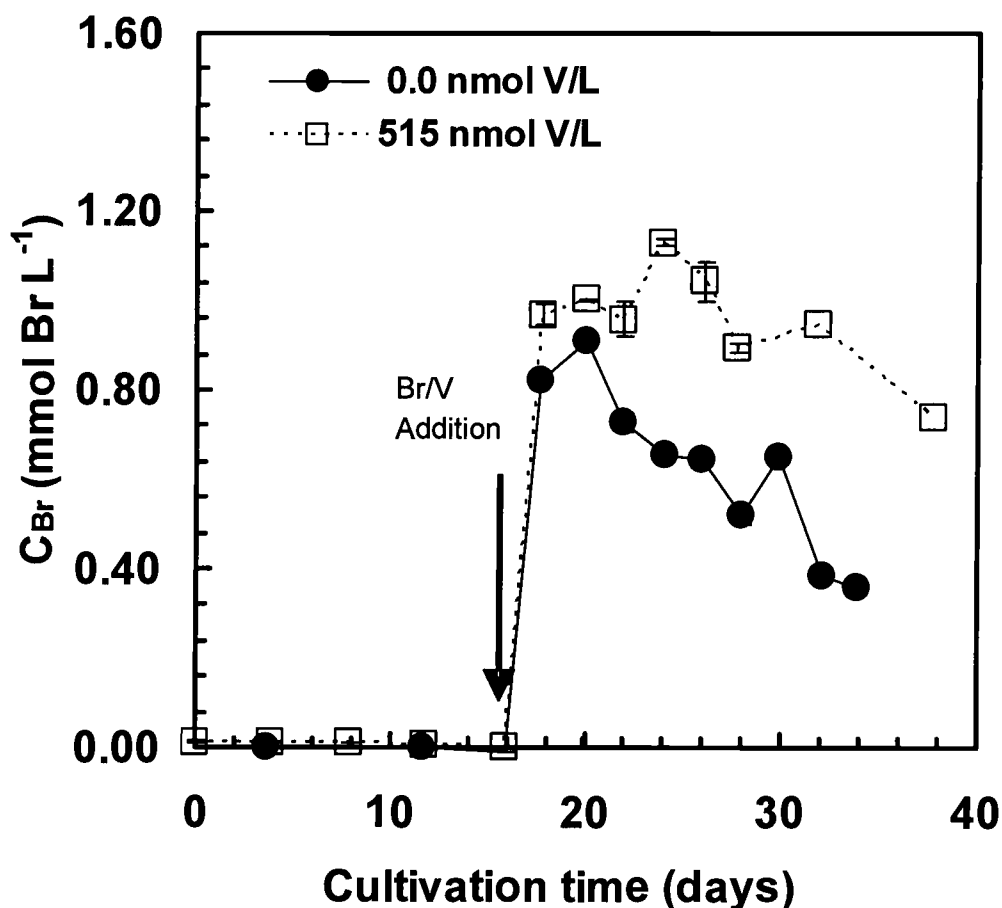


Figure 4-26. Photobioreactor medium bromide concentration profiles for fed-batch bromide delivery cultivations



**Figure 4-27. Photobioreactor medium bromide concentration profiles for fed-batch vanadium delivery cultivations**

The experimental design for fed-batch cultivations called for reactor medium bromide concentrations to be low enough so that consumption of bromide over time could be observed. An attempt was made to reach a low enough bromide concentration such that all bromide pulsed into the vessel would be consumed by the biomass. Figures 4-25 to 4-27 all show that bromide was significantly consumed in all cultivations even at a bromide concentration of  $1.40 \text{ mmol Br L}^{-1}$ . A bromide concentration of  $0.038 \text{ mmol Br L}^{-1}$  was the only non-zero bromide concentration to show a decrease in bromide concentration to zero.

#### 4.2.2.3. Halogenated Monoterpene Kinetic Data

Profiles of the key halogenated monoterpenes identified in section 2.2 are presented in Figures 4-28 to 4-39. Figures 4-28 to 4-33 present the information for cultivations varying bromide concentration from 0.0 to 1.40 mmol Br L<sup>-1</sup>, with a vanadium concentration of between 416 and 515 nmol V L<sup>-1</sup>. Figures 4-34 to 4-39 present the information for cultivations varying vanadium concentration between 0.0 and 515 nmol V L<sup>-1</sup> day<sup>-1</sup>, with a bromide concentration of 1.10 and 1.40 mmol Br L<sup>-1</sup>.

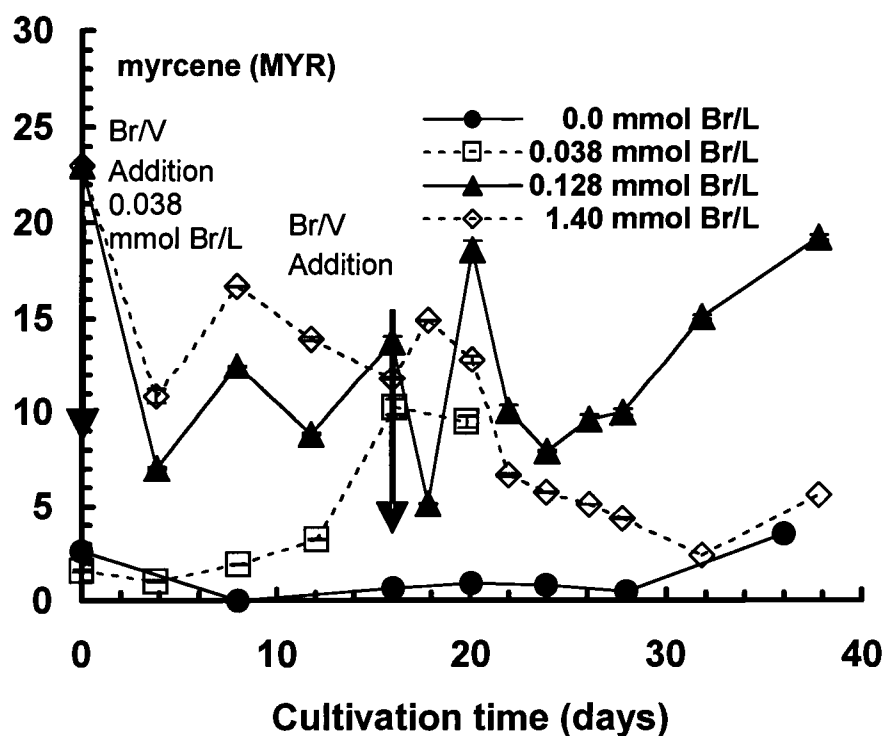


Figure 4-28. Myrcene profiles for fed-batch bromide delivery cultivations

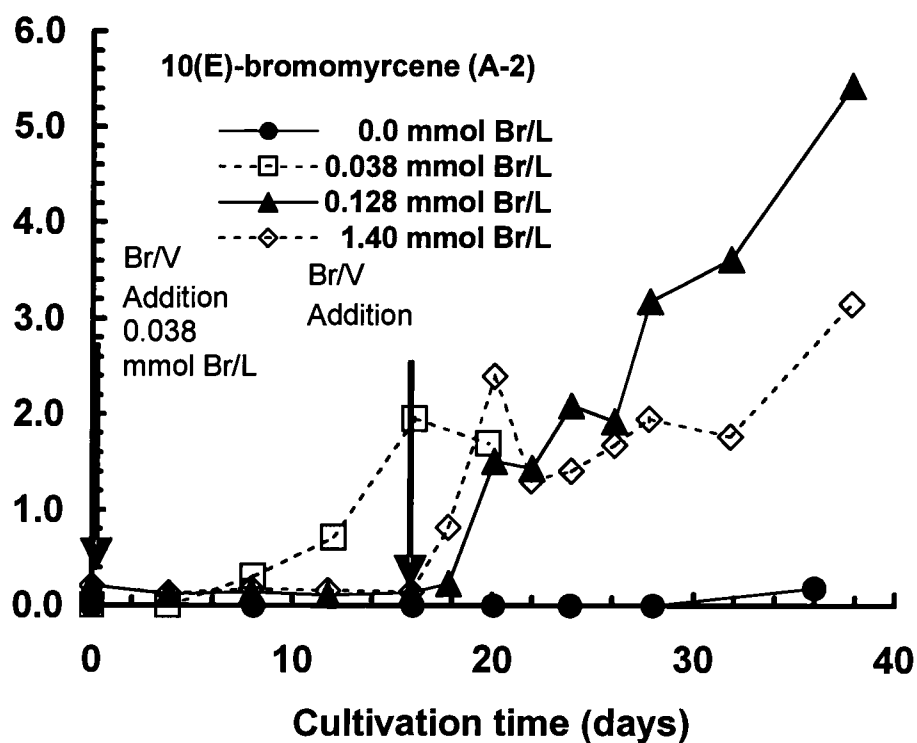
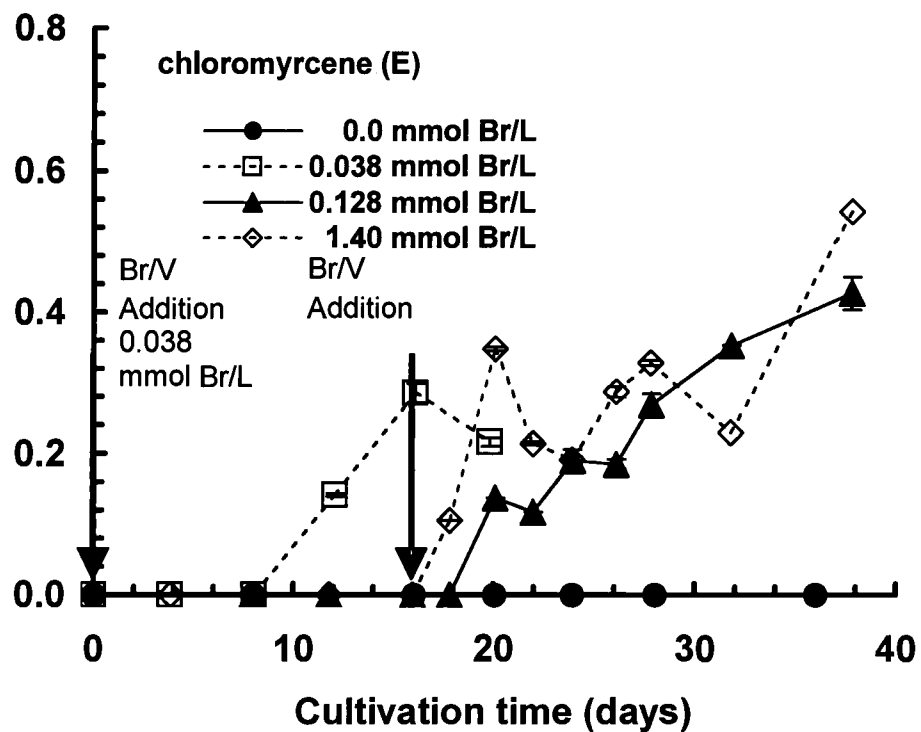
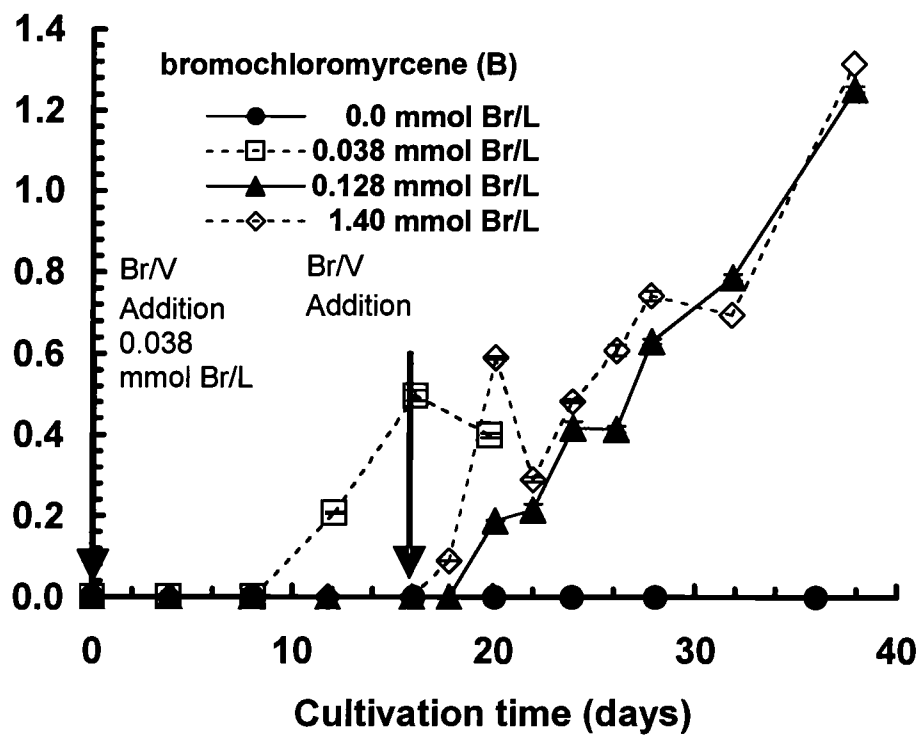


Figure 4-29. Compound A-2 (10(E)-bromomycene) profiles for fed-batch bromide delivery cultivations





**Figure 4-30. Compound E (chloromyrcene) profiles for fed-batch bromide delivery cultivations**



**Figure 4-31. Compound B (bromochloromyrcene) profiles for fed-batch bromide delivery cultivations**

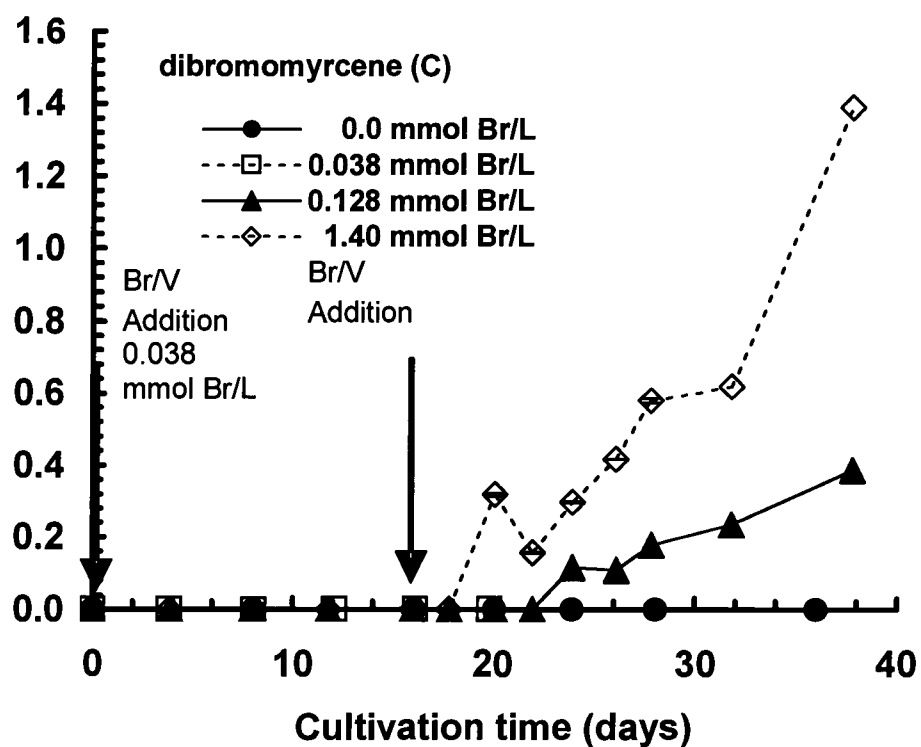


Figure 4-32. Compound C (dibromomyrcene) profiles for fed-batch bromide delivery cultivations

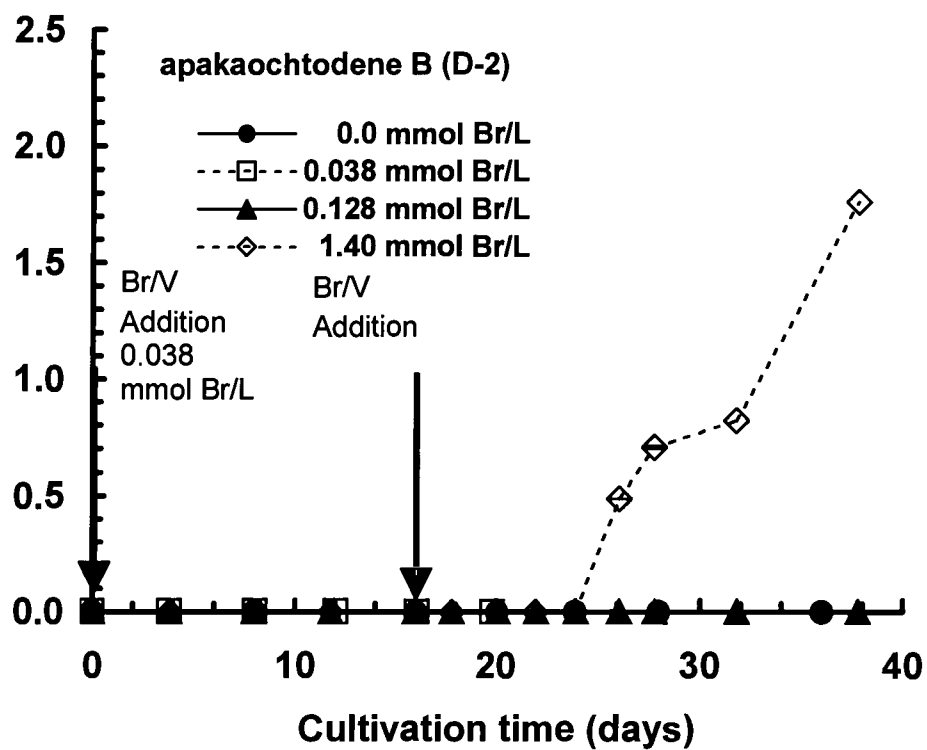


Figure 4-33. Compound D-2 (apakaochtodene B) profiles for fed-batch bromide delivery cultivations

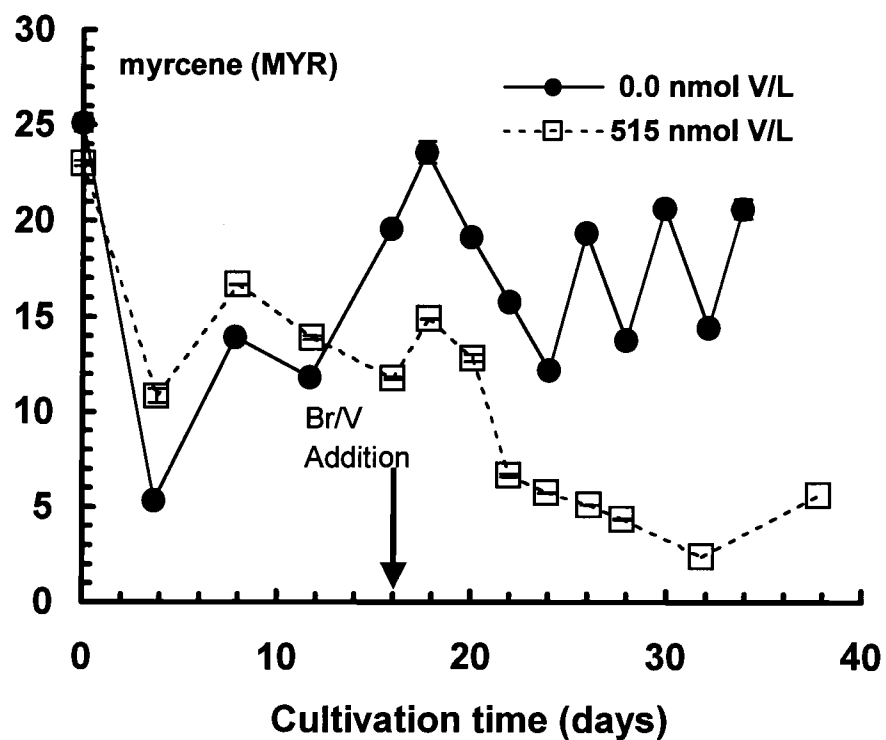


Figure 4-34. Myrcene profiles for fed-batch vanadium delivery cultivations

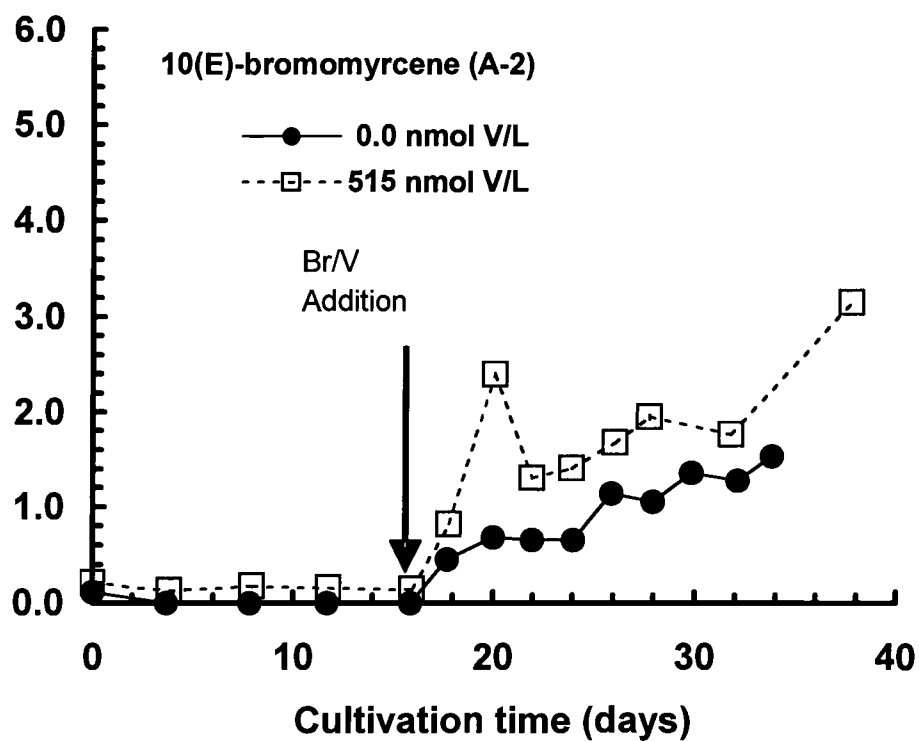
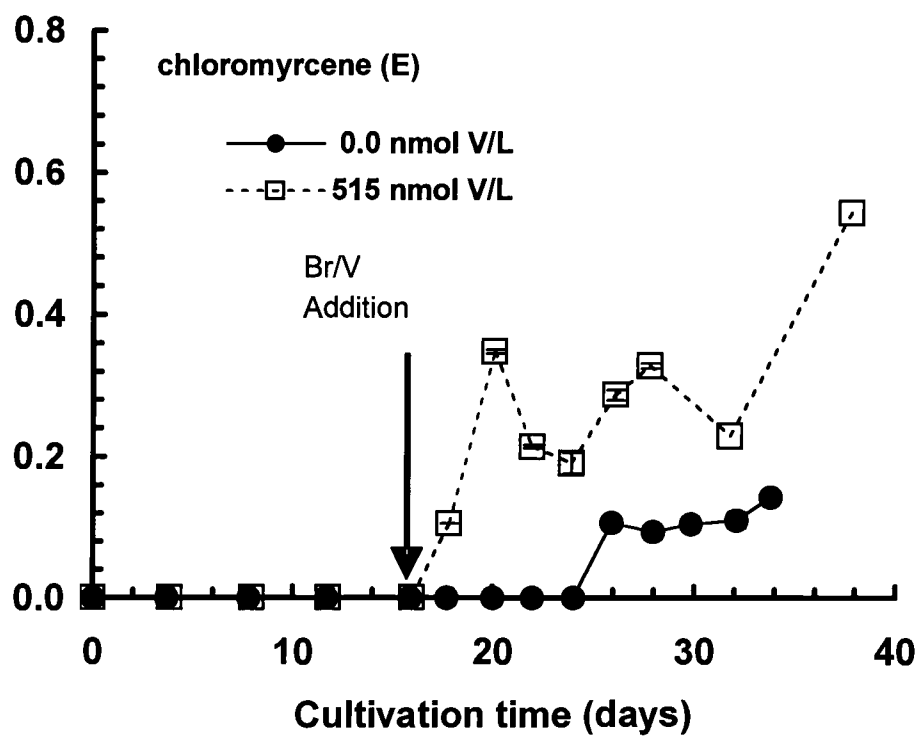
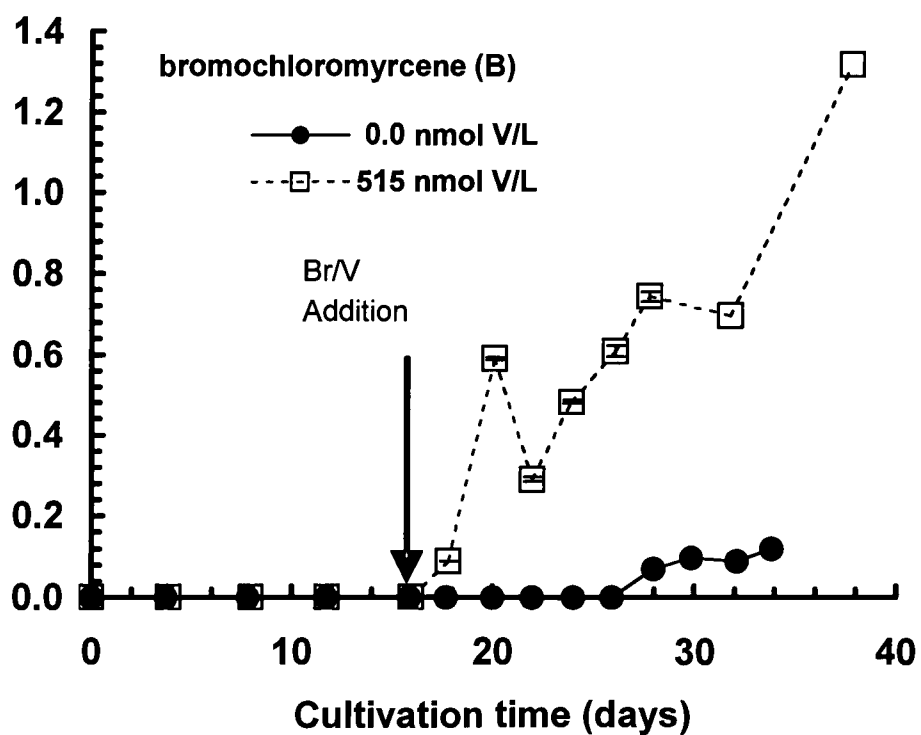


Figure 4-35. Compound A-2 (10(E)-bromomycene) profiles for fed-batch vanadium delivery cultivations



**Figure 4-36. Compound E (chloromyrcene) profiles for fed-batch vanadium delivery cultivations**



**Figure 4-37. Compound B (bromochloromyrcene) profiles for fed-batch vanadium delivery cultivations**



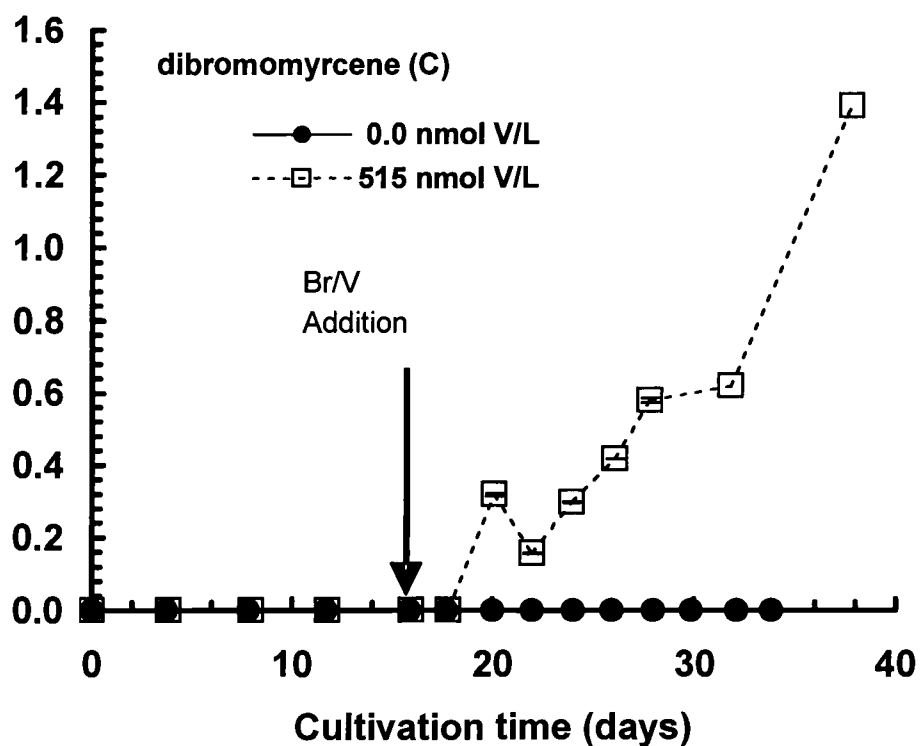


**Figure 4-38. Compound C (dibromomycene) profiles for fed-batch vanadium delivery cultivations**

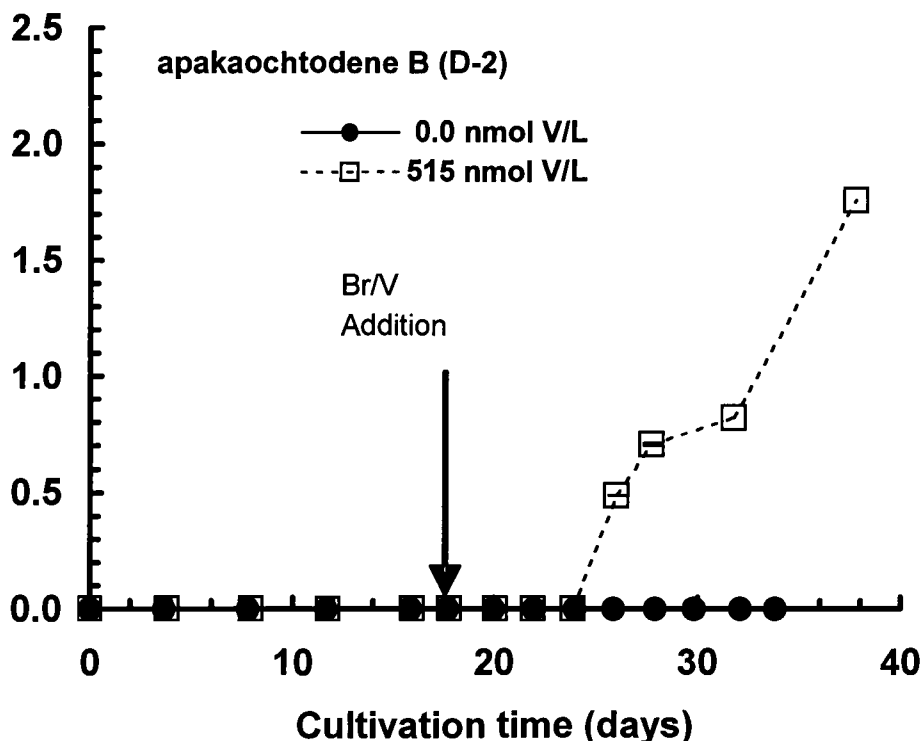


**Figure 4-39. Compound D-2 (apakaochtodene B) profiles for fed-batch vanadium delivery cultivations**

There are no significant differences in halogenated monoterpene yields for cultivations varying bromide concentrations between 0.038 and 1.40 mmol Br L<sup>-1</sup> for compounds A-2, E and B. There is a significant difference in yield between 0.038 and 1.40 mmol Br L<sup>-1</sup>, for compounds C and D-2. For compound C only 0.128 mmol Br L<sup>-1</sup> and 1.40 mmol Br L<sup>-1</sup> show any production, with 1.40 mmol Br L<sup>-1</sup> having a greater yield than 0.128 mmol Br L<sup>-1</sup>. For Compound D-2, only 1.40 mmol Br L<sup>-1</sup> shows any yield. Cultivation at 0.0 mmol Br L<sup>-1</sup> does not show production of any compounds and only slight production of myrcene. Myrcene was limited for 0.0 mmol Br L<sup>-1</sup> cultivation. Myrcene profiles of bromide concentrations between 0.038 and 1.40 mmol Br L<sup>-1</sup> are different, but do not illustrate any trends.

There are differences in yield for several compounds for cultivations varying vanadium concentration between 0.0 and 515 nmol V L<sup>-1</sup>. Cultivation at 515 nmol V L<sup>-1</sup> shows production of all compounds, and cultivation at 0.0 nmol V L<sup>-1</sup> shows production of compounds A-2, E and B. For compounds A-2, E and B the yield at 0.0 nmol V L<sup>-1</sup> was less than the yield at 515 nmol V L<sup>-1</sup>. Myrcene profiles for vanadium concentrations between 0.0 and 515 nmol V L<sup>-1</sup> start off with similar values but 515 nmol V L<sup>-1</sup> shows a reduction in myrcene concentration after day 20 while 0.0 nmol V L<sup>-1</sup> does not show a reduction in myrcene concentration. Myrcene profile for 0.0 nmol V L<sup>-1</sup> shows an oscillatory behavior after day 24. Addition of nutrients as a semi-continuous pulse every 4 days could explain the variations in myrcene concentration. Myrcene concentration has been shown to vary with nutrient concentration (Section 3.2.2).

### 4.3. METABOLIC NETWORK ANALYSIS

#### 4.3.1. Theory and Background

The increased use of genetic engineering to alter biosynthetic pathways of microorganisms has resulted in the increasing importance of metabolic engineering as a tool to formally calculate how genetic modifications affect the biosynthetic pathway (Stephanopoulos, 2002). Metabolic flux analysis allows for the simultaneous analysis of production rate data for every compound of a complex biosynthetic pathway.

Flux is the most critical parameter of a metabolic pathway, and the systematic approach of understanding these fluxes *in vivo* is of central importance to metabolic engineering (Stephanopoulos, et. al. 1998). Metabolic flux analysis

can be used to illustrate the rigidity, or resistance to change, of metabolic branch points to alterations in cultivation conditions, organism strain and genetic modification (Stephanopoulos and Vallino, 1991, Stephanopoulos, et. al. 1998). Once a rigid branch point is identified, genetic modifications can be made to reduce the rigidity or bypass the branch point (Stephanopoulos and Vallino, 1991).

The uniqueness of metabolic flux analysis lies in its approach to understand the entire network as a complex whole and not in the often failed attempt to isolate and understand a simplified limiting step. Attempts to overproduce key enzymes associated with limiting steps have often not resulted in overproduction of the desired metabolite precisely because of the complex control mechanisms in place that resist changes in metabolic flux not essential for growth (Stephanopoulos and Vallino, 1991).

Metabolic flux analysis requires that a metabolic pathway be known or logically proposed. From the pathway, stoichiometric relationships are determined, and can be solved within a set of matrices to estimate the steady-state flux through each step and branch in the pathway. Determination of metabolic fluxes requires the fluxes to adjust to new levels following perturbations to the cultivation. In Stephanopoulos and Vallino (1993) the concentrations of species around key branch points were measured over time in batch culture. The metabolic pathway under investigation was directly involved with primary metabolism, and therefore the changes in cultivation conditions within the batch culture were the perturbations applied. In the current study as well as many other studies (van Gulik, et. al., 2000; Follstad, et. al., 1999; and Aristidou, et. al., 1999), the metabolic pathway under investigation is not involved with primary metabolism, but rather a secondary product. For these studies it is important that primary metabolic flux reach a steady state so that carbon flux to the secondary metabolite can reflect adjustments to applied perturbations not to unsteady state changes in primary metabolism. To

ensure that primary metabolism reaches a steady state, continuous chemostat cultivations are employed (van Gulik, et. al., 2000; Follstad, et. al., 1999; and Aristidou, et. al., 1999).

#### 4.3.2. Biosynthetic Pathway

A proposed biosynthetic pathway for cyclic and acyclic halogenated monoterpene production in *Ochtodes secundiramea* is presented in Figure 4-40. The biosynthesis of halogenated monoterpenes begins with the oxidation of bromide to an enzyme bound bromonium ion ( $\text{Br}^+$ ) at the oxovanadium active site of a vanadium dependent bromoperoxidase (Butler, 1999). Bromoperoxidase has been shown to be present in *Ochtodes secundiramea* (Tucker and Rorrer 2001). The enzyme bound bromonium ion will preferentially attack the  $\Delta^{6-10}$  olefinic bond of myrcene to form a tertiary carbonium ion at C6, with Markovnikov addition of bromide at C10. The loss of hydrogen to eliminate the carbonium ion restores the double bond at C6 to yield 10-bromomyrcene. Addition of a second bromide via the same mechanism will yield di-bromomyrcene.

Chlorinating peroxidases have not been found in marine algae (Butler, 1999), but chlorination can occur by passive attack of a chloride ion on a bromide generated carbonium ion. The addition of  $\text{Br}^+$  to  $\Delta^{6-10}$  and  $\Delta^{2-3}$  followed by attack of  $\text{Cl}^-$  at the carbonium ion at  $\Delta^{2-3}$  generates the  $\text{BrCl}$  derivative. Removal of  $\text{HBr}$  from  $\Delta^{2-3}$  and rearrangement of the double bonds yields the final structure of compound B. This mechanism is likely behind the production of the chlorinated compounds E, B and D-2.

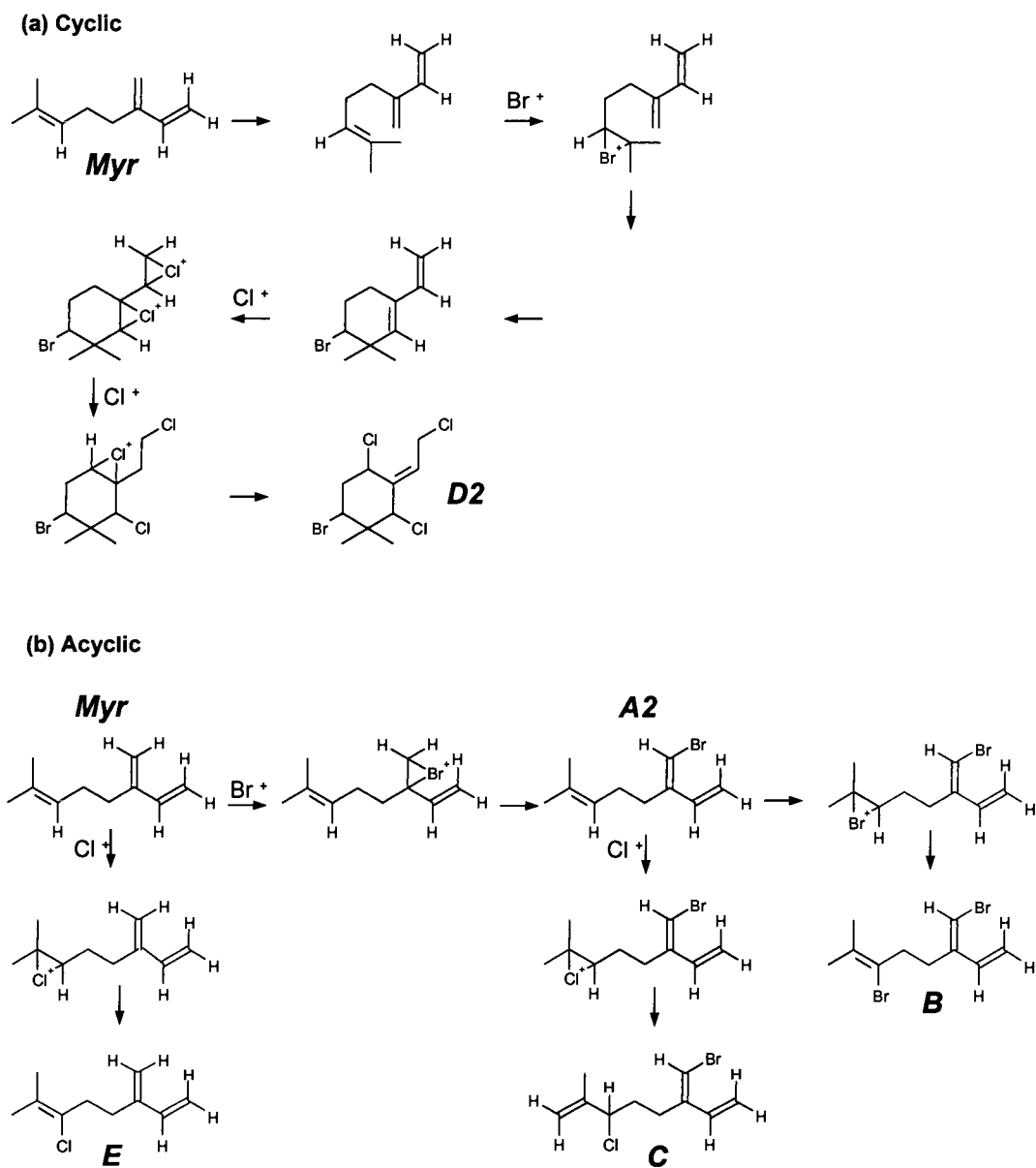


**Figure 4-40. Proposed biosynthetic pathway for production of halogenated monoterpenes in *Ochtodes secundiramea* microplantlets**

### 4.3.3. Metabolic Flux Model Development

A simplified version of the biosynthetic pathway presented in Figure 4-40, illustrating the branch points of the bioreaction network is presented in Figure 4-41.

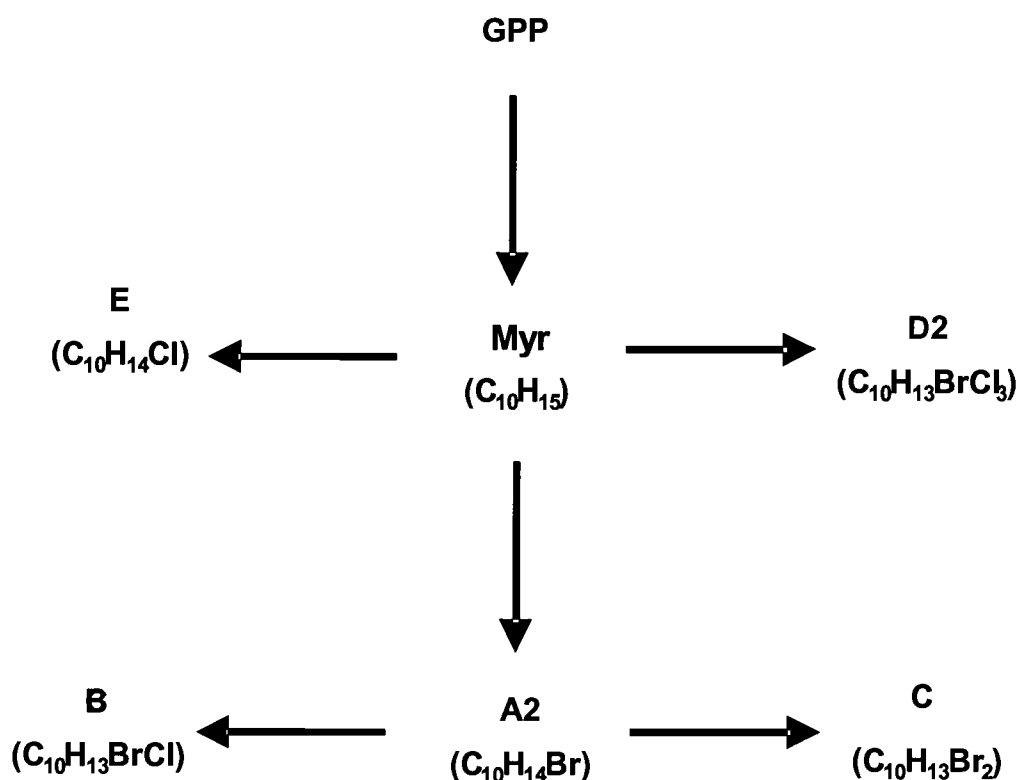


**Figure 4-41. Putative metabolic pathway from myrcene to identified halogenated monoterpenes**

Regio and stereo chemistry and detailed intermediate product formation are not shown in Figure 4-41. Metabolic flux analysis allows for an understanding of branch point control. Since the fluxes through the pathway must be at steady state to be calculated, intermediate steps in a linear pathway can be lumped together and

are not important as individual steps. A detailed knowledge of pathway intermediates is therefore not required.

From the proposed pathway, stoichiometric relationships can be determined and the matrices relating the production rate to the flux can be evaluated. For the pathway described in Figure 4-41 the set of equations relating compound production to flux are:

$$r_{Myr} = v_{Myr-GPP} - v_{A2-Myr} - v_{E-Myr} - v_{D2-Myr} \quad (4-10)$$

$$r_{A2} = v_{A2-Myr} - v_{B-A2} - v_{C-A2} \quad (4-11)$$

$$r_B = v_{B-A2} \quad (4-12)$$

$$r_C = v_{C-A2} \quad (4-13)$$

$$r_E = v_{E-Myr} \quad (4-14)$$

$$r_{D2} = v_{D2-Myr} \quad (4-15)$$

where  $r_i$  is compound  $i$  production rate, and  $v_{i-j}$  is the flux to compound  $i$  from compound  $j$ .

An assumption must be made as to the production rate of myrcene. Myrcene is the key intermediate linking biosynthesis of GPP to the halogenation reactions, and the step change in Br/V concentration should not affect the flux of myrcene. Therefore, myrcene production will be in pseudo-steady state. The pseudo-steady state argument says that changes in metabolic pools adjust quickly to perturbations and can be assumed to not change over time resulting in a zero production rate (Stephanapolous, et. al. 1998). The assumption has been applied by many others in determining metabolic fluxes through pathways in continuous



steady state cultivations. (Aristidou, et. al. 1999; Follstad, et. al., 1999; and van Gulik, et. al., 2000). The above set of equations can be written in matrix form as:

$$R = GV \quad (4-16)$$

$$\begin{pmatrix} r_{myr} \\ r_{A2} \\ r_B \\ r_C \\ r_E \\ r_{D2} \end{pmatrix} = \begin{pmatrix} 1 & -1 & 0 & 0 & -1 & -1 \\ 0 & 1 & -1 & -1 & 0 & 0 \\ 0 & 0 & 1 & 0 & 0 & 0 \\ 0 & 0 & 0 & 1 & 0 & 0 \\ 0 & 0 & 0 & 0 & 1 & 0 \\ 0 & 0 & 0 & 0 & 0 & 1 \end{pmatrix} \begin{pmatrix} v_{Myr-GPP} \\ v_{A2-Myr} \\ v_{B-A2} \\ v_{C-A2} \\ v_{E-Myr} \\ v_{D2-Myr} \end{pmatrix} \quad (4-17)$$

The matrix of pathway fluxes can be easily determined from:

$$V = RG^{-1} \quad (4-18)$$

$$\begin{pmatrix} v_{Myr-GPP} \\ v_{A2-Myr} \\ v_{B-A2} \\ v_{C-A2} \\ v_{E-Myr} \\ v_{D2-Myr} \end{pmatrix} = \begin{pmatrix} r_{myr} \\ r_{A2} \\ r_B \\ r_C \\ r_E \\ r_{D2} \end{pmatrix} \begin{pmatrix} 1 & -1 & 0 & 0 & -1 & -1 \\ 0 & 1 & -1 & -1 & 0 & 0 \\ 0 & 0 & 1 & 0 & 0 & 0 \\ 0 & 0 & 0 & 1 & 0 & 0 \\ 0 & 0 & 0 & 0 & 1 & 0 \\ 0 & 0 & 0 & 0 & 0 & 1 \end{pmatrix}^{-1} \quad (4-19)$$

The matrix analysis allows for easy manipulation of the large set of reaction equations, and can be altered between different proposed pathways by changing the stoichiometric coefficients contained in matrix G.

#### 4.3.4. Flux Rigidity

To illustrate the application of metabolic engineering for the understanding of metabolic pathway control, results from semi-continuous bromide and vanadium delivery cultivations at two different delivery rates will be run through the matrix analysis. Table 4-11 shows the compound production rates estimated by applying equation 4-9 to the compound yield vs time data. Table 4-12 shows the results for the metabolic flux analysis for end cases of bromide and vanadium delivery. Since there is no difference in compound production rate for bromide delivery rates between 0.0074 and 0.13 mmol Br L<sup>-1</sup> day<sup>-1</sup>, the end cases used for the matrix analysis only need to be 0.0 and 0.13 mmol Br L<sup>-1</sup> day<sup>-1</sup>.

**Table 4-11. Compound Production Rates for Key Halogenated Monoterpenes for Semi-continuous Bromide and Vanadium Delivery Cultivations** (all errors  $\pm 1$  s.e.)

		Bromide Delivery Rate		Vanadium Delivery Rate	
		(mmol Br L <sup>-1</sup> day <sup>-1</sup> )		(nmol V L <sup>-1</sup> day <sup>-1</sup> )	
		0.0	0.13	0.0	6.38
Compound	$r_{\text{myr}}$	0.0	0.0	0.0	0.0
Production Rate	$r_{A2}$	0.016 $\pm$ 0.003	0.164 $\pm$ 0.027	0.040 $\pm$ 0.016	0.164 $\pm$ 0.027
( $\mu\text{mol}$	$r_B$	0.0	0.047 $\pm$ 0.010	0.0	0.047 $\pm$ 0.010
compound	$r_C$	0.0	0.011 $\pm$ 0.006	0.0	0.011 $\pm$ 0.006
g DW <sup>-1</sup> day <sup>-1</sup> )	$r_{D2}$	0.0	0.0	0.0	0.0
	$r_E$	0.0	0.022 $\pm$ 0.003	0.0	0.022 $\pm$ 0.003

**Table 4-12. Compound Flux for Semi-continuous Bromide and Vanadium Delivery Cultivations**

		Bromide Delivery Rate		Vanadium Delivery Rate	
		(mmol Br <sup>-</sup> L <sup>-1</sup> day <sup>-1</sup> )		(nmol V L <sup>-1</sup> day <sup>-1</sup> )	
		0.0	0.13	0.0	6.38
Compound Flux ( $\mu\text{mol compound}$ $\text{g DW}^{-1} \text{ day}^{-1}$ )	$V_{\text{Myr-GPP}}$	0.016	0.244	0.040	0.244
	$V_{\text{A2-Myr}}$	0.016	0.222	0.040	0.222
	$V_{\text{B-A2}}$	0.0	0.047	0.0	0.047
	$V_{\text{C-A2}}$	0.0	0.011	0.0	0.011
	$V_{\text{E-Myr}}$	0.0	0.022	0.0	0.022
	$V_{\text{D2-myrr}}$	0.0	0.0	0.0	0.0

The results from the matrix analysis of the cultivation data shows distinctly different compound fluxes between 0.0 and 0.13 mmol Br L<sup>-1</sup> day<sup>-1</sup> for all compounds. Likewise for vanadium delivery between 0.0 and 6.38 nmol V L<sup>-1</sup> day<sup>-1</sup>, there is a significant difference between compound fluxes for all compounds. The flux to compound A-2 is greater than to compound B, which is greater than to compound E. There was no flux to compound C or D-2 for all cases. For the zero delivery rates, only compound A-2 was formed.

Figures 4-9 and 4-15 show that the concentration of myrcene never approaches zero, in fact the concentration of myrcene is 2-3 times higher than the concentration of compound A-2, the halogenated monoterpene with the greatest concentration. Therefore, myrcene biosynthesis did not limit halogenated monoterpene biosynthesis, and would not be a target for enhancement by genetic modification.

The assumption of zero net myrcene production rate causes the flux to myrcene to equal the sum of the fluxes to compounds A-2, D-2 and E. Therefore

any differences in myrcene flux are a result of differences in flux to compounds A-2, D-2 and E. A detailed analysis of the differences in fluxes to compounds A-2, D-2 and E will follow, but a separate analysis of myrcene flux need not be done.

Production of monochlorinated compound E did not occur during bromide limitation suggesting that the mechanism of producing chlorinated compounds in *Ochtodes secundiramea* occurs via a bromonium ion attack on electron rich double bond with replacement by a chloride ion as described in section 4.3.2. Addition of a chloroperoxidase enzyme via genetic modification to *Ochtodes secundiramea* would be a suitable strategy to improve the production of chlorinated compounds E and D-2 relative to other compounds. Cultivation of an altered organism under bromide limitations with an inserted chloroperoxidase enzyme would preferentially produce chlorinated compounds E and D-2.

The production of compound A-2 during zero bromide or vanadium delivery suggests the importance of this branch of the pathway. This step, acting as the first committed step for higher acyclic halogenated monoterpene synthesis, is, however, not likely the rate limiting step. Accumulation of compound A-2 under bromide limitation as well as the absence of compounds B and C under bromide limitation suggests that the rate of production of A-2 is not limiting the production of the other compounds. Also, during high bromide and vanadium delivery, compound A-2 builds up at a higher rate than compounds B and C suggesting again that A-2 production is not limiting the production of higher acyclic halogenated monoterpenes. The bromination of compound A-2 to form compound C and the chlorination of compound A-2 to form compound B are likely the rate limiting steps.

Compounds B and C are not formed when compound A-2 is produced at the zero bromide delivery rate also suggesting that they are substrate limited and

enhancement of the bromoperoxidase enzyme would have no effect on production rate unless bromide concentration was also increased.

Compound B (BrCl derivative) is formed at a higher rate than compound E (Cl derivative) and compound C (Br<sub>2</sub> derivative) for bromide and vanadium delivery rates of 0.13 mmol Br L<sup>-1</sup> day<sup>-1</sup> and 6.38 mmol V L<sup>-1</sup> day<sup>-1</sup>, respectively. This result suggests that passive Cl<sup>-</sup> attack on a bromonium induced carbonium ion occurs more readily when a bromide has already been added to the substrate. There may be allosteric hindrance imposed by the C10 bromide of compound A-2 that reduces the binding ability of the substrate to the active site of the bromoperoxidase enzyme allowing for increased likelihood of chloride attack at C6. Higher production of compound A-2 relative to E would be expected under this theory considering that myrcene contains no bromide to interfere with binding to the bromoperoxidase active site. Modifications of the bromoperoxidase enzyme to improve binding of brominated compound A-2 would likely improve the selectivity for production of compound C over compound B.

Compound A-2 is formed at a higher rate for zero vanadium delivery than for zero bromide delivery. The artificial medium used for the bromide and vanadium free cultivations likely had very low levels of vanadium present as an impurity from the NaCl used for the artificial medium. Zero vanadium delivery experiments likely delivered a very low level of vanadium in addition to adding bromide at a rate of 0.13 mmol Br L<sup>-1</sup> day<sup>-1</sup>. The zero bromide delivery experiments added 6.60 nmol V L<sup>-1</sup> day<sup>-1</sup>. At reduced vanadium levels, the concentration of active bromoperoxidase enzyme should be reduced relative to saturated levels of vanadium. The activity of the bromoperoxidase enzyme was sufficient under vanadium limitation to have a greater production rate of compound A-2 than for cultivations under bromide limitation. The higher rate of compound A-2 production under zero vanadium delivery adds to the evidence of the

importance of bromide availability over enzyme activity to the bromination reactions.

#### 4.4. REFERENCES

- Aristidou, A.A., San, K.Y., and Bennett, G.N. 1999. Metabolic flux analysis of *Escherichia coli* expressing the *Bacillus subtilis* acetolactate synthase in batch and continuous cultures. *Biotechnology and Bioengineering* **63**: 737-749.
- Atkinson, M.J., Smith, S.V. 1983. C:N:P ratios of benthic marine plants. *Limnol Oceanogr* **28**: 568-574.
- Butler, A., and Walker, J.V. 1993. Marine haloperoxidases. *Chemistry Reviews* **93**: 1937-1944.
- Butler, A. 1999. Mechanistic considerations of the vanadium haloperoxidases. *Coordination Chemistry Reviews* **187**: 17-35.
- Fenical, W. 1975. Halogenation in the rhodophyta—a review. *Journal of Phycology* **11**: 245-259.
- Follstad, B.D., Balcarcel, R.R., Stephanopoulos, G.N., and Wang, D.I.C. 1999. Metabolic flux analysis of hybridoma continuous culture steady state multiplicity. *Biotechnology and Bioengineering* **63**: 675-683.
- Huang, Y.M., Maliakal, S., Cheney, D.P., and Rorrer, G.L. 1998. Comparison of development and photosynthetic growth for filament clump and regenerated microplantlet cultures of *Agardhiella subulata* (Rhodophyta, Gigartinales). *Journal of Phycology* **34**: 893-901.
- Kitade, Y., Yamazaki, S., Saga, N. 1996. A method of high molecular weight DNA from the macroalga *Porphyra yezoensis* (Rhodophyta). *Journal of Phycology* **32**: 496-498.
- Maliakal, S., Cheney, D.P., and Rorrer, G.L. 2001. Halogenated monoterpene production in regenerated plantlet cultures of *Ochtodes secundiramea*. *Journal of Phycology* **37**: 1010-1019.

Tucker and Rorrer, 2001. Bromoperoxidase activity in microplantlet suspension cultures of the macrophytic red alga *Ochtodes secundiramea*. *Biotechnology and Bioengineering* **74**: 389-395.

Stephanopoulos, G.N., Aristidou, A.A., Nielsen J. 1998. *Metabolic Engineering: Principles and Methodologies*. San Diego: Academic Press.

Stephanopoulos, G.N., Vallino, J.J. 1991. Network rigidity and metabolic engineering in metabolite overproduction. *Science* **252**: 1675-1681.

Stephanopoulos, G.M. 2002. Metabolic engineering: perspective of a chemical engineer. *AIChE Journal* **48**: 920-926.

Van Gulik, W.M., de laet, W.T.A.M., Vinke, J.L., and Heijnen, J.J. 2000. Application of metabolic flux analysis for the identification of metabolic bottlenecks in the biosynthesis of penicillin-G. *Biotechnology and Bioengineering* **68**: 602-618.

Vallino, J.J., and Stephanopoulos, G.N. 1993. Metabolic flux distribution in *Corynebacterium glutamicum* during growth and lysine overproduction. *Biotechnology and Bioengineering* **41**: 633-646.

## 5. LIGHT DELIVERY

Light delivery experiments were conducted to determine the effect mean light intensity would have on growth rate and monoterpene production rate. To simplify the analysis it was desired to only allow monoterpene production and not allow the formation of halogenated monoterpenes. To prevent halogenated monoterpene production, that pathway was shut down by not adding bromide and vanadium.

The level of light delivery was the manipulated variable and it was varied from 52.5 to 240  $\mu\text{E m}^{-2} \text{s}^{-1}$ . Work was done before cultivations were conducted to determine two key factors for light delivery cultivations. The first factor is light attenuation as a function of biomass density, and it was used to relate the light intensity incident to the vessel wall to the mean light intensity felt by the organism. The second factor is the photosynthetic saturation at increasing light intensities, and it was used to set the level of light delivery from half photosynthetic saturation to above saturation.

### 5.1. MATERIALS AND METHODS

#### 5.1.1. Culture Maintenance

Plantlets of the macrophytic tropical red alga *Ochtodes secundiramea* used for light delivery cultivation experiments were derived and maintained under the same conditions as the culture used for the bromide and vanadium delivery experiments detailed in chapter 4. The composition of the medium and methods for stock culture maintenance were the same as described in chapter 4.



### 5.1.2. Photobioreactor Design and Operation

The airlift photobioreactor design used for experiments detailed in chapter 4 was utilized for light delivery experiments. A detailed description of the cultivation conditions used for light delivery experiments are presented in Table 5-1. The mean light intensity provided to the culture was the variable under study and was altered to 3 different values. Continuous medium perfusion was implemented to maintain adequate nutrient levels, and the composition of the initial and perfusion medium is provided in Table 5-2.

The sampling protocol described in chapter 4 was implemented for light delivery cultivations. The cell biomass, medium nitrate concentration, medium phosphate concentration and metabolite extraction and quantification procedures described in chapter 4 were also used in light delivery cultivations.

**Table 5-1. Experimental Process Conditions for Light Delivery Cultivations**

Process parameter	Mean Light Intensity		
	$I_m$		
	$(\mu\text{E m}^{-2} \text{ s}^{-1})$		
	52.5	125	240
Planes of illumination, $\alpha$	4	4	4
Photoperiod (h ON:h OFF LD)	14:10	14:10	14:10
Bromide conc. ( $\text{mmol Br L}^{-1}$ )	0.0	0.0	0.0
Vanadium conc. ( $\text{nmol V L}^{-1}$ )	0.0	0.0	0.0
Medium perfusion rate ( $\text{mL day}^{-1}$ )	412	392	418
Working volume, $V$ (mL)	2050	1900	2000
Vessel inner diameter, $d_o$ (cm)	10.0	10	10
Draft tube inner diameter, $d_i$ (cm)	6.0	6.0	6.0
Aeration rate, $v_e$ ( $\text{L min}^{-1}$ )	630	630	630
Aeration rate, $v_e / V$ ( $\text{L air L}^{-1} \text{ min}^{-1}$ )	0.31	0.33	0.32
$\text{O}_2$ mass transfer, $k_L a$ ( $\text{h}^{-1}$ )	21.5	21.5	21.5
$\text{CO}_2$ Partial pressure, (ppm)	3500	3500	3500
$\text{CO}_2$ - $TR_{max}$ ( $\text{mmol CO}_2 \text{ L}^{-1} \text{ h}^{-1}$ )	2.23	2.23	2.23
$n_{\text{CO}_2}$ ( $\text{mmol CO}_2 \text{ L}^{-1} \text{ h}^{-1}$ )	2.65	2.65	2.65
Setpoint pH	8.0	8.0	8.0
Average pH	$7.9 \pm 0.1$	$7.8 \pm 0.1$	$7.9 \pm 0.3$
Culture removal rate, $v_f / V$ ( $\text{mL day}^{-1}$ )	54.0	42.5	51.0
Temperature ( $^{\circ}\text{C}$ )	26	26	26
Final cultivation time (days)	36.0	36.0	36.0
Solids content ( $\text{g DW g}^{-1} \text{ FW}$ )			
Inoculation	25.74%	26.80%	28.21%
Final	27.43%	33.25%	29.24%
Initial plantlet density, $X_o$ ( $\text{g DW L}^{-1}$ )	1.14	1.27	1.13
Final plantlet density, $X_o$ ( $\text{g DW L}^{-1}$ )	0.69	1.68	2.39

**Table 5-2. Medium Composition for Light Delivery Cultivations**

Parameter	Mean Light Intensity $I_m$ ( $\mu\text{E m}^{-2} \text{s}^{-1}$ )		
	52.5	125	240
Initial and perfusion medium composition			
Bromide conc. (mmol Br L <sup>-1</sup> )	0.0	0.0	0.0
Vanadium conc. (nmol V L <sup>-1</sup> )	0.0	0.0	0.0
Nitrate conc. ( $\mu\text{mol N L}^{-1}$ )	3415	3684	3500
Phosphate conc. ( $\mu\text{mol P L}^{-1}$ )	180	195	185
Micronutrient conc. (x base medium)	2	2	2

### 5.1.3. Mean Light Intensity

A representative PI curve for *Ochtodes secundiramea* microplantlets, cultivated under the above conditions, is presented in Figure 5-1. Measurements of the photosynthetic oxygen evolution rate (OER) were performed using the apparatus and procedures described by Huang et al. (1998). Although the vessel and DO cell are curved, the most conservative estimate for  $I_m$  results from light transfer across the vessel diameter,  $d$  (cm), i.e., the longest light path. Consequently, for one-dimensional light transfer across the vessel diameter,  $I_m$  for the vessel is

$$I_{mv} = \frac{\alpha_v I_{ov}}{k' d_v} \left( 1 - e^{-k' d_v} \right) \quad (5-1)$$

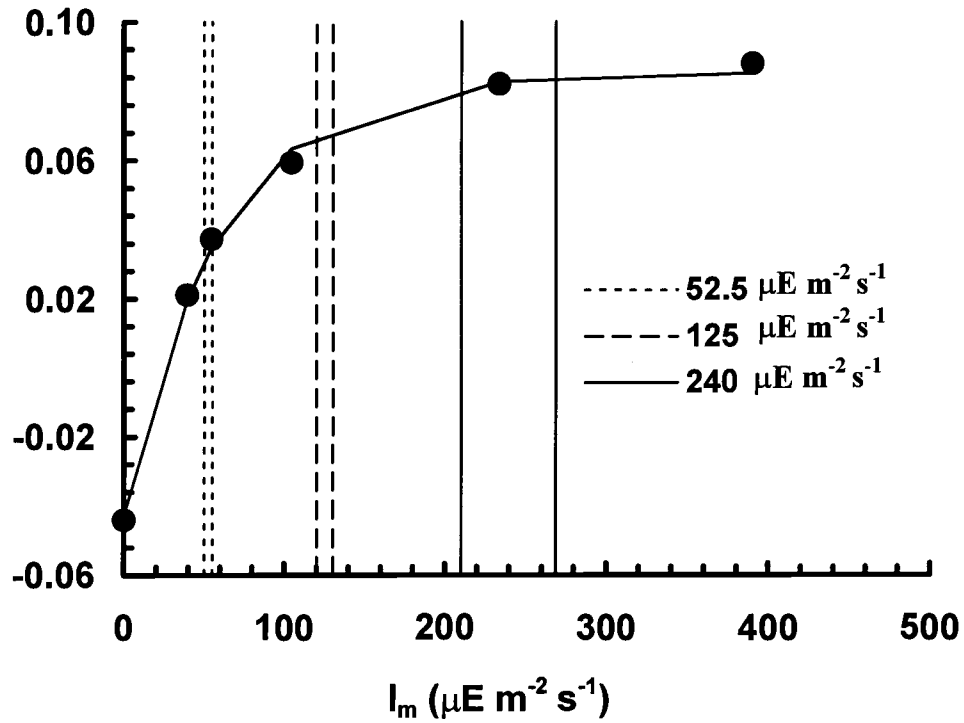


**Figure 5-1. Photosynthetic oxygen evolution rate vs mean light intensity (PI) curve for *Ochtodes secundiramea* microplantlets**

and for the DO cell

$$I_{mc} = \frac{\alpha_c I_{oc}}{k' d_c} (1 - e^{-k' d_c}) \quad (5-2)$$

where  $\alpha_v$  is the number of planes of light delivery to the vessel,  $\alpha_c$  is the number of planes of light delivery to the DO cell, and  $k'$  ( $\text{cm}^{-1}$ ) is the light attenuation constant for the cultivation medium. The light attenuation constant was determined experimentally using the apparatus and procedures described in Huang

& Rorrer (2002). Figure 5-2 shows the light attenuation constant for increasing values of biomass concentration.

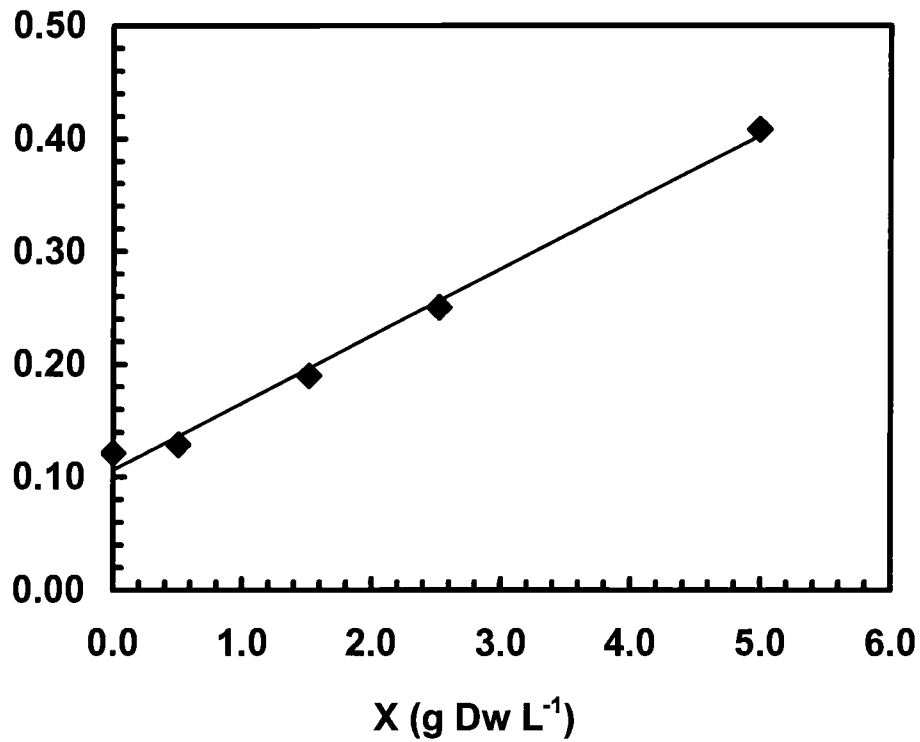


**Figure 5-2. Dependence of the light attenuation constant on biomass density**

The equation describing the light attenuation constant is linear and is given by

$$k' = k_o + k_c X \quad (5-3)$$

where  $k_o$  (cm<sup>-1</sup>) is the light attenuation through cell free media and  $k_c$  (L cm<sup>-1</sup> g DW<sup>-1</sup>) is the specific light attenuation constant of the biomass,  $X$  (g DCW L<sup>-1</sup>).

Values for  $k_o$  and  $k_c$  as well as an estimation of the mean light intensities for all light delivery cultivations are given in Table 5-3.

The mean light intensities for each cultivation are presented on the PI curve, Figure 5-1, as vertical lines. Two vertical lines display the maximum and minimum mean light intensity provided at the maximum and minimum biomass densities achieved during the cultivation. The three mean light intensities used for the light delivery cultivations are in three different zones of the PI curve. The highest mean light intensity is in the saturated zone, meaning no additional light delivery will have an impact on the oxygen evolution. The second mean light intensity is at approximately 75% saturation and the lowest mean light intensity is at half saturation. Consequently, all three light delivery experiments are at distinctively different mean light intensities.

**Table 5-3. Estimation of Mean Light Intensity** (all errors  $\pm 1$  s.e.)

	Mean Light Intensity		
	$I_m$		
	$(\mu\text{E m}^{-2} \text{ s}^{-1})$		
	52.5	125	240
$\alpha_v$	4	4	4
$d_v$ (cm)	10	10	10
$k_o$ (cm <sup>-1</sup> )	0.107 $\pm$ 0.0074	0.107 $\pm$ 0.0074	0.107 $\pm$ 0.0074
$k_c$ (L g DW <sup>-1</sup> cm <sup>-1</sup> )	0.059 $\pm$ 0.0029	0.059 $\pm$ 0.0029	0.059 $\pm$ 0.0029
$X_o$ (g DW L <sup>-1</sup> )	1.14	1.27	1.13
$X_f$ (g DW L <sup>-1</sup> )	0.69	1.68	2.37
$I_m(X_o)$ ( $\mu\text{E m}^{-2} \text{ s}^{-1}$ )	49.8	130	269
$I_m(X_f)$ ( $\mu\text{E m}^{-2} \text{ s}^{-1}$ )	55.1	120	210

#### 5.1.4. Specific Biomass Growth Rate

Calculation of the specific biomass growth rate for light delivery cultivations was done using equations 4-1 through 4-4, developed in chapter 4, section 4.1.5. An alternative estimate for the specific growth rate based on the photosynthetic oxygen evolution rate is

$$\mu = P_o \cdot Y_{x/o_2} \cdot f \quad (5-4)$$

where  $f$  is the fractional photoperiod,  $Y_{x/o_2}$  is the biomass yield coefficient based on  $O_2$  evolution, equal to  $30 \text{ g DCW mol}^{-1}$ , given by the Redfield ratio for phototrophic organisms (Atkinson and Smith, 1983).  $P_o$  is the photosynthetic oxygen evolution rate calculated from

$$P_o = P_{o,\max} \left( 1 - e^{-I_m/I_k} \right) + Q_o \quad (5-5)$$

where  $P_{o,\max}$  ( $\text{mmol } O_2 \text{ g DCW}^{-1} \text{ hr}^{-1}$ ),  $I_k$  ( $\mu\text{E m}^{-2} \text{ s}^{-1}$ ) and  $Q_o$  ( $\text{mmol } O_2 \text{ g DCW}^{-1} \text{ hr}^{-1}$ ) are all obtained from a non-linear regression of the PI curve data presented in Figure 5-2 with equation 5-5. The values of the fitted parameters are presented in Table 5-5.

#### 5.1.5. GC-MS Analysis

Samples from cultivations of *Ochthodes secundiramea* microplantlets performed under light delivery manipulations, showed GC-FID chromatograms different than cultivations performed under nutrient or bromide/vanadium delivery manipulations. A GC-MS analysis was performed on shutdown biomass from a run conducted at mean light intensity of  $125 \mu\text{E m}^{-2} \text{ s}^{-1}$  to identify the differences. The biomass extract was obtained following the procedure outlined in Chapter 2, but a different GC-MS procedure was used. The biomass extracts were analyzed by GC-MS using a Hewlett Packard 6890 gas chromatograph and quadrupole mass selective detector. Compounds were profiled on a 30 m by 0.32 mm HP-5 capillary



column (Phenomenex, 5% phenyl- 95% dimethylpolysiloxane film, 0.25  $\mu\text{m}$  thickness) under the following temperature program: injector temperature 250  $^{\circ}\text{C}$ , column temperature 50  $^{\circ}\text{C}$  initial, 20  $^{\circ}\text{C min}^{-1}$  ramp to 320  $^{\circ}\text{C}$ , 6.5 min hold at 320  $^{\circ}\text{C}$ . The carrier gas flowrate through the column was 2.0  $\text{mL min}^{-1}$  at 9.54 psi column head pressure. The ionization voltage of the MS detector was 70 eV. Sample injection volume was 1.0  $\mu\text{L}$ . All reported mass spectra were obtained from the scan taken at the apex of the chromatographic peak corresponding to a given compound. The reported relative signal intensity for a given mass fragment was not averaged from several scans nor subtracted from the baseline abundance signal.

## 5.2. RESULTS AND DISCUSSION

### 5.2.1. Growth Data

Light delivery cultivations were performed to determine the effect of light delivery on growth and halogenated monoterpene production. Nutrient and  $\text{CO}_2$  delivery were set to approach or exceed saturation levels, making mean light intensity the only independent variable. Nutrient and  $\text{CO}_2$  delivery rates are detailed in Tables 5-1 and 5-2.

Figure 5-2 shows the cultivation mean light intensities relative to the PI curve. The cultivation mean light intensities cover a range from above saturation (240  $\mu\text{E m}^{-2} \text{s}^{-1}$ ) to two values below saturation (52.5  $\mu\text{E m}^{-2} \text{s}^{-1}$  and 125  $\mu\text{E m}^{-2} \text{s}^{-1}$ ). Over this range, mean light intensity should affect growth. Table 5-4 presents the specific growth rate, calculated by equations 4-1 through 4-4, and Table 5-5 shows the specific growth rate calculated by equations 5-4 and 5-5. Values calculated by estimation of the specific oxygen evolution rate, equations 5-4 and 5-

5 vary from  $0.086 \text{ day}^{-1}$  to  $0.12 \text{ day}^{-1}$  over the range of experimental mean light intensities. The specific growth rates calculated by equations 4-1 through 4-4 vary from  $0.018 \text{ day}^{-1}$  to  $0.051 \text{ day}^{-1}$ . While the calculated value does not exactly match the experimental value, the trend in the specific growth rate, shown in Figure 5-3, as a function of mean light intensity is the same for both calculated and experimental specific growth rates. The mean light intensity was capable of affecting the specific growth rate as illustrated by Figure 5-3.

The nitrate and phosphate concentrations of the liquid medium were measured over the cultivation time. These results are presented in Figures 5-4 and 5-5. Nitrate concentrations for all cultivations do not reach zero during the cultivation, and phosphate concentrations for all cultivations reach zero after 10 days. The phosphate concentration for the two lowest mean light intensities,  $52.5 \mu\text{E m}^{-2} \text{ s}^{-1}$  and  $125 \mu\text{E m}^{-2} \text{ s}^{-1}$ , show a slow increase after day 20. Growth was therefore limited by the rate of phosphate delivery for cultivations at  $52.5 \mu\text{E m}^{-2} \text{ s}^{-1}$  and  $125 \mu\text{E m}^{-2} \text{ s}^{-1}$  during an interval between 10 and 20 days. The cultivation at  $240 \mu\text{E m}^{-2} \text{ s}^{-1}$  was phosphate limited after day 10 and for the remainder of the cultivation. Phosphate and nitrate delivery rates were set to an N:P ratio of 19:1 as determined by Atkinson and Smith, 1983 for balanced growth of red marine algae. An increase in the ratio of phosphate to nitrate would be required to prevent phosphate limitation. For the current study the N:P ratio was set to ensure consistency with earlier studies.

**Table 5-4. Measured Specific Growth Rates for Light Delivery Cultivations**  
(all errors  $\pm 1$  s.e.)

	Mean Light Intensity $I_m$ ( $\mu\text{E m}^{-2} \text{ s}^{-1}$ )		
	52.5	125	240
$M_o$ (g)	2.33	2.41	2.27
$M_f$ (g)	1.41	3.48	4.74
$t_o$ (day)	0	0	0
$t_f$ (day)	36	36	36
$\dot{R}_s$ (g/day)	$0.059 \pm 0.0011$	$0.051 \pm 0.0010$	$0.092 \pm 0.0021$
$\mu$ ( $\text{day}^{-1}$ )	0.018	0.028	0.051

**Table 5-5. Specific Growth Rate Calculated from Estimation of Photosynthetic Oxygen Evolution**

	Mean Light Intensity		
	$I_m$ $(\mu\text{E m}^{-2} \text{ s}^{-1})$		
	52.5	125	240
$P_{o,\max}$ (mmol $\text{O}_2$ g DCW $^{-1}$ hr $^{-1}$ )	0.128	0.128	0.128
$Q_o$ (mmol $\text{O}_2$ g DCW $^{-1}$ hr $^{-1}$ )	0.043	0.043	0.043
$I_k$ ( $\mu\text{E m}^{-2} \text{ s}^{-1}$ )	58.5	58.5	58.5
$I_m$ ( $\mu\text{E m}^{-2} \text{ s}^{-1}$ )	53	125	240
$f$ (-)	0.583	0.583	0.583
$Y_{x/\text{O}_2}$ (g DCW mol $^{-1}$ )	30.0	30.0	30.0
$P$ (mmol $\text{O}_2$ g DCW $^{-1}$ hr $^{-1}$ )	0.119	0.156	0.169
$\mu$ (day $^{-1}$ )	0.050	0.065	0.071

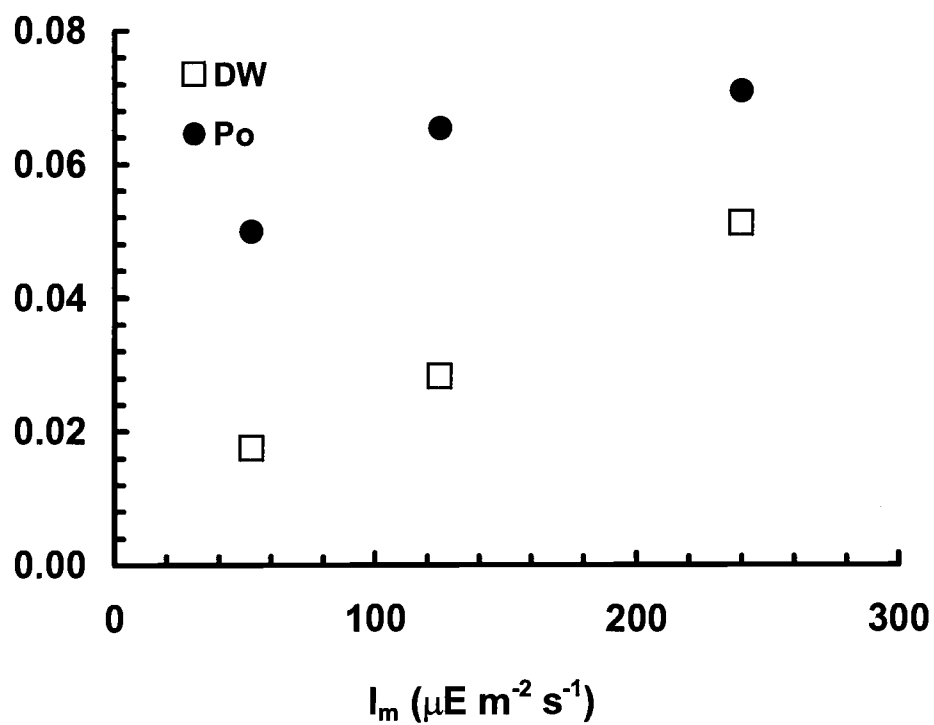


**Figure 5-3. Calculated specific growth rates for light delivery cultivations based on measurements of biomass during cultivation, and from photosynthetic oxygen evolution calculation**

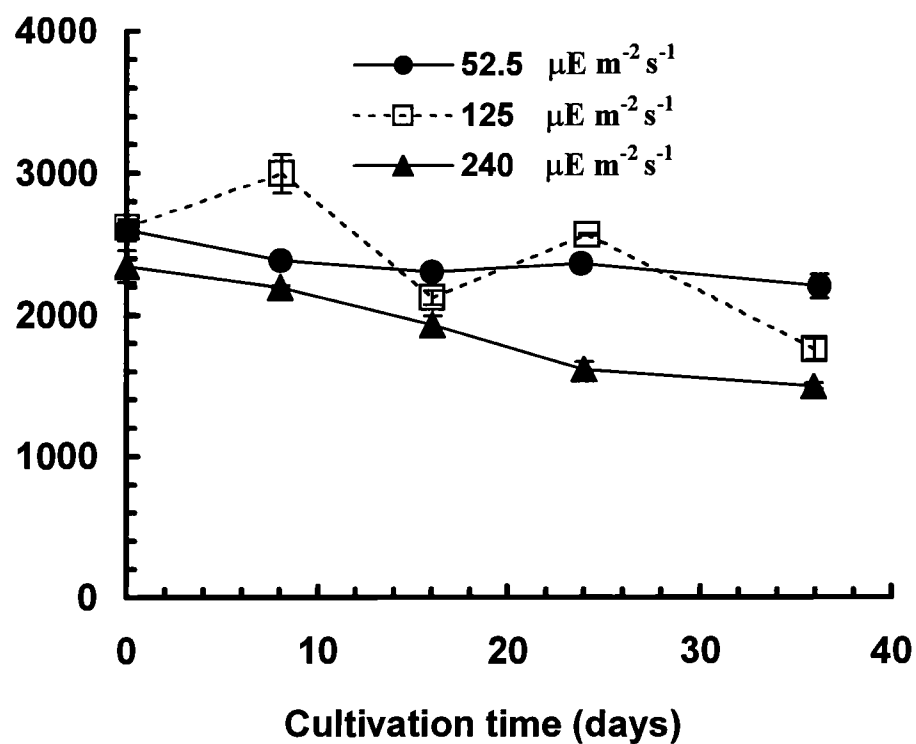


**Figure 5-4. Photobioreactor medium nitrate concentration profiles for light delivery cultivations**

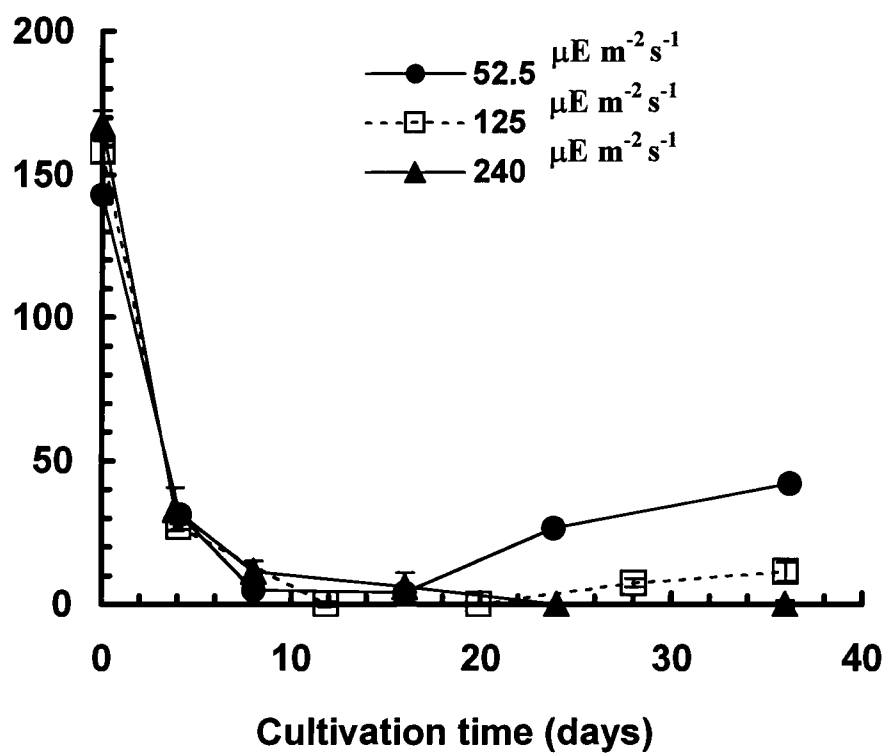


**Figure 5-5. Photobioreactor medium phosphate concentration profiles for light delivery cultivations**

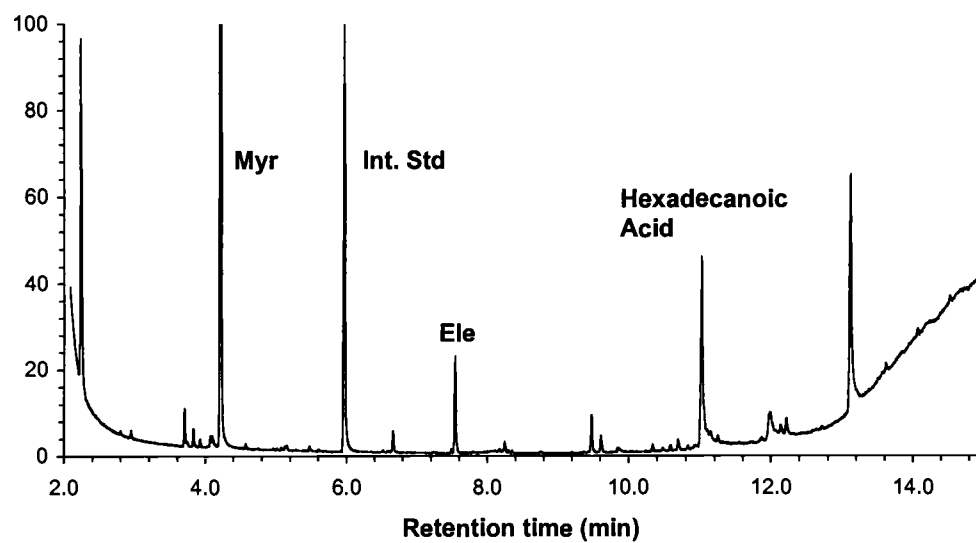


**Figure 5-6. GC-TIC plots of DCM extracts of *Ochtodes secundiramea* microplantlets showing terpenes and no halogenated compounds**



### 5.2.2. GC-MS Analysis

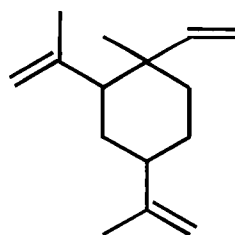
The dichloromethane (DCM) extract from the photobioreactor cultured *O. secundiramea* plantlets grown without bromide or vanadium under a mean light intensity of  $125 \mu\text{E m}^{-2} \text{s}^{-1}$  contained no halogenated monoterpenes, one monoterpene, one sesquiterpene, as well as other hydrocarbons. Gas chromatography (GC) profiles of a representative DCM extract using TIC mode of detection is presented in Figure 5-6. Mass spectral data from selected peaks profiled by GC-TIC are presented in Table 5-6. The peak at 4.22 min retention time on GC-TIC was myrcene,  $\text{C}_{10}\text{H}_{16}$ , an acyclic monoterpene with characteristic mass signals at  $m/z$  136 (parent molecular ion  $\text{M}^+$ ), 93 ( $\text{M}^+$  less  $m/z$  43  $\text{C}_3\text{H}_7$  fragment), and  $m/z$  69 ( $\text{C}_5\text{H}_9$  fragment). The peak at 7.54 min retention time was beta-elemene,  $\text{C}_{15}\text{H}_{24}$ , a cyclic sesquiterpene with characteristic mass signals at  $m/z$  189 (parent molecular ion  $\text{M}^+$  less  $m/z$  15  $\text{CH}_3$  fragment), 93 ( $\text{M}^+$  less  $m/z$  111  $\text{C}_8\text{H}_{15}$  fragment), and  $m/z$  81 ( $\text{M}^+$  less  $m/z$  123  $\text{C}_9\text{H}_{15}$  fragment).

**Table 5-6. Dominant Terpenes in DCM Extracts of Photobioreactor Cultivated *O. secundiramea* Microplantlets**

Label	Retention Time (min)		Characteristic Mass Signals ( $m/z$ )			Mol. Formula (cyclization)	Mol. Weight
	TIC	FID	100% peak	M-C <sub>3</sub> H <sub>7</sub> (43), M-C <sub>8</sub> H <sub>15</sub> (111)	M+		
MYR	4.63	4.44	93	93(100) (Myr-43)	136(5)	C <sub>10</sub> H <sub>16</sub> (acyclic)	136.24
ELE	7.54	8.22	93	161(31) (M-43) 93(100) (M-111)	n.d.	C <sub>15</sub> H <sub>24</sub> (cyclic)	204

### 5.2.3. Terpene Kinetic Data

Myrcene concentration profiles are presented in Figure 5-7, and beta elemene profiles are presented in Figure 5-8. Beta-elemene is a sesquiterpene with the following structure.



beta-Elemene

An analysis of the myrcene profiles reveals that there is a time lag for myrcene production that does vary between the three light intensities: 8, 16 and 20 days for the mean light intensities of 240, 125 and 52.5  $\mu\text{E m}^{-2} \text{s}^{-1}$ , respectively.

The slope of the myrcene profiles following the time lag is the same for all three light intensities. The transfer of the culture from its maintenance state to the photobioreactor constitutes a step change in mean light intensity. The intermediate compounds of the non-mevalonate pathway, the likely biogenic source of monoterpenes, are not at saturation levels at inoculation because the maintenance culture is not exposed to saturated levels of light. The non-mevalonate pathway is coupled to photosynthesis (Rohmer, 1999), and the concentrations of the compounds in the pathway will increase to saturation levels faster at higher light intensity. According to this rationale, once the saturation levels are reached, the rate of production of myrcene will be equal for all three light intensities. At mean light intensities above  $52.5 \mu\text{E m}^{-2} \text{s}^{-1}$  there is no sensitivity of myrcene production in *Ochtodes secundiramea* microplantlets on light intensity.

Beta-elemene profiles show no time lag and have equal production rates. Beta-elemene is a sesquiterpene that is likely formed from a different biogenic pathway than myrcene, so differences in lag are not expected. At mean light intensities above  $52.5 \mu\text{E m}^{-2} \text{s}^{-1}$  there is no sensitivity of beta-elemene production in *Ochtodes secundiramea* microplantlets on light intensity.

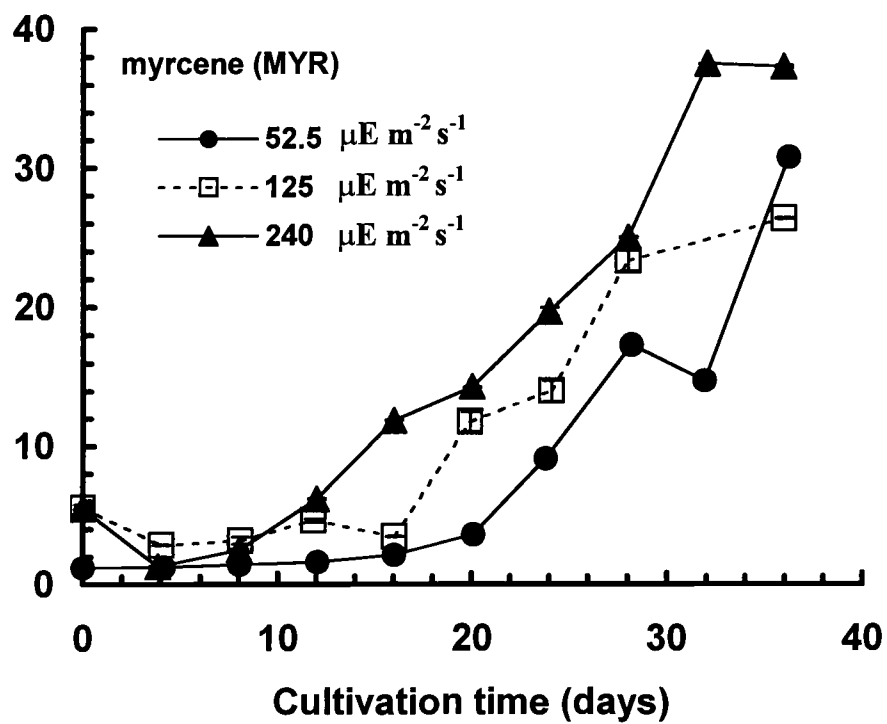


Figure 5-7. Myrcene profiles for light delivery cultivations

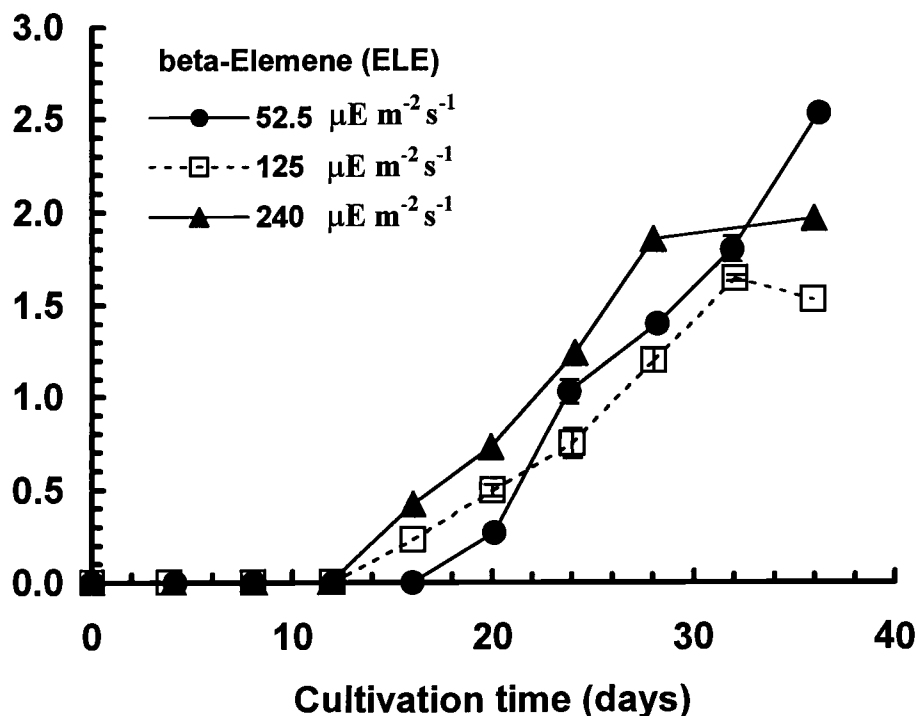


Figure 5-8. beta-Element profiles for light delivery cultivations

### 5.3. REFERENCES

- Atkinson, M.J., Smith, S.V. 1983. C:N:P ratios of benthic marine plants. *Limnol Oceanogr* **28**: 568-574.
- Huang, Y.M., Maliakal, S., Cheney, D.P., and Rorrer, G.L. 1998. Comparison of development and photosynthetic growth for filament clump and regenerated microplantlet cultures of *Agardhiella subulata* (Rhodophyta, Gigartinales). *Journal of Phycology* **34**: 893-901.
- Huang, Y.M., and Rorrer, G.L. 2002. Dynamics of oxygen evolution and biomass production during cultivation of *Agardhiella subulata* microplantlets in a bubble-column photobioreactor under medium perfusion. *Biotechnology Progress* **18**: 62-71.

Rohmer, M. 1999. The discovery of a mevalonate-independent pathway for isoprenoid biosynthesis in bacteria, algae, and higher plants. *Nat. Prod. Rep.* **16**: 565-574.

## 6. SUMMARY AND CONCLUSIONS

Several factors have been identified that affect the growth and halogenated monoterpene production of *Ochtodes secundiramea* microplantlets. The areas of focus for this study centered around understanding the effects of nutrient delivery, bromide/vanadium delivery and light delivery. These areas were chosen for their likelihood of having an impact on growth and halogenated monoterpene production, and each area is presumed to effect growth and halogenated monoterpene production in different ways. Crossover between the groups is limited.

The area of nutrient delivery showed a straightforward and significant effect on growth rate and a complex and subtle effect on halogenated monoterpene production. Secondary metabolite synthesis, and terpenoid synthesis in particular, are complex, with many intermediates, enzymes, co-factors and control points. Growth on the other hand is more easily understood and simpler to model. Increasing nutrient delivery from  $0.0063 \text{ mmol N L}^{-1} \text{ day}^{-1}$  to  $0.74 \text{ mmol N L}^{-1} \text{ day}^{-1}$  caused an increase in final biomass density and specific growth rate. In red algae, nitrogen is not only a component of proteins and DNA, but is also a component of photosynthetic pigments. For a nutrient delivery of  $0.74 \text{ mmol N L}^{-1} \text{ day}^{-1}$ , the photosynthetic oxygen evolution rate increases to a peak value and then decreases. As more nitrogen was brought into the microplantlets, the maximum photosynthetic rate increases. After medium nitrate concentrations reduce, nitrogen is shifted from pigments back to protein and DNA, and we observe a decrease in the photosynthetic rate. The nitrogen containing pigments complicate growth models because they are a significant destination for nitrogen that changes over the course of the cultivation. Any accurate model of biomass growth, and nutrient

concentrations would need to account for the incorporation of nitrogen into photosynthetic pigments.

For the production of the secondary metabolites in the halogenated monoterpene biosynthetic pathway, increasing nutrient delivery causes an increase in production of myrcene, bromomyrcene and chloromyrcene, but does not have an effect on bromochloromyrcene. Production rates of apakaochtodene B and dibromomyrcene are slightly higher for nutrient delivery of  $0.077 \text{ mmol N L}^{-1} \text{ day}^{-1}$  than for  $0.74 \text{ mmol N L}^{-1} \text{ day}^{-1}$ . Nutrient delivery of  $0.0063 \text{ mmol N L}^{-1} \text{ day}^{-1}$  showed reduced production of all compounds. Increasing nutrient delivery shows a selectivity for mono-halogenated monoterpenes, while the higher halogenated monoterpenes are preferred for the lower nutrient delivery rate of  $0.077 \text{ mmol N L}^{-1} \text{ day}^{-1}$ . Decreasing nutrient delivery to  $0.0063 \text{ mmol N L}^{-1} \text{ day}^{-1}$  does not produce appreciable amounts of any compounds, and is likely severely nutrient limited at an early stage of cultivation.

Nutrient delivery cultivations were conducted to test the carbon-nutrient balance hypothesis. Assuming that the higher halogenated monoterpenes, in particular apakaochtodene B, are defense compounds, our results with *Ochtodes secundiramea* microplantlets partially follows the CNBH theory. The lowest nutrient delivery was not sufficient to produce any compounds illustrating a minimum nutrient delivery must be reached to allow for production of defense compounds.

For semi-continuous and fed-batch bromide and vanadium delivery cultivations, the production of halogenated monoterpenes can be completely shut off by denying the culture bromide and vanadium. If either bromide or vanadium is supplied while denying the other, the monohalogenated compound bromomyrcene can still be formed. The comparison of production rates for bromomyrcene under



conditions of saturated bromide and zero vanadium versus saturated vanadium and zero bromide, shows an increased production rate for the vanadium denied cultivation. This result likely illustrates the catalytic nature of vanadium versus the substrate bromide.

In semi-continuous cultivations, under conditions of zero bromide delivery, the chlorinated compound chloroperoxidase is not formed. The lack of production of chloromyrcene under saturated chlorine concentrations, and zero bromide concentration shows there is not likely a chloroperoxidase enzyme in *Ochtodes secundiramea* that could add chlorine directly to myrcene. The production of chloromyrcene is likely tied to the production of a bromonium ion-myrcene intermediate that can be attacked by a chloride ion. Lack of bromide to form the bromonium ion-myrcene intermediate prevents formation of chloromyrcene.

Semi-continuous bromide and vanadium delivery experiments show that even at the lowest possible bromide delivery rate, the mass of bromide delivered was above saturation levels for halogenated monoterpene production. For fed-batch cultivations, it was possible to reduce the mass of bromide delivered to below saturation levels for two of the halogenated monoterpenes. The reduced mass of bromide delivered to the culture has a complex effect on halogenated monoterpene production. Bromomyrcene, chloromyrcene and bromochloromyrcene production rates show that  $0.038 \text{ mmol Br L}^{-1}$  delivered to the culture was enough to provide excess bromide for production of these compounds. Production of dibromomyrcene shows sensitivity on bromide mass delivered, with  $1.40 \text{ mmol Br L}^{-1}$  making more dibromomyrcene than  $0.128 \text{ mmol Br L}^{-1}$  with zero production for  $0.0$  and  $0.038 \text{ mmol Br L}^{-1}$ . Apakaoctodene is only produced at a bromide mass delivered of  $1.4 \text{ mmol Br L}^{-1}$ .

There was no significant effect of bromide and vanadium delivery rates on biomass growth rate and final biomass yield. As the microplantlets grew, they did not divide but continued to grow larger and larger. The microplantlets approached a diameter which made them difficult to suspend and difficult to remove from the vessel. The liquid medium was well mixed as shown by the nitrate, phosphate and bromide concentration curves, but the biomass sampled was not representative of the biomass concentration. Therefore, only significant differences in growth rate for different bromide and vanadium delivery rates would be meaningful. There were no significant differences in growth rate for any bromide and vanadium delivery rate.

Light delivery experiments showed that increasing mean light intensity does not increase production of myrcene. The lowest mean light intensity tested was still high enough to saturate the production of myrcene. During light intensity cultivations in which halogenated monoterpene production was shut down by removing bromide and vanadium, appreciable amounts of beta-elemene were formed. Nutrient delivery cultivations, and bromide/vanadium delivery cultivations did not show the production of beta-elemene. Shutting off the halogenation reactions for the entire cultivation allowed for the accumulation of beta-elemene, illustrating that other metabolite pathways can be affected by changing the halogenated monoterpene pathway.

Light delivery cultivations were able to have an effect on growth rate and biomass yield. The mean light intensity delivered for these cultivations spanned a range from above saturation to half saturation. The profiles of growth rate estimated from biomass samples, and calculated from photosynthetic oxygen evolution rates show similar patterns.

For all cultivations performed, the phosphate concentration reached zero at some point during the cultivation. For all but fed-batch cultivations, the nitrate concentration also reached zero at some point during the cultivation. Phosphate concentration always reached zero faster than nitrate concentration. The microplantlets were phosphate limited for much of their cultivation. Since the phosphate limitation was the same for the different groups of experiments, the limitation likely did not contribute to the differences observed. An increase in the nitrogen:phosphorous ratio should be an objective of future work in this area.

Other areas for future work include isolation and identification of the remaining un-known compounds of the halogenated monoterpene pathway. Knowing the structure of the compounds would give more evidence to the likely pathway and reaction mechanism for halogenated monoterpene production.

Much work has been done to study the activity of the bromoperoxidase enzyme. Studying the reactions of myrcene with the enzyme under different conditions would also give insight as to the mechanism of reactions. Understanding the reaction mechanics and pathway should be at the root of all future work in this area.

If the reaction mechanism and pathway can be elucidated, I would recommend that genetic engineering be done to enhance higher halogenated monoterpenes. I would recommend inserting a chloroperoxidase and cyclase enzyme into *Ochtodes secundiramea* to study any change in the product yields.

It is interesting to note that none of the compounds isolated from field collections of *Ochtodes secundiramea* were identified in this study. I would propose work be done to understand the differences between photobioreactor

cultivated biomass vs field collected biomass, in particular the differences in any enzymes or enzyme activity.

## BIBLIOGRAPHY

- Aristidou, A.A., San, K.Y., and Bennett, G.N. 1999. Metabolic flux analysis of *Escherichia coli* expressing the *Bacillus subtilis* acetolactate synthase in batch and continuous cultures. *Biotechnology and Bioengineering* **63**: 737-749.
- Arnold, T.M., Tanner, C.E., and Hatch, W.I. 1995. Phenotypic variation in polyphenolic content of the tropical brown alga *Lobophora variegata* as a function of nitrogen availability. *Marine Ecology Progress Series* **123**: 177-183.
- Atkinson, M.J., Smith, S.V. 1983. C:N:P ratios of benthic marine plants. *Limnol Oceanogr* **28**: 568-574.
- Barahona, L.F., and Rorrer, G.L. 2003. Isolation of halogenated monoterpenes from bioreactor-cultured microplantlets of the macrophytic red-algae *Ochtodes secundiramea* and *Portieria hornemannii*. *Journal of Natural Products* **66**: 743-751.
- Bramley, P.M. 1997. Isoprenoid metabolism. In: *Plant Biochemistry*, P.M. Dey and J.B. Harborne, Ed., Academic Press: San Diego, CA, pp 417-439.
- Burreson, B.J., Woolard, F.X., and Moore, R.E. 1975. Evidence for the biogenesis of halogenated myrcenes from the red alga *Chondrococcus hornemannii*. *Chemistry Letters*: 1111-1114.
- Butler, A., and Walker, J.V. 1993. Marine haloperoxidases. *Chemistry Reviews* **93**: 1937-1944.
- Butler, A. 1998. Acquisition and utilization of transition metal ions by marine organisms. *Science* **281**: 207-210.
- Butler, A. 1999. Mechanistic considerations of the vanadium haloperoxidases. *Coordination Chemistry Reviews* **187**: 17-35.
- Carte, B.K. 1996. Biomedical potential of marine natural products. *BioScience* **46**: 271-285.
- Crews, P. 1977. Monoterpene halogenation by the red alga *Plocamium oregonum*. *Journal of Organic Chemistry* **42**: 2634-2636.

- Crews, P., Myers, B.L., Naylor, S., Clason, E.L., Jacobs, R.S., and Staal, G.B. 1984. Bio-active monoterpenes from red seaweeds. *Phytochemistry* **23**: 1449-1451.
- Cronin, G., and Hay, M.E. 1996. Effects of light and nutrient availability on the growth, secondary chemistry, and resistance to herbivory of two brown seaweeds. *Oikos* **77**: 93-106.
- de Boer, E., and Wever, R. 1988. The reaction mechanism of the novel vanadium-bromoperoxidase. *Journal of Biological Chemistry* **263**: 12326-12332.
- Fenical, W. 1975. Halogenation in the rhodophyta—a review. *Journal of Phycology* **11**: 245-259.
- Fenical, W. 1982. Natural products chemistry in the marine environment. *Science* **215**: 923-928.
- Firmage, D. 1981. Environmental influences on the monoterpene variation in *Hedeoma drummondii*. *Biochemical Systematics and Ecology* **9**: 53-58.
- Follstad, B.D., Balcarcel, R.R., Stephanopoulos, G.N., and Wang, D.I.C. 1999. Metabolic flux analysis of hybridoma continuous culture steady state multiplicity. *Biotechnology and Bioengineering* **63**: 675-683.
- Fuller, R.W., Cardellina II, J.J., Kato, Y., Brinen, L.S., Clardy, J., Snader, K.M., and Boyd, M.R. 1992. A pentahalogenated monoterpene from the red alga *Portieria hornemannii* produces a novel cytotoxicity profile against a diverse panel of human tumor cell lines. *Journal of Medical Chemistry* **35**: 3007-3011.
- Fuller, R.W., Cardellina II, J.J., Jurek, J., Scheuer, P.J., Alvarado-Lindner, B., McGuire, M., Gray, G.N., Steiner, J.R., Clardy, J., Menez, E., Shoemaker, R.H., Newman, D.J., Snader, K.M., and Boyd, M.R. 1994. Isolation and structure/activity features of halomon-related antitumor monoterpenes from the red alga *Portieria hornemannii*. *Journal of Medical Chemistry* **37**: 4407-4411.
- Gerwick, W.H. 1984. 2-Chloro-1,6(S\*),8-tribromo-3-(8)(Z)-octodene: a metabolite of the tropical red seaweed *Ochtodes secundiramea*. *Phytochemistry* **23**: 1323-1324.
- Gribble, G.W. 1992. Naturally occurring organohalogen compounds—a survey. *Journal of Natural Products* **55**: 1353-1395.

Grob, R.L. 1995. Modern practice of gas chromatography, 3<sup>rd</sup> ed. New York: Wiley-Interscience.

Huang, Y.M., Maliakal, S., Cheney, D.P., and Rorrer, G.L. 1998. Comparison of development and photosynthetic growth for filament clump and regenerated microplantlet cultures of *Agardhiella subulata* (Rhodophyta, Gigartinales). *Journal of Phycology* 34: 893-901.

Huang, Y.M., and Rorrer, G.L. 2002a. Dynamics of oxygen evolution and biomass production during cultivation of *Agardhiella subulata* microplantlets in a bubble-column photobioreactor under medium perfusion. *Biotechnology Progress* 18: 62-71.

Huang, Y M.; Rorrer, G L. 2002b. Optimal temperature and photoperiod for the cultivation of *Agardhiella subulata* microplantlets in a bubble-column photobioreactor. *Biotechnology and Bioengineering* 79: 135-144.

Huang, Y.M., and Rorrer, G.L. 2003. Cultivation of microplantlets derived from the marine red alga *Agardhiella subulata* in a stirred tank photobioreactor. *Biotechnology Progress* 19: 418-427.

Ichikawa, N., Naya, Y., and Enomoto, S. 1974. New halogenated monoterpenes from *Desmia (Chondrococcus) hornemanni*. *Chemistry Letters*: 1333-1336.

Ireland, C.M., Roll, D.M., Molinski, T.F., McKee, T.C., Zabriske, T.M., and Swersey, J.C. 1988. Uniqueness of the marine environment: categories of marine natural products from invertebrates. In: *Biomedical Importance of Marine Organisms*, D.G. Fautin, Ed., California Academy of Sciences: San Francisco, CA, pp. 41-57.

Itoh, N., Quamrul, H., Izumi, Y., and Yamada, H. 1988. Substrate specificity, regiospecificity and stereospecificity of halogenation reactions catalyzed by non-heme-type bromoperoxidase of *Corallina pilulifera*. *European Journal of Biochemistry* 172: 477-484.

Ilvessalo, H., and Tuomi, J. 1989. Nutrient availability and accumulation of phenolic compounds in the brown alga *Fucus vesiculosus*. *Marine Biology* 101: 115-119.

Kitade, Y., Yamazaki, S., Saga, N. 1996. A method of high molecular weight DNA from the macroalga *Porphyra yezoensis* (Rhodophyta). *Journal of Phycology* 32: 496-498.

- Konig, G.M., Wright, A.D., and Sticher, O. 1990. A new polyhalogenated monoterpene from the red alga *Plocamium cartilagineum*. *Journal of Natural Products* **53**:1615-1618.
- Lerdau, M., Litvak, M., and Monson, R. 1994. Plant chemical defense: monoterpenes and the growth-differentiation balance hypothesis. *TREE* **9**: 58-61.
- Maliakal, S., Cheney, D.P., and Rorrer, G.L. 2001. Halogenated monoterpene production in regenerated plantlet cultures of *Ochtodes secundiramea*. *Journal of Phycology* **37**: 1010-1019.
- McConnell, O.J., and Fenical, W. 1978. Ochtodene and ochtodiol: novel polyhalogenated cyclic monoterpenes from the red seaweed *Ochtodes secundiramea*. *Journal of Organic Chemistry* **43**: 4238-4241.
- Naylor, S., Hanke, F.K., Manes, L.V., and Crews, P. 1983. XXX. *Prog. Chem. Nat. Prod.* **44**: 189.
- Paul, V.J., McConnell, O.J., and Fenical, W. 1980. Cyclic monoterpenoid feeding deterrents from the red marine alga *Ochtodes crockeri*. *Journal of Organic Chemistry* **45**: 3401-3407.
- Paul, V.J. Hay, M.E., Duffy, J.E., Fenical, W., and Gustafson, K. 1987. Chemical defense in the seaweed *Ochtodes secundiramea* (Montagne) Howe (Rhodophyta): effects of its monoterpenoid components upon diverse coral-reef herbivores. *Journal of Experimental Marine Biology and Ecology* **114**: 249-260.
- Puglisi, M.P., and Paul, V.J. 1997. Intraspecific variation in the red alga *Portieria hornemannii*: monoterpene concentrations are not influenced by nitrogen or phosphorus enrichment. *Marine Biology* **128**: 161-170.
- Qi, H., and Rorrer, G.L. 1995. Photolithotrophic cultivation of *Laminaria saccharina* gametophyte cells in a stirred-tank bioreactor. *Biotechnology and Bioengineering* **45**: 251-260.
- Radmer, R.J. 1996. Algal diversity and commercial algal products. *BioScience* **46**: 263-270.
- Rorrer, G.L., Mullikin, R., Huang, Y.M., Gerwick, W.H., Maliakal, S., and Cheney, D.P. Production of bioactive metabolites by cell and tissue cultures of marine macroalgae in bioreactor systems. 1999. In: *Plant Cell and Tissue Culture for the Production of Food Ingredients*, Fu et al., Ed., Kluwer Academic/Plenum: New York, pp 165-184.



Rorrer, G.L., Polne-Fuller, M., and Zhi, C. 1996. Development and bioreactor cultivation of a novel semi-differentiated tissue suspension derived from the marine plant *Acrosiphonia coalita*. *Biotechnology and Bioengineering* **49**: 559-567.

Rorrer, G.L., J. Modrell, C. Zhi, H.-D. Yoo, D.N. Nagle and W.H. Gerwick. 1995. Bioreactor seaweed cell culture for production of bioactive oxylipins. *Journal of Applied Phycology* **7**: 187-198.

Stephanopoulos, G.N., Aristidou, A.A., Nielsen J. 1998. *Metabolic Engineering: Principles and Methodologies*. San Diego: Academic Press.

Stephanopoulos, G.N., Vallino, J.J. 1991. Network rigidity and metabolic engineering in metabolite overproduction. *Science* **252**: 1675-1681.

Stephanopoulos, G.M. 2002. Metabolic engineering: perspective of a chemical engineer. *AIChE Journal* **48**: 920-926.

South, G.R., Whittick, A. 1987. *Introduction to phycology*. Oxford: Blackwell Scientific Publications.

Tucker and Rorrer, 2001. Bromoperoxidase activity in microplantlet suspension cultures of the macrophytic red alga *Ochtodes secundiramea*. *Biotechnology and Bioengineering* **74**: 389-395.

Turpin, D.H. 1991. Effects of inorganic N availability on algal photosynthesis and carbon metabolism. *Journal of Phycology* **27**: 14-20.

Vallino, J.J., and Stephanopoulos, G.N. 1993. Metabolic flux distribution in *Corynebacterium glutamicum* during growth and lysine overproduction. *Biotechnology and Bioengineering* **41**: 633-646.

Van Gulik, W.M., de Laat, W.T.A.M., Vinke, J.L., and Heijnen, J.J. 2000. Application of metabolic flux analysis for the identification of metabolic bottlenecks in the biosynthesis of penicillin-G. *Biotechnology and Bioengineering* **68**: 602-618.

Wise, M.L., and Croteau, R. Monoterpene biosynthesis. 1999. In: *Comprehensive Natural Products*, S. Barton, K. Nakanishi, O.M. Cohn, and D.E. Cane, Ed., Elsevier: Amsterdam, pp 97-153.

Yamaura, T., Tanaka, S., and Tabata, M. 1989. Light-dependent formation of glandular trichomes and monoterpenes in thyme seedlings. *Phytochemistry* **28**: 741-744.

Zhi C., and Rorrer, G.L. 1996. Photolithotrophic cultivation of *Laminaria saccharina* gametophyte cells in a bubble-column bioreactor. *Enzyme and Microbial Technology* **18**: 291-299.